TRANSPORTATION RESEARCH RECORD 633

Pavement Surface Properties and Performance

TRANSPORTATION RESEARCH BOARD

COMMISSION ON SOCIOTECHNICAL SYSTEMS
NATIONAL RESEARCH COUNCIL

NATIONAL ACADEMY OF SCIENCES
WASHINGTON, D.C. 1977

Transportation Research Record 633
Price $2.80
Edited for TRB by Dolores Breslaw

subject areas
21 photogrammetry
25 pavement design
26 pavement performance
40 maintenance, general
51 highway safety

Transportation Research Board publications are available by ordering directly from the board. They may also be obtained on a regular basis through organizational or individual supporting membership in the board; members or library subscribers are eligible for substantial discounts. For further information, write to the Transportation Research Board, National Academy of Sciences, 2101 Constitution Avenue, N.W., Washington, D.C. 20418.

Notice
The project that is the subject of this report was approved by the Governing Board of the National Research Council, whose members are drawn from the councils of the National Academy of Sciences, the National Academy of Engineering, and the Institute of Medicine. The members of the committee responsible for the report were chosen for their special competence and with regard for appropriate balance.

This report has been reviewed by a group other than the authors according to procedures approved by a Report Review Committee consisting of members of the National Academy of Sciences, the National Academy of Engineering, and the Institute of Medicine.

The views expressed in this report are those of the authors and do not necessarily reflect the view of the committee, the Transportation Research Board, the National Academy of Sciences, or the sponsors of the project.

Library of Congress Cataloging in Publication Data
National Research Council. Transportation Research Board.
Pavement surface properties and performance.

(Transportation research record; 633)
Includes bibliographical references.
1. Pavements–Design and construction–Addresses, essays, lectures. 2. Pavements–Evaluation–Addresses, essays, lectures. 3. Pavements–Testing–Addresses, essays, lectures. I. Title. II. Series.
TE7.H5 no. 633 [TE250] 380.5'08s [625.8]
ISBN 0-309-02659-8 78-2815

Sponsorship of the Papers in This Transportation Research Record

GROUP 2–DESIGN AND CONSTRUCTION OF TRANSPORTATION FACILITIES
Eldon J. Yoder, Purdue University, chairman

Pavement Design Section
Carl L. Monismith, University of California, Berkeley, chairman

Committee on Surface Properties-Vehicle Interaction
Don L. Ivey, Texas A&M University, chairman
Glenn G. Balmer, Frederick E. Behn, A. Y. Casanova III, Peter M. W. Elsenaar, Robert D. Ervin, Michael W. Fitzpatrick, Kenneth D. Hankins, Rudolph R. Hegmon, Kenneth J. Law, David C. Mahone, James A. Matthews, W. E. Meyer, Thomas H. Morrow, Jr., W. Grigg Mullen, Arthur H. Neill, Jr., Bayard E. Quinn, John J. Quinn, Hollis B. Rushing, Richard K. Shaffer, Elson B. Spangler, James C. Wambold, M. Lee Webster, E. A. Whitehurst, Ross G. Wilcox

Committee on Pavement Condition Evaluation
K. H. McGhee, Virginia Highway and Transportation Research Council, chairman
Frederick Roger Allen, Frederick E. Behn, Max P. Brokaw, Edwin J. Dudka, Karl H. Dunn, Asif Faiz, Wouter Gulden, Ralph C. G. Haas, R. G. Hicks, William H. Highter, W. Ronald Hudson, L. B. R. Hunter, David J. Lambiotte, J. W. Lyon, Jr., Alfred W. Maner, William A. Phang, Bayard E. Quinn, Freddy L. Roberts, Lawrence L. Smith, Elson B. Spangler, Robert J. Weaver, Loren M. Womack, Eldon J. Yoder

Lawrence F. Spaine, Transportation Research Board staff

Sponsorship is indicated by a footnote at the end of each report. The organizational units and officers and members are as of December 31, 1976.

Contents

Technique for Evaluating Hydroplaning Potential of Pavements

S. K. Agrawal and J. J. Henry, Department of Mechanical Engineering, Pennsylvania State University

Hydroplaning potential of pavement is defined as the inability of the accumulated water to escape from the tire-pavement contact area. The potential is measured in terms of the speed above which hydroplaning occurs; that is, the vehicle tires are lifted off the pavement and supported by a water wedge formed between tire surface and pavement. For the standardization of the measurement system, various test conditions and tires were investigated. An inflation pressure of 165 kPa (24 lb/in^2) and a vertical tire load of 2891 N (650 lbf) were chosen as the optimum parameters. The test results in a stationary trough show that the combination of the above test parameters and the ASTM designation E 524 tire gives very low values of friction force at 80.5 km/h (50 mph) when the water-film thickness is 1.27 mm (0.05 in). We also found that water films as thick as 1.3 mm (0.05 in) were obtained from the tester water when the water jet was delivered approximately 2 m (6.5 ft) ahead of the tire. Also, the tests on different pavements show that the hydroplaning potential of a pavement is determined by measuring the water-film thickness and the average texture depth.

When the water film on a pavement is of a certain thickness, vehicles may hydroplane; i.e., the tires may be separated from the pavement by the water wedge formed between the tire surface and the pavement surface. Total hydroplaning occurs when the fluid pressure forces (generated as a result of change in momentum of the fluid particles) in the water-wedge region exceed the total downward load on the tire.

Hydroplaning can be controlled by changing tire and pavement designs. Such changes, however, may adversely affect the performance of vehicles on dry pavements. The most logical approach is to prevent water accumulation on the pavement. Grooving the pavement and providing a course texture finish are effective in reducing the water-film buildup under the tire. The measures, however, lose effectiveness when depressions and ruts from which water cannot drain develop in the pavement. Such depressions can develop on heavily traveled, flexible pavements and pavements on which studded tires are extensively used. Regions of large temperature variations are also susceptible to the development of undulations in the pavements.

Measurement of the hydroplaning potential of pavements (of the inability of the accumulated water to escape from the tire-pavement contact area) affords a useful criterion for ranking the performance of the pavements. This measurement indicates the speed above which hydroplaning will occur if a specified water-film thickness exists on the pavement and if a set of other specified test parameters are used. Ideally, the method of measurement will permit extrapolation or interpolation to water-film thicknesses other than those of the test. The method is simple enough that minor modifications can be incorporated in the friction testers currently used for routine skid testing to convert the testers into hydroplaning-potential measuring systems. To engineer the method, one must have a knowledge of all the factors that both promote and inhibit hydroplaning.

The research culminating in these findings was divided into two phases. In the first phase the hydroplaning behavior of two tires, ASTM designation E 249 and designation E 524, was determined under various tire-inflation pressures, tire-vertical deflections, and water-film thicknesses in a stationary trough. In the second phase a mobile system for measuring potential hydroplaning was designed and demonstrated on various pavements having different textures.

PHASE I: TESTING IN THE STATIONARY TROUGH

Selection of Test Parameters

The selection of test parameters was done on a portion of pavement that is not yet open to public traffic. The pavement has a portland cement concrete (PCC) surface with nonuniform transverse burlap drag and an average texture height of 0.45 mm (0.0178 in) as measured by the sand-patch method. The test section has a longitudinal slope of 0.15 percent (0.045 m/30.48 m, 0.15 ft/100 ft) and a superelevation of 0.8 percent (0.24 m/30.48 m, 0.8 ft/100 ft) and provides sufficiently long approaches to accelerate and decelerate the test vehicle.

The inflation pressures selected were 124, 165, and 207 kPa (18, 24, and 30 lb/in^2). The vertical tire deflections selected were 12.7, 15.9, and 19.1 mm (0.5, 0.625, and 0.75 in). Those deflections correspond to vertical loads between 2607 and 4284 N (586 and 963 lb). The main consideration in selecting the above test parameters was to obtain a set of variables that would enable testing at speeds that could be obtained easily on public highways without endangering the other vehicles.

Experimental Procedure

A stationary trough was installed over an approximately straight section of the pavement surface. The trough was 61 m (200 ft) long and 0.56 m (22 in) wide (Figure 1). A 3.785-m^3 (1000-gal) truck provided the water for testing.

The locked-wheel mode of operation was selected rather than the spin-down method used by some researchers (1, 2). The choice was based on a few tests in both the modes. We observed that at lower water-film thicknesses, no distinct spin down occurred within the trough length at the speeds the tests were run. Also, we realized that the method to be used later for measuring hydroplaning potential should not require higher speeds.

The Pennsylvania Transportation Institute road friction tester (3) was used for the research. Brake force coefficient (BFC), the ratio of friction force to vertical load on tire when testing is done in the locked-wheel mode, and vehicle speed (measured with a fifth wheel) were automatically recorded. BFC is represented as 100 times the ratio. The vehicle speed was controlled within ±0.8 km/h (±0.5 mph) by an audio speed monitor (4). Water film as thick as 2.54 mm (0.1 in) was measured by the National Aeronautics and Space Administration (NASA) water level depth gauge, model ML-365, and water film thicker than 2.54 mm (0.1 in) was measured by a modified version of this gauge. In the modified version, the length of each of the tripod legs was increased by equal amounts by use of the brass caps that fit over the existing conical ends.

Results of Testing in the Stationary Trough

Theoretically, the friction force present at the tire-pavement interface during total hydroplaning should be zero. In practice, however, the friction force is not zero because of viscous and hydrodynamic drag present at the tire-pavement interface. To measure the hydroplaning speed, therefore, one must use either a direct method (record the speed when complete tire-pavement

Figure 1. Layout of test facility.

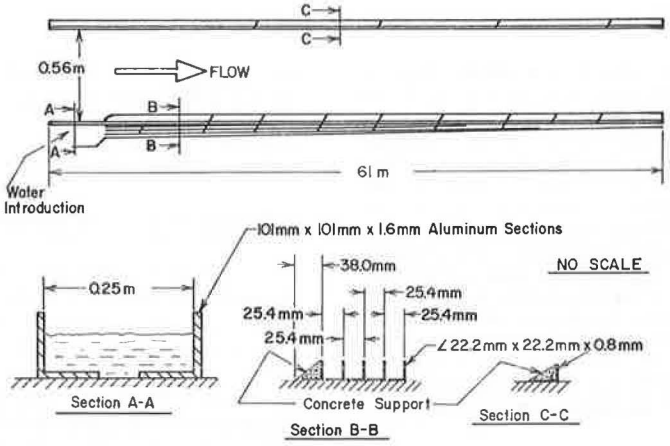

Figure 2. BFC versus vehicle speed at various water-film thicknesses.

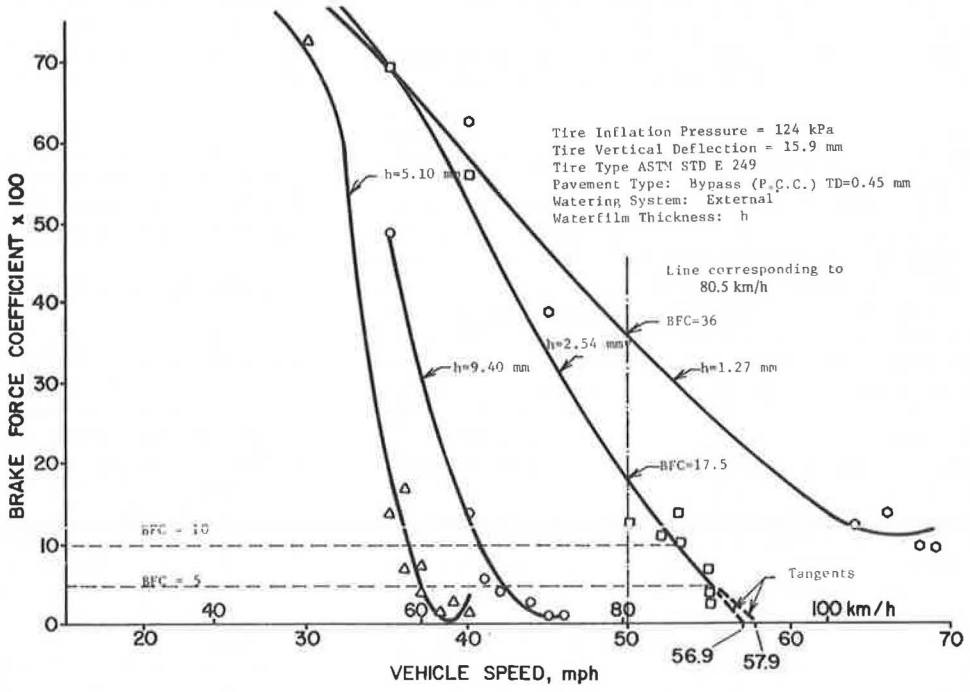

Table 1. Hydroplaning speed as a function of tire-inflation pressure, water-film thickness, and vertical tire deflection.

Tire Inflation Pressure (kPa)	Vertical Tire Deflection (mm)	Hydroplaning Speed (km/h)							
		h = 1.27 mm		h = 2.54 mm		h = 5.10 mm		h = 9.40 mm	
		BFC = 5	BFC = 10	BFC = 5	BFC = 10	BFC = 5	BFC = 10	BFC = 5	BFC = 10
124	12.7	107.4[a]	107.4	86.1	86.1	60.7	58.3	67.4	66.0
	15.9	113.5[b]	113.5[b]	93.2	91.6	61.0	60.4	70.5	77.1
	19.0	130.8	107.7	98.2	92.2	79.7	74.8	—[c]	—[c]
165	12.7	86.9	86.9	77.6	77.2	75.0	74.4	78.9	77.9
	15.9	96.7	95.1	85.8	86.7	71.0	71.1	77.9	77.9
	19.0	108.8	108.8	85.8	84.0	73.4	72.6	—[c]	—[c]
207	12.7	113.5	113.9	94.5	95.3	83.7	82.1	90.4	87.4
	15.9	105.9	105.9	95.8	95.9	81.0	80.5	87.5	80.5
	19.0	98.7	98.7	95.8	92.1	77.7	77.1	84.0	84.3

Note: h = water-film thickness; BFC = brake force coefficient; 1 mm = 0.04 in; 1 kPa = 0.145 lb/in^2; 1 km/h = 0.6 mph.

[a]Since the BFC = 5 line does not cross the polynomial, the hydroplaning speed corresponds to BFC = 10. [b]Obtained from graph. [c]Test data not available.

separation occurs) or some indirect method. The former is not practical because of the difficulties involved in the measurement of film thickness under the tire. Thus, an indirect method must be used to obtain a characteristic speed.

Various possibilities exist (5). In the present research, the hydroplaning speed is defined as the intercept of a tangent from a point on the BFC-speed curve with the speed axis (Figure 2). A third-order polynomial curve was fitted through the data. The tangents were drawn at the points corresponding to BFC = 5 and BFC = 10. We found that the two tangents gave nearly the same value of hydroplaning speeds (Table 1). Figure 3 shows the hydroplaning speed as a function of tire-inflation pressure. When the inflation pressure is reduced from 165 to 124 kPa (24 to 18 lb/in^2), higher hydroplaning speeds at 1.27 and 2.54-mm (0.05 and 0.1-in) film thickness may be due to a larger contact area at the lower inflation pressure or to a partial dry contact because of uneven water film under the tire or to both. When the film thickness increases, a well-accepted trend represented by the equation $V = 10.35\sqrt{P}$ is obtained (6). The hydroplaning speed is least sensitive to water-film thickness at 165-kPa (24-lb/in^2) inflation pressure and 12.7-mm (0.5-in) tire deflection.

The data can be plotted in an alternate way: BFC at 80.5 km/h (50 mph) as a function of water-film thickness (Figure 4). Here the BFC values are obtained from the individual curves between BFC and speed under various test conditions [Figure 2 shows that BFC = 17.5 at 124-kPa (18-lb/in^2) inflation and 15.9-mm ($^5/_8$-in) vertical deflection]. If the BFC-speed curve terminated before 80.5 km/h (50 mph) [h = 9.4 and 5.1 mm (0.37 and 0.2 in) in Figure 2], a zero was assumed as the value of BFC at that condition. The assumption is reasonable since the increase in BFC will probably start at a speed

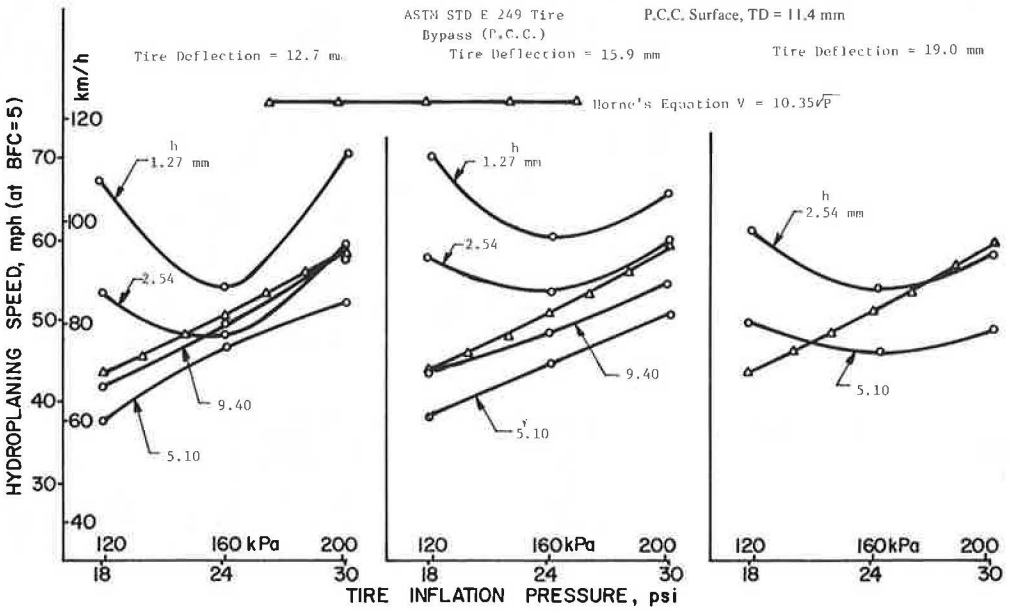

Figure 3. Hydroplaning speed as a function of tire-inflation pressure

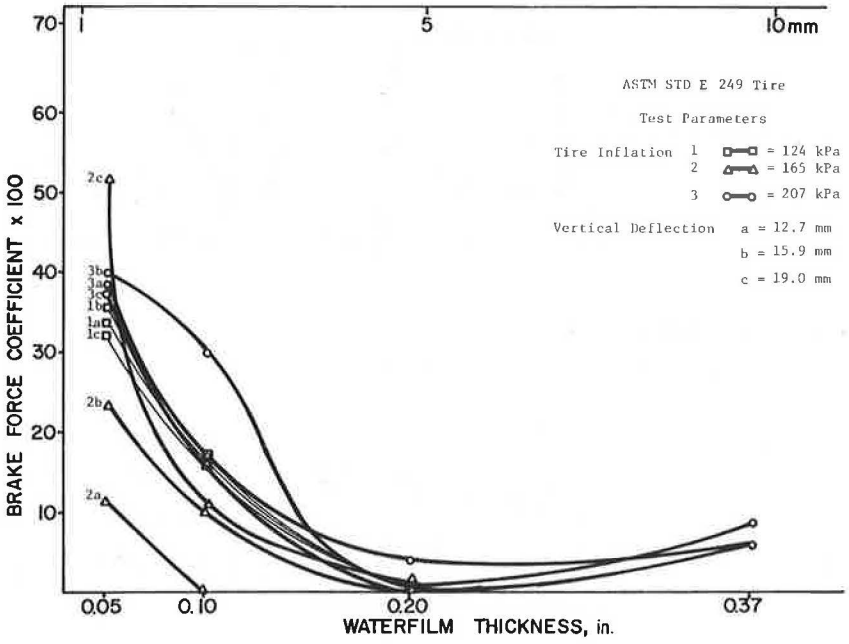

Figure 4. Effect of water-film thickness on friction characteristics of PCC surface (TD = 0.45 mm) at constant vehicle speed of 80.5 km/h.

much higher than 80.5 km/h (50 mph) when the viscous drag starts to play an important role. Figure 4 shows that, at 165-kPa (24-lb/in^2) inflation pressure and 12.7-mm (0.5-in) vertical deflection, a BFC range of 0 to 12 is obtained when the water-film thickness is 2.54 mm (0.1 in) or less.

Figure 5 shows the BFC-speed characteristics of the ASTM designation E 524 tire (smooth version of E 501 tire) at various tire-inflation pressures and vertical loads. The water-film thickness was kept constant at 1.27 mm (0.05 in). At 80.5 km/h (50 mph) the lowest values of BFC are obtained at 165 kPa (24 lb/in^2) at any vertical load. The above results indicate that the ASTM designation E 524 tire is the most likely candidate to be

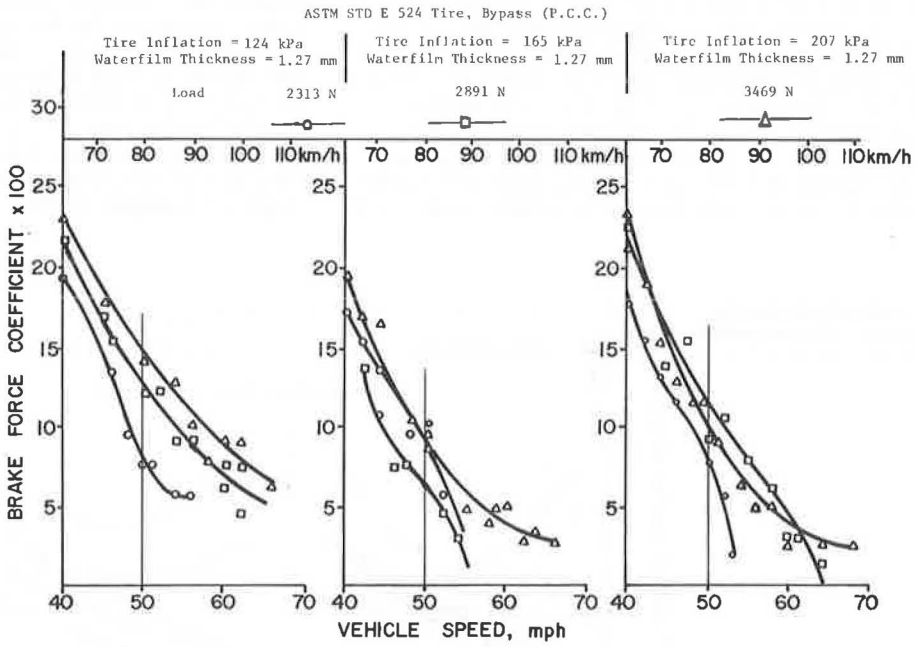

Figure 5. BFC versus vehicle speed at various inflation pressures and vertical loads.

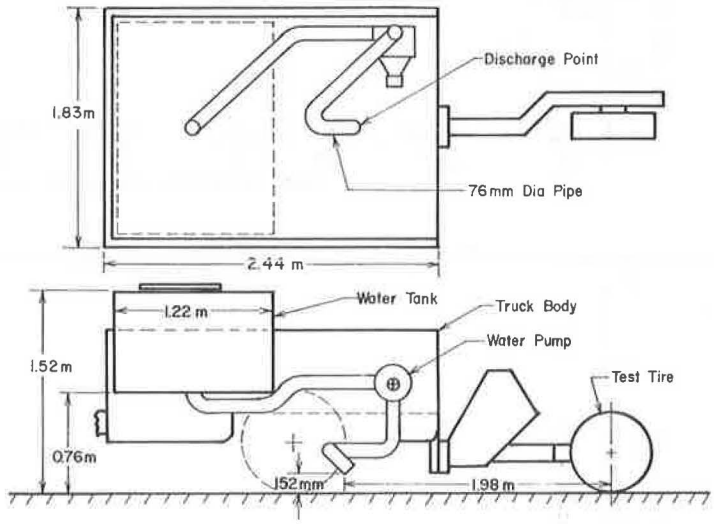

Figure 6. Schematic of water-delivery system.

Table 2. Description of surfaces at skid test facility.

Number	Name	Texture Depth (mm)	Description
1	Jennite	0.39	ID-2A surface treated with a first coat of Jennite (1963 m^2/m^3)
2	Sand epoxy	0.43	ID-2A surface treated with coal-tar-modified epoxy resin compound (736 m^2/m^3) and saturated with 20-40 flint-shot Ottawa sand
3	Concrete, burlap drag	0.29	Portland cement concrete (20.3 cm) reinforced and finished with light application of transverse burlap drag
4	ID-2A wearing course	0.76	Pennsylvania specification hot-mixed bituminous concrete, 5.5 percent asphalt concrete 2000 asphalt, Pennsylvania type A limestone aggregate consisting of 42 percent 1-B (close) graded coarse (12.7 mm max size) and 58 percent crushed stone fines

tested at an inflation pressure of 165 kPa (24 lb/in^2) and a vertical load of 2891 N (650 lb).

PHASE II: MEASURING SYSTEM FOR POTENTIAL MOBILE HYDROPLANING

Having selected the type of tire and the operating parameters, we directed our attention to finding a means for providing water films under the tire that were thick enough for hydroplaning. When a water pump rated up to 946-L/min (250-gal/min) flow at 96.6 km/h (60 mph) did not prove satisfactory (i.e., the pump did not reduce the values of the friction force compared to those obtained with a low-capacity water pump), we decided to

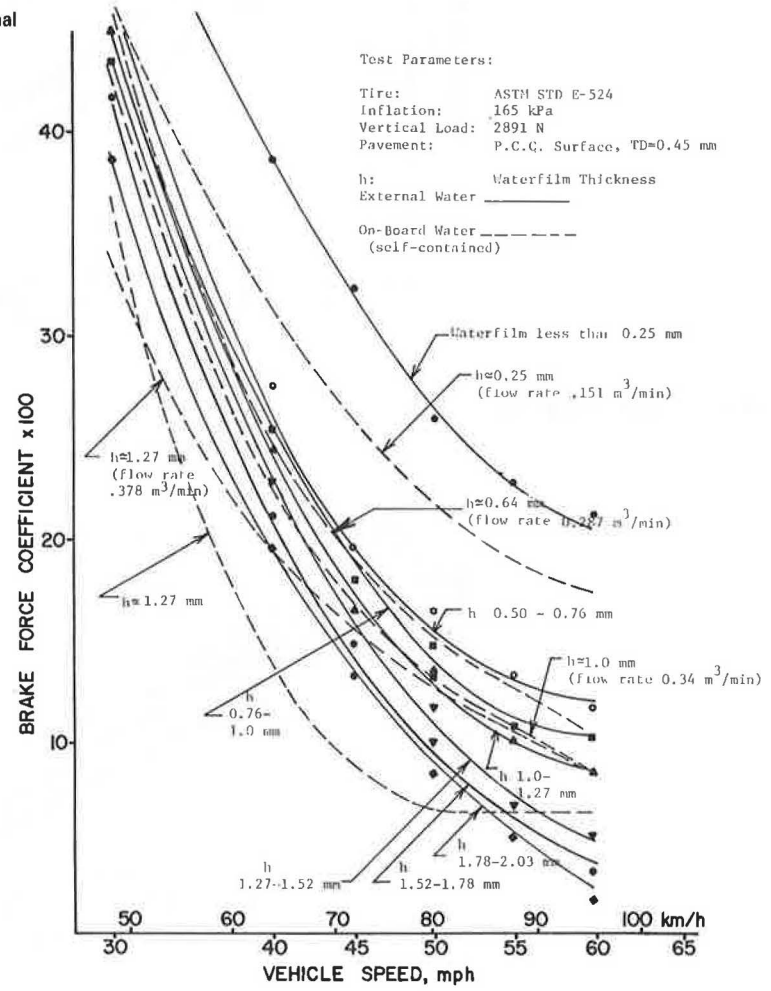

Figure 7. BFC versus vehicle speed with external and on-board watering systems.

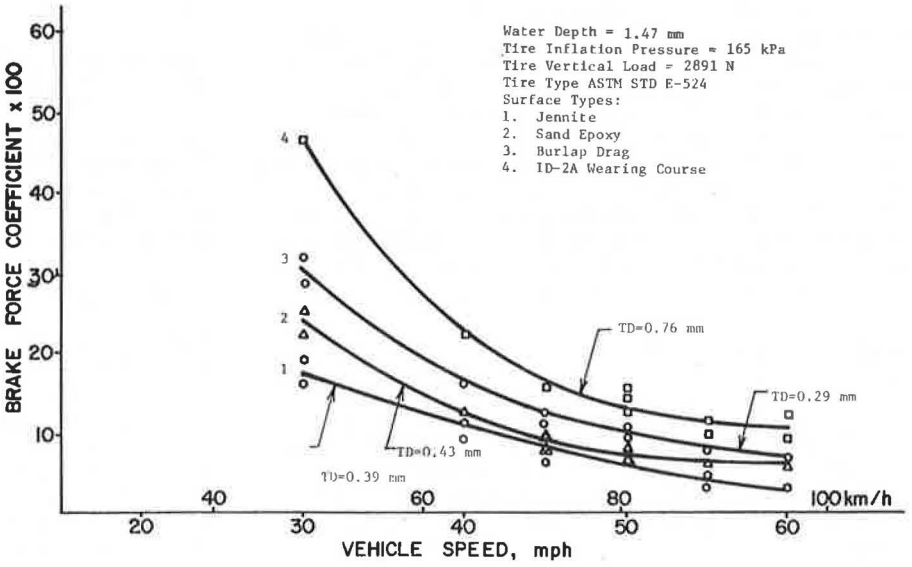

Figure 8. BFC versus vehicle speed for four pavement surfaces.

Figure 9. Hydroplaning speed versus water depth.

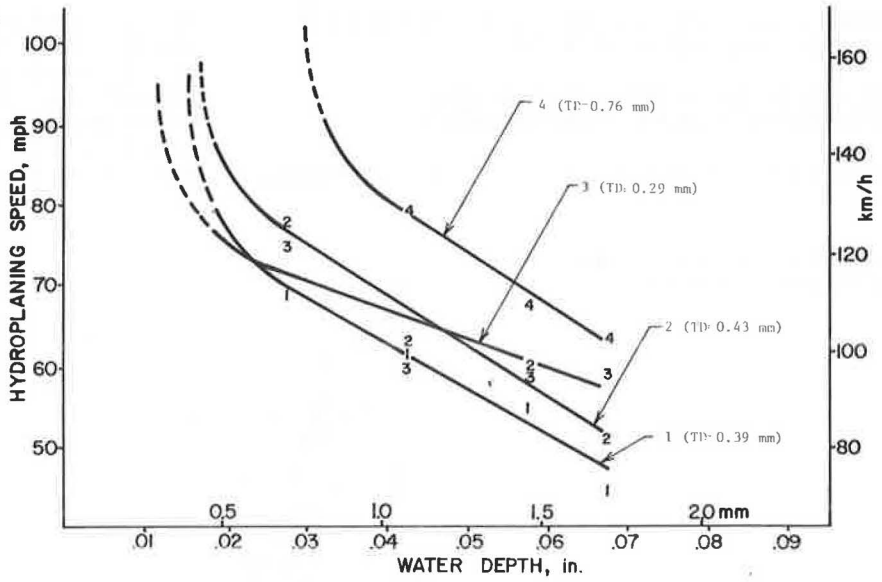

Figure 10. Hydroplaning speed versus water film thickness.

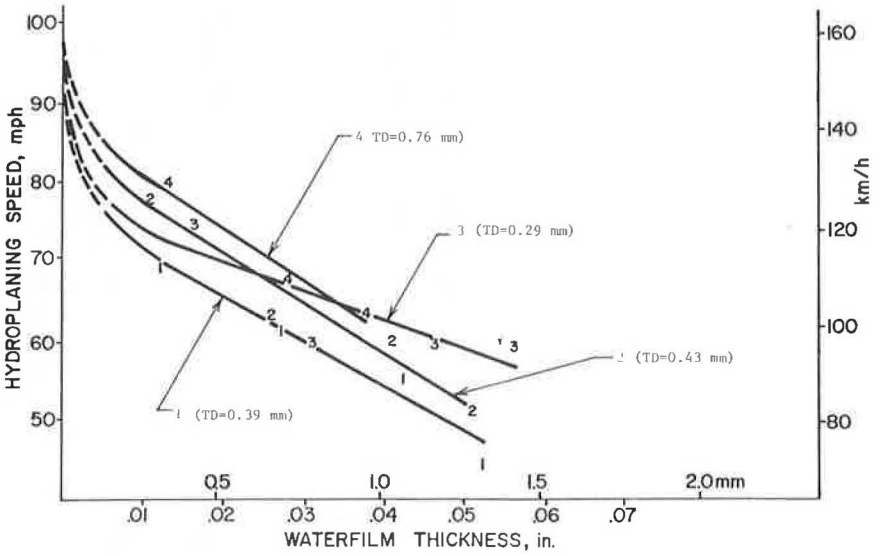

modify the water-delivery system. Tests were performed in which a variety of nozzle shapes and sizes were used. The water-delivery point ahead of the tire was also investigated. We found that delivering the water approximately 2 m (6.5 ft) ahead of the tire (Figure 6) provided a water-film thickness equivalent to 1.27 mm (0.05 in) obtained with externally supplied water on the trough. The above conclusion was based on a comparison of the test results (under similar conditions) on the trough with both external and on-board water. We also found that the flow rate was not excessive [378 L/min at 96.5 km/h (100 gal/min at 60 mph)].

Experimental Procedure

The modified water-delivery system was installed, and tests were performed at four different water-flow rates: 151 L/min at 64.4 km/h (40 gal/min at 40 mph), 288 L/min at 64.4 km/h (76 gal/min at 40 mph), 341 L/min at 64.4 km/h (90 gal/min at 40 mph), and 378 L/min at 64.4 km/h (100 gal/min at 40 mph). The flow rates were linear between 48.3 and 96.6 km/h (30 and 60 mph). The BFC and speed were recorded in each case.

Measurements of Hydroplaning Potential of Pavements

The tests were carried out on four test surfaces at the Pennsylvania Transportation Institute's skid test facility. Each test surface was 1.8 m (6 ft) wide and 61 m (200 ft) long. The four surfaces of the skid test facility are described in Table 2.

Results and Discussion

Figure 7 shows the BFC-speed relationship with both the external and the on-board watering systems. Film thicknesses in the external water tests (solid lines) were measured with the NASA depth gauge, although the equivalent film thicknesses in the on-board watering tests (dashed lines) were obtained by interpolation. The resulting film thicknesses are 0.25, 0.635, 1, and 1.27 mm (0.01, 0.025, 0.04, and 0.05 in). The corresponding flow rates are also shown in the figure.

Figure 8 shows the BFC-speed relationship on the different pavement textures. The mean effective water depth in the figure represents the water delivery per unit area and is equal to the sum of water-film thickness (measured with the NASA gauge) and the texture depth of the PCC surface where the comparison of on-board and of external watering systems was made. Similar curves were obtained for three other water depths. In each case, the data were fitted to a third-order polynomial. Texture depth of each pavement is also shown in the figure (texture depth was measured by the sand-patch method). From this figure, the hydroplaning speed was computed by use of the previously discussed method (tangents were drawn at BFC = 15 because the lower values of BFC were not attainable on all the pavements without exceeding legal speed limits).

Figure 9 shows the hydroplaning-speed and water-depth relationship obtained from the individual curves similar to those shown in Figure 8. Figure 10 shows the hydroplaning-speed and water-film-thickness relationship. This was obtained from Figure 9 by shifting the individual curves to start at zero water-film thickness; i.e., the texture depth was subtracted from the water depth. In both figures, the straight portions of the curves represent the least square fit to the data. The dashed lines are drawn on the assumption that very high hydroplaning speeds result when the water depth approaches the texture depth (water-film thickness approaches zero).

Figure 10 illustrates that the slope of the hydroplaning-speed and water-film-thickness curve for the rigid pavement (PCC surface 3) is larger than that for the flexible pavements (asphalt pavements with overlays 1, 2, and 4). Because only one rigid pavement was used, more data are required to determine if the two kinds of pavements can be grouped separately according to their hydroplaning potential. To determine the hydroplaning speed from these curves, one needs to know the water-film thickness, texture depth, and type of pavement. All the data presented here were gathered with the smooth tire (ASTM designation E 524). Under similar conditions, any other tire would probably hydroplane at a higher speed. Further testing at higher water-film thicknesses is desirable to determine the point (on the hydroplaning and water-film-thickness curve) at which the effect of pavement texture is insignificant.

CONCLUSIONS

1. The ASTM designation E 524 tire, tested under 165-kPa (24-lb/in^2) inflation pressure and 2891-N (650-lb) vertical load on the PCC surface having a water-film thickness of 1.27 mm (0.05 in), developed the lowest values of the brake force coefficient. The test conditions provided a suitable combination to be used in the second phase of testing.
2. The standard skid tester (conforming to ASTM method E 274) can be modified to deliver an equivalent water depth of up to 1.78 mm (0.07 in) by delivering the water jet about 2 m (6.5 ft) ahead of the tire. The water flow must also be increased.
3. The speed above which hydroplaning will occur (hydroplaning potential) on pavements having different texture depths can be determined from the hydroplaning speed versus water-depth curves by measuring the water film present and the average texture depth of the pavement.
4. The hydroplaning potential of the rigid pavements (PCC surfaces) and of the flexible pavements can be grouped separately according to the slopes of the hydroplaning-speed-equivalent and water-film-thickness curves.

ACKNOWLEDGMENTS

This research was sponsored by the Pennsylvania Department of Transportation in cooperation with the Federal Highway Administration. The progress of the research was aided by valuable suggestions from W. E. Meyer of the Pennsylvania Transportation Institute. The contents of this paper are ours and do not necessarily reflect the views of the sponsoring agencies.

REFERENCES

1. I. R. Ehrlich, A. R. Shaefer, and G. A. Wray. Parameters Affecting Model-Tire Hydroplaning and Rolling Restoration. Davidson Laboratory, Stevens Institute of Technology, Hoboken, N.J., Rept. SIT-DL-20-1405, March 1970.
2. A. J. Stocker, J. T. Dotson, and D. L. Ivey. Automobile Tire Hydroplaning—A Study of Wheel Spin-Down and Other Variables. Texas Transportation Institute, Research Rept. 147-3F, Aug. 1974.
3. S. K. Agrawal and J. D. Decker. PTI Mark II Road Friction Tester. Pennsylvania Transportation Institute, Pennsylvania State Univ., in preparation.
4. W. E. Meyer, R. R. Hegmon, and T. D. Gillespie. Locked-Wheel Skid Tester Correlation and Calibration Techniques. NCHRP, Rept. 151, 1974, 100 p.
5. S. K. Agrawal, W. E. Meyer, and J. J. Henry. Measurement of Hydroplaning Potential. Pennsylvania Transportation Institute, Pennsylvania State Univ., Final Rept., Feb. 1977.
6. W. B. Horne and R. C. Dreher. Phenomena of Pneumatic Tire Hydroplaning. National Aeronautics and Space Administration, Technical Note TD D-2056, Nov. 1963.

Publication of this paper sponsored by Committee on Surface Properties-Vehicle Interaction.

Effects of Pavement Grooving on Friction, Braking, and Vehicle Control

J. E. Martinez, Texas Transportation Institute, Texas A&M University

Pavement grooving is a technique by which longitudinal or transverse cuts are introduced on a surface to increase skid resistance and reduce the number of wet-weather accidents. The objective of the research was to determine the effect of pavement grooving on motorist safety by studying the effects of grooving on friction, braking, and vehicle control by computer simulation and full-scale testing. Vehicles considered were automobiles, motorcycles, and automobile and towed-vehicle combinations. The computer simulation was developed by obtaining test data for a variety of conditions and performing a regression analysis of the data. The result was a set of equations that were incorporated into vehicle-handling models that predicted vehicle response due to the grooves. The motorcycle rider detected a perceptible difference between worn and unworn grooving. The effect of grooving on motorcycle response could not be detected by electronic instruments that measured steering angle and torque. No significant difference was found for various grooving geometries. Electronic instrumentation could not detect the effects of grooving on a typical small automobile and towed-vehicle combination at different speeds for various trailer and tongue loads. Based on computer simulation, the effect of grooving is more beneficial for low-friction than for high-friction pavement; also, grooves provide a noticeable increase in the directional stability of a vehicle.

Pavement grooving is becoming a widely accepted means of improving the stability of vehicles on pavements. Grooving is primarily longitudinal on highways in the United States and transverse on aircraft runways and in other countries. For a given pattern, various dimensions of the groove width, depth, and spacing have been studied; however, an optimum pattern has not been accepted. Most studies of highway grooving have relied on measurements on in-service roadways. Factors such as skid numbers, texture or surface wear, and accident rates were investigated before and after grooving. To a limited extent, driver response and vehicle behavior were monitored, primarily by public response.

When grooves were first introduced, motorcyclists filed a large number of complaints with the state highway departments and motorcycle magazines (1). The riders claimed that the grooved pavements produced uncomfortable and hazardous riding. Experience has shown that the effect of grooving on motorcycles varies with the width of the grooves. Farnsworth states that 6.4-mm (0.25-in) wide grooves generated complaints from motorcyclists and drivers of small automobiles and that 3.2-mm (0.125-in) wide grooves still brought complaints, though fewer, from motorcyclists (1, 2). In addition, narrower grooves were just as effective in controlling skids as wider grooves.

This paper presents the findings of a study that involved laboratory and full-scale tests in which various groove geometries and pavements were used and the effects of slip, camber and approach angles, normal load, tire geometry, pavement, speed, groove geometry, and wet or dry conditions were considered. The data were collected by using the Texas Transportation Institute (TTI) low-speed tire tester and the Highway Safety Research Institute (HSRI) mobile tire tester.

The direct advantage of grooved pavement under rainfall conditions in producing large values of lateral friction and the indirect advantage in reducing accidents are thoroughly documented. Therefore, this study placed primary emphasis on the determination of vehicle handling or stability problems on dry pavements. The wet-pavement data were obtained only because the process for doing so was readily available. Consequently, a wet pavement merely refers to a pavement with a particular skid number as obtained by the HSRI tester; the truck-borne water systems produced low friction levels but not low enough to be consistent with rain-wetted surfaces (3, 4).

Free-rolling and braking data were taken with the two machines. The data were next used as input to a regression model that produced a functional relation for the grooved side or circumferential force in terms of the variables mentioned previously. These representations for the free-rolling and braking cases were next integrated with computer programs for the handling of automobiles, motorcycles, and towed vehicles.

A regression analysis resulted in a model that produced results consistent with data found in the literature. The trends were quite realistic.

Full-scale tests were performed with an instrumented motorcycle and a small automobile and towed-vehicle combination. The results of the motorcycle study are presented in this paper, and the results of the automobile and towed-vehicle study are presented in another report (5).

The conclusions presented are based on contact with leading researchers in the field, on evaluation of grooved pavements by automobile drivers and motorcyclists, and on laboratory, full-scale test data, and computer simulation.

EXPERIMENTAL APPROACH

The degree of slip, camber, and approach angles of tires that were considered in the tests are given below.

Vehicle	Slip	Camber	Approach
Automobile	4	0	-10
	8	5	0
	16	10	10
			45
			90
Trailer	4	0	—
	8	5	—
	16	10	—
Motorcycle	0	0	-10
	6	20	0
		40	10
			45
			90

The load values in newtons (1 N = 0.225 lbf) of the tires that were considered are given below.

Automobile	Trailer	Motorcycle
2891.3	1779.0	889.6
4003.3	2891.3	1779.0
6227.5	4003.3	
	6227.5	

Types of tires considered are given in Table 1. The effect of various tires was accounted for through the use of $(\mu_y)_{max}$ and $(\mu_x)_{max}$ [i.e., the ratio of the peak side (free-rolling) or circumferential (braking) force to the normal load] and

through the use of a tire cornering or camber coefficient. The tire coefficient was computed as the slope of the side force versus slip angle (for automobile and trailer tires) or camber angle (for motorcycle tires) at zero slip angle divided by the normal load for free-rolling cases and as the slope of the braking force versus percentage of slip at zero slip angle divided by load for the braking cases.

The groove width, depth, and spacing in millimeters (1 mm = 0.039 in) that were used in the tests are given below.

Test	Width	Depth	Spacing
Laboratory	2.8	3.2	19.0
	3.2	6.4	25.4
	5.6	9.5	38.0
Full scale	2.8	3.2	19.0
			25.4

The tester operated at a speed of 3.62 km/h (2.25 mph) in the laboratory tests and at speeds of 32.2 and 64.4 km/h (20 and 40 mph) in the full-scale tests.

The effect of the various pavements was accounted for through the use of the locked-wheel skid number obtained with the Goodyear custom power cushion tire in the full-scale tests and with the ASTM E-249 tire in the laboratory tests.

In the full-scale tests, longitudinal grooves were cut in two straight sections of portland cement concrete (PCC) and two curved sections of asphaltic concrete (AC) as follows (1 m = 3.3 ft and 1 mm = 0.039 in):

Type	Dimension (m)	Curvature Radius (m)	Groove (mm)
Straight, PCC	48.8 x 11	–	2.8 x 3.2 x 25.4
Straight, AC	48.8 x 7.3	–	2.8 x 3.2 x 25.4
Straight, PCC and AC	91.4 x 6.7	106.7	2.8 x 3.2 x 19

In the laboratory tests, grooves were cut in PCC and AC slabs approximately 1.8 m × 61 cm × 5 cm (6 ft × 2 ft × 2 in). The grooves were cut longitudinally, transversely, and at skewed angles of -10, 10, and 45° as follows:

2.8 × 3.2 × 25.4 mm,
2.8 × 3.2 × 19 mm,
3.2 × 3.2 × 19 mm,
3.2 × 3.2 × 25.4 mm, and
5.6 × 6.4 × 38 mm.

FULL-SCALE TESTING

A preliminary motorcycle test at the TTI Research Annex on the grooved pavements determined the rider's evaluation of the grooving. An uninstrumented 1974 Yamaha RD 350 motorcycle was used that had a standard ribbed Dunlop front tire and a Dunlop K-87 rear tire.

Table 1. Types of tires used in tests.

Vehicle	Manufacturer	Size	Rated Load (N)	Pressure (kPa)
Automobile	Goodyear custom power cushion	8.25×14	7206.1	220.6
	ASTM E-249	7.50×14	4826.3	165.5
	Goodyear custom G8	5.60×15	4314.8	220.6
Motorcycle	Trials knobby	3.50×18	–	–
	Dunlop Gold Seal F7	3.00×18	–	–
	Dunlop K-95	3.50×18	–	–
Small trailer	Goodyear super rib	4.80×4.00×18	–	–

Note: 1 N = 0.225 lbf; 1 kPa = 0.145 lbf/in².

Three riders were selected. One was a highly skilled professional who had considerable experience; one was an average rider who had approximately 2 years of experience on dirt and street riding; and one was an inexperienced rider, the principal investigator of the research project, who had less than 1 year of experience on street riding only.

The inexperienced and average riders rode over the grooved surfaces at speeds up to 112.6 km/h (70 mph); however, the highly skilled rider was allowed to ride at speeds exceeding 112.6 km/h (70 mph). Most of the riding was done on an 18-deg curve paved with PCC. The maneuvers consisted of in-lane and lane-change travel. The three riders agreed that at speeds below 80.5 km/h (50 mph) there was no noticeable effect on the handling. At speeds above 80.5 km/h (50 mph), but below 96.5 km/h (60 mph), a slight wobble was detected when no attempt was made to follow the grooves. This wobble disappeared, however, when an effort was made to follow the grooves. The consensus of the riders was that a perceptible wobble was present at speeds between 96.5 and 112.6 km/h (60 and 70 mph) when the grooves were not followed, but only a slight wobble was evident when the grooves were followed. At speeds exceeding 112.6 km/h (70 mph), the skilled rider reported a feeling of hazardousness when he did not try to follow the grooves and a feeling of uneasiness when he did try.

This first series of tests was performed on a curved pavement section that had newly cut grooves. Another series of tests was done on a straight pavement section that had worn grooves. That section was 6.4 km (4 miles) of the eastbound and westbound lanes of Loop 410 in San Antonio between the Blanco Road exit on the east and the Fredericksburg exit on the west. The inexperienced rider and the motorcycle were the same as those involved in the first tests. A TTI vehicle equipped with a motion picture camera followed the motorcycle to photograph any wobble that might be caused by the grooved pavement.

Runs with speeds well exceeding 88.5 km/h (55 mph) were made when safe traffic conditions were present, and the motion picture showed no wobble. The rider felt only a slight vibration through the seat at the high speed, but not at the low speed whether he followed the grooves or changed lanes.

The test motorcycle was then equipped with new Trials Universal (semiknobby) tires, commonly used on dual-purpose motorcycles for riding on streets and dirt roads. When no attempt was made to follow the grooves, the rider felt a slight wobble at speeds of 88.5 km/h (55 mph) and an uneasy feeling at 105 km/h (65 mph). The rider had not previously ridden on semiknobby tires, which do not handle the same way as street tires do.

In later tests with worn semiknobby tires, the rider could reach speeds above 105 km/h (65 mph) before he felt uneasy. The reason may partially be that he had become accustomed to semiknobby tires.

The motorcycle, equipped with both street and semiknobby tires, was also ridden on pavement with a metal tine texture, which is sometimes mistaken for a grooved texture. The rider felt more uncomfortable on the tine surface than on the grooved surface. The motorcycle tended to drift, even at speeds below 88.5 km/h (55 mph), and tended to drift even more and slightly wobble at higher speeds. In some instances, the motorcycle tended to follow the wavy pattern of the metal tine texture, and perhaps some tire-groove interlock took place. In other instances, the motorcycle tended to drift across the lane of travel. In a strong crosswind and heavy traffic, riding a motorcycle on metal tine texture could be hazardous.

Motorcycle testing was also conducted on an 0.8-km (0.5-mile) grooved portion of I-45 in Navarro County near

Angus, Texas. Several runs made with and without a steering damper produced no disturbing effects at speeds below 88.5 km/h (55 mph). Wobble seemed to increase with speed when no steering damper was used. The wobble continued until the speed was reduced to approximately 80.5 km/h (50 mph). The wobble did not occur immediately at any speed but seemed to take approximately 30.5 to 61 m (100 to 200 ft) to develop depending on the speed.

The runs made in Navarro County indicated that pavement grooving affects motorcycle handling, and the effect depends on the physical properties of the motorcycle. In the opinion of the test rider, the wobble is not hazardous, except perhaps to someone who is inexperienced. (Many other motorcyclists, however, do not agree with this opinion.) The rider felt that the longer distance gave the disturbance more time to become evident and that significant differences were experienced between ungrooved pavements.

A roadway disturbance analysis was conducted in Navarro County. The full-scale test data included motorcycle steering torque and steering angle time histories over the segment of grooved pavement. The test speeds varied from 64.4 to 120.7 km/h (40 to 75 mph). Data from the angle and torque transducers were telemetered to a mobile base station where the data were recorded on FM analog magnetic tape and simultaneously displayed on visicorder paper. Unfortunately, inspection of raw signals for grooved pavement showed no startling differences from those of ungrooved pavement, although the driver experienced a perceptible difference. These signals were used as input to a motorcycle-handling computer program (6).

Figure 1. Lateral velocity in HVOSM computer simulation.

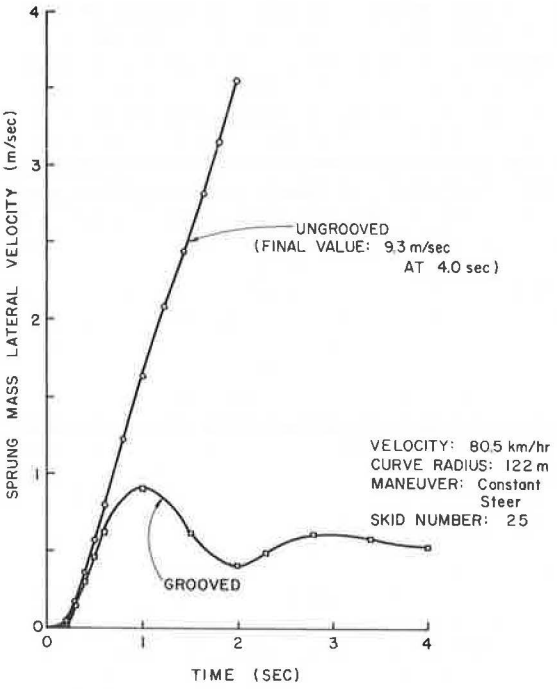

Figure 2. Lateral acceleration in HVOSM computer simulation.

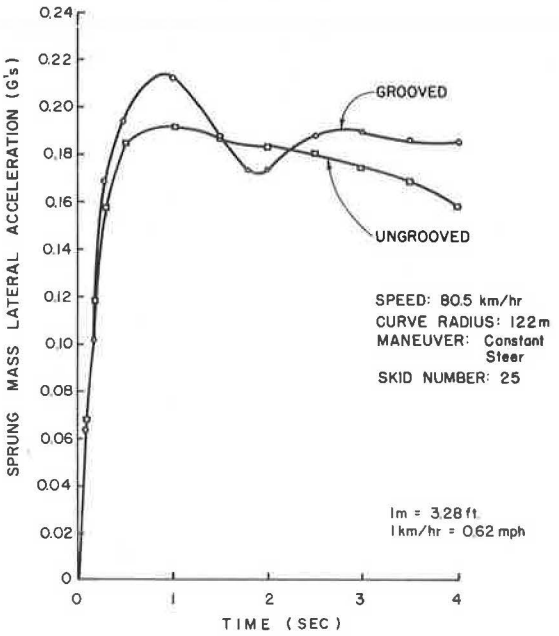

Figure 3. Yaw rate in HVOSM computer simulation.

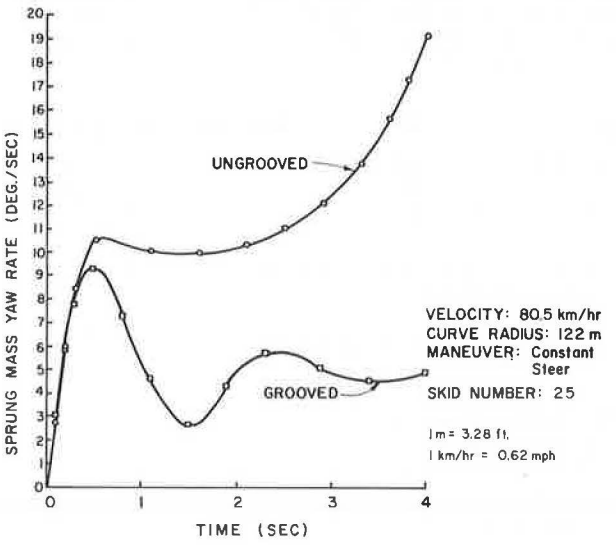

Figure 4. Yaw angle in HVOSM computer simulation.

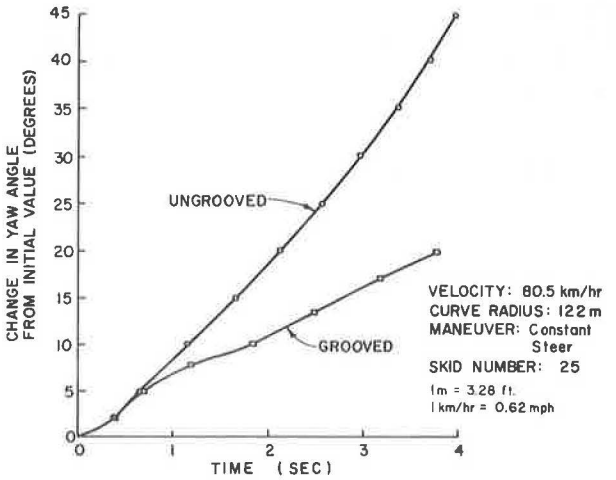

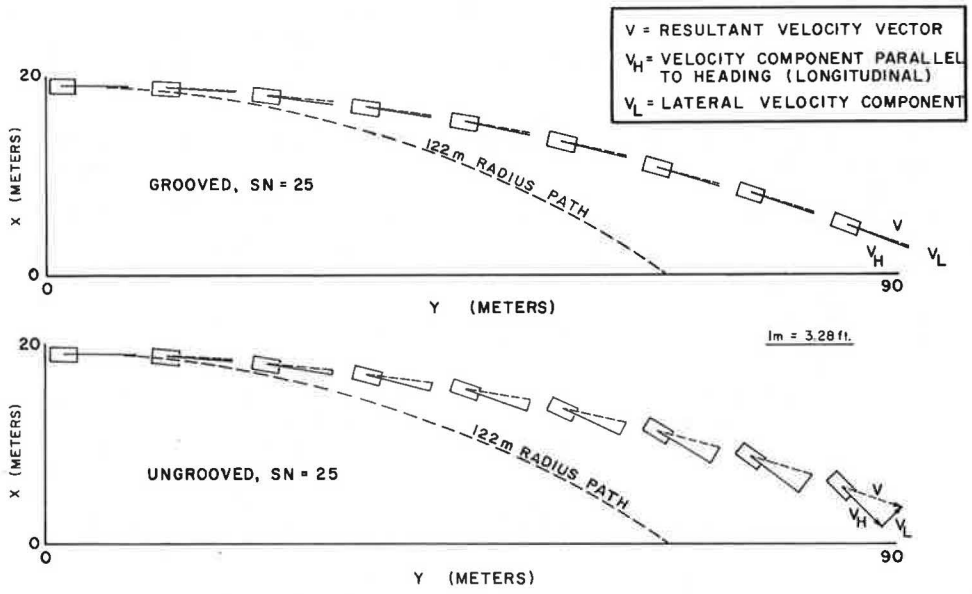

Figure 5. Constant steer maneuver at 80.5 km/h (50 mph) on low-friction pavement in HVOSM simulation.

THEORETICAL APPROACH

A regression analysis was performed on the data, and equations were developed to describe the effects of the pavement grooving. The equations considered the effect of the following parameters: side force and circumferential force for smooth pavement, side-slip angle, camber angle, grooving approach angle, normal load, groove width, groove depth, groove spacing, pavement, tire, circumferential slip, and velocity. The two equations that were developed for automobile tires considered free-rolling and braking effects, and the one equation that was developed for motorcycle tires considered only free-rolling effects.

The computer simulation was carried out by using three distinct vehicle-handling computer models: a highway-vehicle-object simulation model (HVOSM) (7), a motorcycle-handling model developed by CALSPAN Corporation (6), and a model for articulated vehicles developed by HSRI (8). These models incorporated the results of the regression analysis.

DISCUSSION OF RESULTS

The results obtained by the HSRI computer simulation of an articulated vehicle in free-rolling and braking conditions on both grooved and smooth (ungrooved) pavements closely match results obtained by HSRI in tests in which a new B.F. Goodrich Silvertown belted 8.25 × 14 tire inflated to 165.5 kPa (24 lbf/in^2) was driven on a smooth TTI test pad (9). The computer runs were made for a 1636.5-kg (3600-lb) vehicle towing a 954.6-kg (2100-lb) trailer at 48.3 km/h (30 mph) on dry, grooved concrete pavement. Results from 12 computer runs show that the smooth and grooved roads do not differ significantly (5).

The results of the motorcycle study were inconclusive. The model simulated a motorcycle following the line of the roadway on a section of grooved pavement. Steering torque data were obtained in full-scale tests by a torque sensor located between the handlebars and front fork of the test motorcycle. The data were digitized and used as a disturbance input to the motorcycle computer simulation. The steer angle was also recorded and used in comparisons. The front and rear tire side forces resulting from the disturbance were modified by using the grooving function.

Since steer angle was the only parameter that could be used in comparisons, no firm conclusions could be reached on how well the simulation results compare with full-scale test results. The agreement between simulated and experimental steer responses was not close. No oscillations of the motorcycle that could be termed weave or wobble were noted either in the simulated or experimental steering time histories. One conclusion that can be reached is that pavement grooving has little effect on motorcycle response under the conditions studied.

Several computer runs made with HVOSM considered different pavements (SN = 75 and SN = 25) and constant steer maneuvers for a medium-weight vehicle traveling on a 122-m (400-ft) radius curve at 80.5 km/h (50 mph). Grooving caused a slight increase in lateral force on the high-friction pavement and had a significantly beneficial effect on the low-friction pavement. Figures 1 through 5 show that the vehicle is considerably more stable on the grooved pavement than on the ungrooved pavement. The vehicle attains its maximum available lateral force on all four tires during the 4-s maneuver on the ungrooved pavement; only the front two tires saturate on the grooved pavement. Figures 1 and 5 indicate that the grooves provide vehicle directional control as evidenced by the small lateral velocity component. Figure 2 shows that lateral acceleration is dependent on steer input on grooved pavements and indepdendent of steer input on ungrooved pavements. Figure 3 shows that the oscillations in yaw rates seem to decay to a steady-state value on grooved pavements and diverge rapidly after 2 s on ungrooved pavements. Figure 4 shows that the yaw angle is larger on ungrooved pavements than on grooved pavements and continues to increase throughout the simulation. These results seem to indicate that the beneficial effects of pavement grooving are greater for the low-friction pavements. However, the results at the low skid number represent an extrapolation of measured data.

CONCLUSIONS

Pavement grooving helps to drain pavements, provides directional stability, and consequently reduces the number of accidents during wet-weather periods. However, some motorcyclists have expressed concern about riding on grooved pavements. This study could find no detrimental effects of pavement grooving on motorcycle

handling. At high speed, the motorcycle rider did have an insecure feeling because of the presence of the grooved pavement. The testing, theoretical hypotheses, and riding experiments suggest that the tire-groove interaction does excite certain resonant frequencies in motorcycles; the effect is so subtle as to be almost undetectable except at very high speeds or for a poorly damped motorcycle.

The results of the HSRI computer simulation of the articulated vehicle did not show much difference between the smooth and grooved pavements. The braking results revealed that slightly higher friction is available on grooved than on smooth pavements. The full-scale testing of the instrumented automobile-trailer combination revealed that the effects of the grooving could not be detected by the instrumentation used.

The study showed that variations in the groove dimensions and approach angle do not produce a significant difference between grooved and ungrooved pavement.

Specific conclusions drawn are given below, some of which are based on analyses contained in another report (5).

Motorcycle

Rider Evaluation

1. Worn grooves are not so evident to the rider as are unworn or newly cut grooves.
2. Grooves have no detrimental effects at speeds no higher than 88.5 km/h (55 mph).
3. At speeds approaching 112.6 km/h (70 mph), the rider experiences a perceptible wobble (side-to-side, front-wheel movement) when he does not follow the grooves and only a slight wobble when he does.
4. The effect of the grooves does not occur immediately and is more evident when the testing is performed over a 0.8-km (0.5-mile) length of pavement.
5. The effect of a steering damper on the response of the motorcycle to the grooves could not be clearly detected.
6. The effect of grooves on motorcycle response is more noticeable for knobby tires than for factory-equipped, street tires.
7. Riding over transverse grooves (perpendicular to approach direction) does not produce undesirable effects.
8. Lowering the tire-inflation pressure by 68.9 kPa (10 lb/in^2) from the recommended pressure does not affect the motorcycle response on grooves.
9. A more noticeable disturbance is produced on steel-time, longitudinally textured pavement than on grooved pavements.
10. Pavement grooving cannot be considered hazardous for speeds under 112.6 km/h (70 mph) except perhaps to the most inexperienced rider.

Electronic Instrumentation and Computer Simulation

1. The effects of pavement grooving cannot be detected.
2. Motorcycle response is almost the same on grooved and smooth pavements.
3. No motorcycle oscillations that could be termed weave or wobble were noted.

Small Automobile and Towed-Vehicle Combination

1. Based on instrumented full-scale testing, the effects of grooving cannot be detected at different speeds for various trailer and tongue loads.
2. Based on driver evaluation, a slight vibration occurs in the steering wheel at a speed of 80.5 km/h (50 mph) even though the system remains extremely stable.
3. Based on full-scale testing and driver evaluation, pavement grooving is not detrimental.
4. Based on computer simulation in which grooving function resulting from single-tire test data is used, no significant difference is observed for cornering maneuvers on smooth and grooved pavements.

Automobile (HVOSM Simulation)

1. In a braking situation, grooving is quite beneficial at higher speeds (data were only collected at skid numbers of 60 and above).
2. In a free-rolling situation, grooving is more beneficial on the low-friction pavements (Figure 4), the effect of the grooving approach angle (angle between wheel velocity vector and the grooves) is minor, and the side forces are larger on grooved than on smooth pavement.
3. At 80.5 km/h (50 mph) on a 122-m (400-ft) radius curve, grooves have a slightly beneficial effect for a constant steer maneuver on a high-friction pavement (SN = 75) and significant beneficial effect for a turning maneuver on a low-friction pavement (SN = 25).

ACKNOWLEDGMENTS

This study was conducted by the Texas Transportation Institute and sponsored by the Federal Highway Administration, U.S. Department of Transportation. I wish to express my appreciation to R. R. Hegmon, contract manager, for his guidance and helpful advice during the course of the study. His continual interest assured the successful execution of the objectives of the research. The opinions, findings, and conclusions expressed in this paper are mine and not necessarily those of the sponsor.

REFERENCES

1. E. Farnsworth and D. Johnson. Reduction of Wet Pavement Accidents on Metropolitan Freeways. SAE, Rept. 710574, June 1971.
2. R. J. Rasmussen. Pavement Surface Texture and Restoration for Highway Safety. Paper presented at the 53rd Annual Meeting, HRB, 1974.
3. B. M. Gallaway and J. G. Rose. Macro-Texture, Friction, Cross Slope and Wheel Track Depression Measurements on 41 Typical Texas Highway Pavements. Texas Transportation Institute, Texas A&M Univ., College Station, Research Rept. 138-2, June 1970.
4. D. L. Ivey, H. E. Ross, G. G. Hayes, R. D. Young, and J. C. Glennon. Side Friction Factors Used in the Design of Highway Curves. Texas A&M Research Foundation, Texas Transportation Institute, College Station, Final Rept. 628-2, revised June 1971; NCHRP, Project 20-7.
5. J. E. Martinez. Effects of Pavement Grooving on Friction, Braking and Vehicle Control. Texas Transportation Institute, Texas A&M Univ., College Station, Final Rept., Aug. 1976.
6. R. Roland. Simulation Study of Motorcycle Stability at High Speed. Second International Congress on Automotive Safety, San Francisco, Paper 73020, July 1973.
7. R. R. McHenry and N. J. Deleys. Automobile Dynamics: A Computer Simulation of Three-

Dimensional Motions for Use in Studies of Braking Systems and of the Driving Task. CALSPAN Corp., Buffalo, CAL Rept. VJ-2251-V-7, Aug. 1970.
8. J. E. Bernard and others. A Computer Based Mathematical Method for Predicting the Directional Response of Trucks and Tractor-Trailers. Highway Safety Research Institute, Univ. of Michigan, Ann Arbor, Technical Rept. UM-HSRI-PF-73-1, June 1973.
9. J. E. Bernard and others. Vehicle in Use Limit Performance and Tire Factors: The Tire in Use. Highway Safety Research Institute, Univ. of Michigan, Ann Arbor, Rept. DOT-HS-801-439, March 1975.

Publication of this paper sponsored by Committee on Surface Properties-Vehicle Interaction.

Notice: The Transportation Research Board does not endorse products or manufacturers. Trade and manufacturers' names appear in this report because they are considered essential to its object.

Photographic Technique for Estimating Skid Number and Speed Gradients of Pavements

L. Bruce McDonald,* Allen Corporation, Alexandria, Virginia
Robert R. Blackburn, Midwest Research Institute, Kansas City, Missouri
Donald R. Kobett,* Black and Veatch Engineers, Kansas City, Missouri

A technique has been developed for determining skid number and speed gradients of pavements from a moving vehicle. Photographs were made of the pavement by using a light at low-incidence angle to project shadows across the peaks and valleys of pavement macrotexture. The photographs were compared to standard photographs of pavements with known gradients. The ratings were converted to estimated skid number and speed gradient by using a regression equation. The technique is economical, valid, and reliable.

A study was made to determine the relations between skid number (coefficient of friction × 100) and wet-pavement accident rates. Wet-pavement accident records and the matching skid-number measurements provided by the states participating in the study were used. Skid number measurements are needed that correspond to the operating speed of the roadway.

The skid number data collected by the states are generally measured at a speed of 64 km/h (40 mph), and the skid number is known to decrease as speed increases. Thus, to determine skid number at the operating speed of the roadway at the time of the accident, we must know the skid number-speed gradient (G = Δ skid number/Δ speed). For example, if we know that the skid number at 64 km/h (40 mph) is 45 and the speed gradient is 0.50, then the skid number at an operating speed of 97 km/h (60 mph) is 45 - (0.50 × 60 - 40) = 45 - 10 = 35.

The most obvious method of obtaining the gradient for a section of pavement is to measure the skid number at various speeds and determine the gradient empirically. Because this is an expensive procedure and states have only limited budgets for skid measurement, the gradients have been determined for only a small number of pavement sections. A review of previous work was thus made to determine the technique best suited to estimate gradients.

PREVIOUS WORK

Several research projects have been directed toward alternate methods of determining the skid number-speed gradient of selected pavements. The most productive study was done by Schulze and Beckman (1), who found that the skid number-speed gradient from 20 to 60 km/h (12 to 37 mph) is correlated with the mean width of surface voids. The larger void width produces a flatter speed gradient primarily because of better water drainage.

The method for obtaining the mean void width is described by Schulze (2). Stereophotographs were taken of pavement sections and magnified 25 to 1. The outline of each individual void was then traced onto paper, and the width of each void was measured. Needless to say, this procedure would be much too expensive for any major speed-gradient inventory.

Gillespie (3) found mean void widths from pavement profile traces by using an electromechanical roughness meter. The mean void width was defined as the mean distance between peaks on the trace. When mean void width was compared to the known skid number-speed gradient from 60 to 80 km/h (37 to 50 mph), the comparison with the extrapolated Schulze and Beckmann curve was excellent.

Goodman (4) developed several techniques for measuring pavement texture from a moving vehicle; his validation, however, was limited to stationary, laboratory studies. One proposed technique involved photography. A narrow slit of light was projected vertically onto the surface of the pavement, and the resulting line was photographed from an angle of 30° to horizontal. In the resulting photograph, the strip of light delineated the peaks and valleys along the strip. The number of peaks per centimeter, inverse of mean void width, from this photographic technique agreed well with the results from an electromechanical roughness meter applied to the same strip of pavement.

Howerter and Rudd (5) developed a technique that uses stereophotography and computer interpretation to obtain skid-resistance parameters. However, the technique in its present form would be quite expensive for large pavement inventory projects.

After a thorough review of the literature, we elected to obtain the pavement-surface-texture data photographically because that approach appeared to offer the highest probability of success and liberal use could be made of off-the-shelf components.

PHOTOGRAPHIC EQUIPMENT AND TESTING

Photographs of pavement surfaces were made from a moving van at the same time other highway inventory data were being collected. Approximately 4 photographs were taken each 1.5 km (4 photographs/mile) of the left wheel track area, where most pavement skid number data are measured. The data were taken while the van was moving at 64 km/h (40 mph) because stopping the van on the highway was impractical.

Equipment

Figure 1 shows the configuration of the photographic equipment, which consists of a projection system, a camera system, and a light shroud.

The projection system projects a high-intensity, short-duration, shadow-bar pattern on the pavement surface. Since pictures were taken from a van moving at 64 km/h (40 mph), a flash duration of 0.5 to 1 μs was needed to stop the motion of the pavement relative to the camera. The shadow-bar pattern was projected on the pavement at a 20° angle with respect to the horizontal. This low-incidence light served to delineate the roughness of the pavement. On a smooth surface the interface between a band of light and dark was essentially straight. The rougher the surface became, the more crooked the interface line became because of the shadows cast by the peaks in the surface.

A camera system was needed with adequate format to portray salient surface texture features and durability to withstand several thousand kilometers of travel in the van. The system selected was composed of 35-mm data camera and magazine, 105-mm lens, electromechanical shutter, appropriate film, and combination housing and mounting structure.

A light shroud was provided to shield the pavement area illuminated by the projector from ambient light. The shroud was needed because ambient light reflecting from the surface would wash out the image of texture detail formed by the oblique lighting of the projection.

Equipment Testing

The complete photographic system was assembled, tested in the laboratory, and then installed in the van. Test photos were then taken for different pavement types, vehicle speeds, light-shroud position, time of day, and direction of travel (relative to the sun as ambient light source).

The developed test film showed that good, usable pictures could be obtained provided the light shroud was lowered to between 1 and 3 cm (0.5 and 1 in) above the pavement surface when the van was at a standstill. When the shroud was raised higher, ambient light effects obscured surface texture features. Vehicle speed and bouncing had no obvious effect. Pavement color change, e.g., portland cement concrete (PCC) to asphalt concrete (AC), altered the appearance of the photographs but visibility of surface texture was retained.

PRELIMINARY ANALYSIS OF PHOTOGRAPHS

The pavement was photographed from directly above and with oblique lighting. The spot of light contained shadow lines intended to delineate the peaks and valleys along a trace of the surface. The flash duration was sufficiently short to obtain streak-free photographs at 64 km/h (40 mph), but light leakage under the shroud produced minor streaking in most of the photographs.

The first nonlaboratory test of the photographic procedure was made while the vehicle was stationary. A photograph (Figure 2) was taken of a spot of open-textured asphaltic concrete in a parking lot. An impression of the surface was then made, and the surface texture was later duplicated with a plaster-of-paris replica.

The negative film photograph of the spot was placed on a standard library 35-mm film reader and magnified 2.2 times. The number of peaks per centimeter was determined by two methods. First, the shadow line was traced onto a piece of tracing paper and the number of peaks per centimeter were counted by hand. Second, a ruler was placed on the viewer screen and the number of peaks along the ruler edge was determined by changes in shades of gray. Then the number of peaks per centimeter in the same areas of the plaster-of-paris replica were counted by hand. For the shadow line trace, direct measurement, and plaster-of-paris replica there were 7, 6, and 4 peaks/cm (18, 15, 11 peaks/in) respectively. The oblique lighting in the photograph appeared to magnify the size of some of the microtexture, which was mistaken for macrotexture.

Another method used for analyzing the tracing paper outline of the shadow edge was to directly measure the mean void width. The width, parallel to the shadow bar, of each shadow projecting into a void was measured. This method produced unsatisfactory results for the same reasons as stated above, accumulated measurement errors, and was quite tedious and time consuming.

The analysis technique was then applied to the photographs taken from a moving vehicle in the field. Several of the macrotexture photographs were taken on pavement sections with known speed gradients. The film was reviewed and rated as to quality of photographs. (Quality indicates resolution or clarity of the photograph and was determined by comparison to reference photographs.) Rating was influenced primarily by motion streaking made visible by ambient light leaking under the light shroud. Experience showed that the minor streaking was helpful in interpreting the photograph; however, too much or too little streaking was undesirable. The average quality photograph is shown in Figure 3. A decision was made to test the film-reading procedure only on average quality photographs to avoid any bias that might be introduced by differences in photographic quality. Fortunately, 75 to 80 percent of all photographs were of the desired quality.

The known gradient photographs were analyzed by two methods. First, the shadow line was traced from the viewer screen onto tracing paper and the number of peaks per centimeter was counted by hand. Second, a ruler was placed in the lighted portion of the photograph, and the number of discernible changes in shades of gray along the ruler was counted. From this the number of peaks per centimeter was determined. A discernible peak on the negative film was defined as a darker area separated from the next darker area along the ruler by a lighter area. The two methods (tracing and direct reading) produced essentially the same results. Because the direct reading method was considerably faster, this method was selected as the primary reading method for subsequent work.

The number of peaks per centimeter on the known gradients was determined by the direct reading method described above. Only average quality photographs were read to prevent any bias that photographic quality might introduce. An average of six photographs was read for each known gradient and the mean of these readings was used. The mean number of peaks per centimeter was inverted to yield mean void width.

Mean void width may be converted to an index of speed gradient by using the Schulze and Beckman formula:

$$y = 13.5 - 72.6x + 103.6x^2 \quad (1)$$

where

y = mean width of surface voids (0.254 mm or 0.01 in) and
x = coefficient of friction at 20 km/h (12 mph) - coefficient of friction at 60 km/h (37 mph).

Solving the equation for x yields

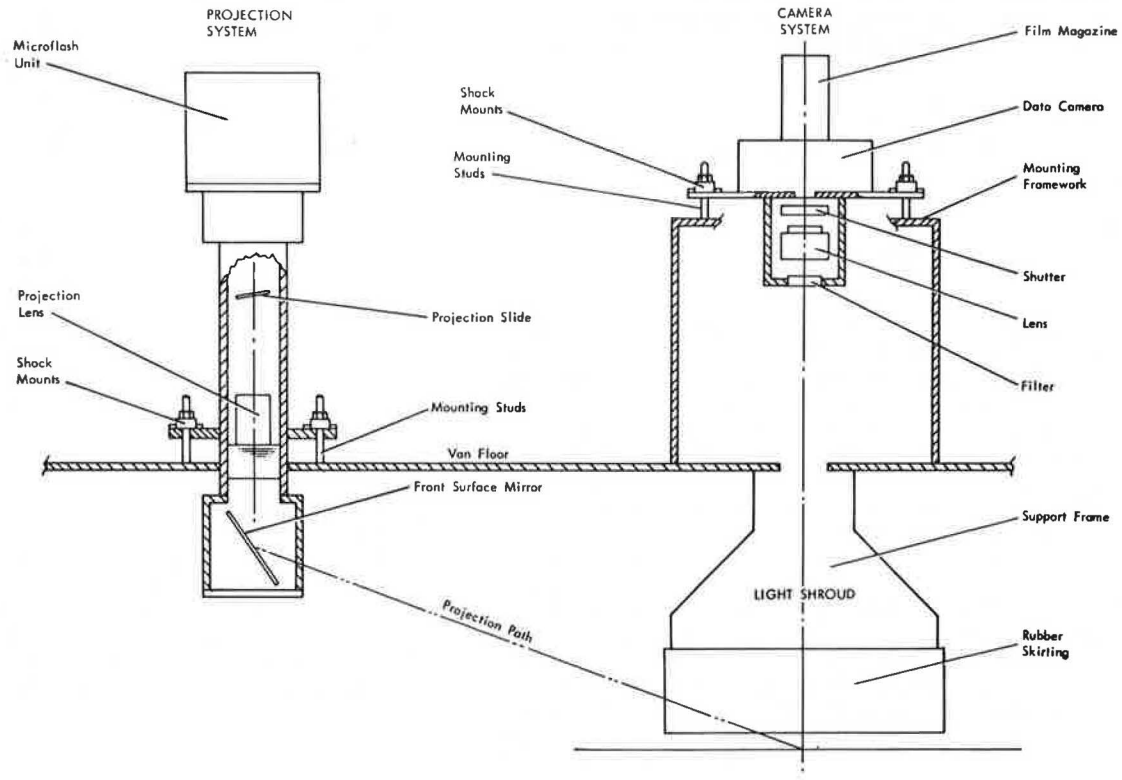

Figure 1. Principal components of photographic system.

Figure 2. Photograph of pavement macrotexture from stationary vehicle.

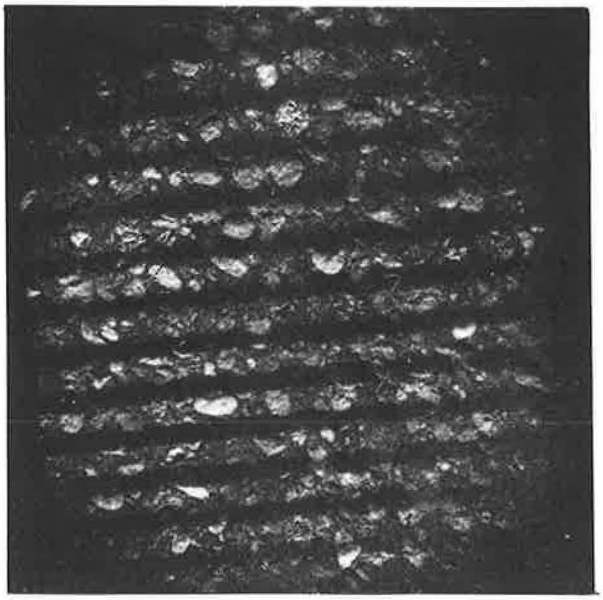

Figure 3. Photograph of average quality taken from moving vehicle.

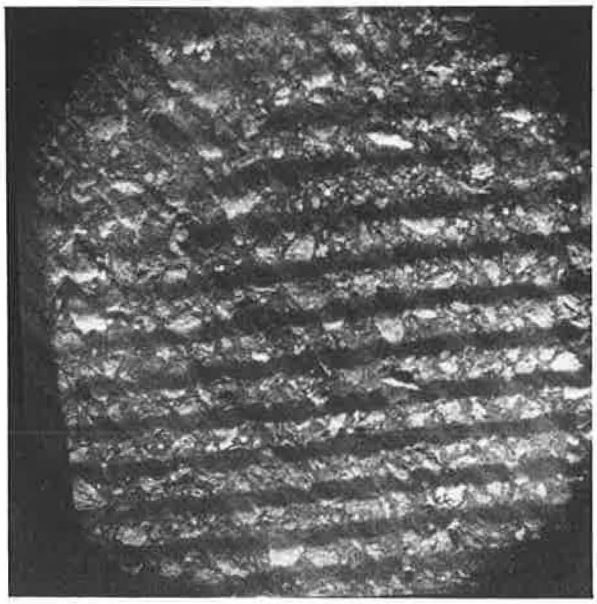

$$x = 0.350\,38 - \sqrt{-0.007\,542\,86 + 0.009\,653y} \quad (2)$$

or the change (Δ) in coefficient of friction (CF) between 20 and 60 km/h. A much more useful term would be $\Delta SN/\Delta km/h$, where SN = 100 CF and 1 km = 0.62 mile. We multiply the right side of the above equation by [(100) (1.609)]/40 = 4.023 to yield

$$x = G = 1.4097 - \sqrt{-0.122\,077\,6 + 0.156\,229\,3y} \quad (3)$$

where $G = \Delta SN/\Delta km/h$. The curve in Kummer and Meyer (6) is based on this last equation.

The mean void width for each known gradient was converted to SN - G by using Equation 3. The G estimated from photographs and measured by skid trailer at various speeds are given below (1 km = 0.62 mph).

	Measured			
Estimated (km/h)	48 to 64 km/h	64 to 80 km/h	80 to 97 km/h	48 to 97 km/h
0.82	0.63	0.53	0.42	0.53
0.91	0.74	0.44	0.34	0.51
0.78	0.28	0.45	0.18	0.30
0.72	0.31	0.59	0.09	0.33

Based on this small sample, the method appeared to be accurate enough to be of value to the study. Considering the high variance in the known gradient data, the photo-estimated values appeared to be reasonable.

The film-reading method adopted for this study appeared to work better on photographs gathered in the field than on laboratory photographs. We believed this difference to be due to the light leakage under the shroud in the field. This light leakage created some streaking on the photograph and reduced the resolution somewhat. This loss in resolution obliterated the shadows cast on the microtexture (small irregularities in void surfaces that are not meaningful to drainage) by the oblique lighting, and only the macrotexture shadows could be seen. Consequently, the streaked photographs from the field produced better results than the laboratory photographs.

However, this photographic technique had limitations. We had field photographs of PCC pavement on which the sand patch test was done. Although mean texture depth is not synonymous with mean void width, one would expect them to be positively correlated.

Macrotexture photographic data were available for two pavements: The mean texture depth of one was 0.17 cm (0.066 in), and the other was 0.030 cm (0.012 in). The latter surface was considered very smooth. The field photographs of those pavements were read, and the mean void width on the first pavement was estimated to be 0.17 cm (0.07 in). The film reader reported that photographs of the smoother surface were unreadable. When told that the surface was very smooth and to try again, the reader was able to estimate the mean void width to be 0.18 cm (0.25 in). Based on these results, we assumed that our photo-estimation technique was not capable of determining the mean void width for very smooth pavements.

PRIMARY ANALYSIS OF PHOTOGRAPHS AND RELIABILITY OF MEASUREMENTS

For any measurement technique to be valid, it must yield essentially the same results from multiple measurements of the same data. This concept is known as test-retest reliability. A total of 83 photographs taken from a moving vehicle were read twice; a 2-month delay occurred between the first and second readings. The direct-measurement technique (using the ruler as described above) was used both times to determine the number of peaks per centimeter. The Pearson correlation coefficient (γ) between first and second reading on each photograph was found to be only 0.01. We then grouped the data into three classes as given in the table below (1 mm = 0.04 in, 1 km/h = 0.62 mph).

Class	Peaks (per mm)	Mean Void Width (mm)	Gradient ($\Delta SN/\Delta km/h$)
1	0.0 to 5.0	∞ to 2.0	0.0 to 0.21
2	5.1 to 8.0	2.0 to 1.3	0.21 to 0.37
3	>8	1.3 to 0.0	>0.37

The correlation coefficient between first and second reading in this case was 0.73. This finding indicated that the pavements could be reliably rated as to high, medium, or low gradients. When the readings were grouped into five classes, as given in the following table, the correlation dropped to 0.11, which indicated that the rater could not reliably rate the pavement into five classes.

Class	Peaks (per mm)	Mean Void Width (mm)	Gradient ($\Delta SN/\Delta km/h$)
1	0.0 to 4.5	∞ to 2.3	0.0 to 0.17
2	4.6 to 5.5	2.3 to 1.8	0.18 to 0.26
3	5.6 to 7.5	1.8 to 1.3	0.27 to 0.37
4	7.6 to 12.5	1.3 to 0.8	0.38 to 0.50
5	>12.5 +	0.8 to 0.0	>0.51 +

Subjective Rankings of Pavement Texture

At this point a decision was made to develop a method of ranking the photographs of pavements into several classes without directly counting peaks. Five studies were performed to determine how reliably a number of raters could rate pavement molds and photographs so that standards could be developed for the individual classes of pavement texture. One macrotexture photograph was selected as the standard for each class, and a photograph of a macrotexture of unknown gradient was compared to the standard to determine the gradient.

Study 1

The first study used 13 molds of pavement texture of known gradients, as follows:

Mold Number	Pavement Type	G ($\Delta SN/\Delta km/h$)	Mold Number	Pavement Type	G ($\Delta SN/\Delta km/h$)
1	AC	0.31	8	AC	0.12
2	PCC	0.24	9	Special	0.08
3	AC	0.27	10	Special	0.05
4	PCC	0.31	11	Special	0.18
5	AC	0.31	12	Special	0.15
6	AC	0.18	13	Special	0.09
7	AC	0.21			

Molds were positive duplications of the pavement surfaces and were molded from negative silicone impressions. The positive molds were made of white hydro stone. Gradients were calculated from multiple speed skid measurements provided by the states and the 64 to 97-km/h (40 to 60-mph) values were used when available. The raters consisted of 12 staff members, 6 of whom were primarily highway safety engineers and 6 stenographers and analysts.

Asphalt concrete (AC), portland cement concrete (PCC), and special pavement molds were hot mixed so that the rating would not be contaminated. The AC molds were rated first, the PCC molds second, and the special pavement third. Because some of the special pavement

molds were exceptionally rough or smooth, extra rough and extra smooth were added to the classes of smooth, medium, and rough.

The relation between SN - G and mean texture rating (T) is shown in Figure 4; goodness of fit is described by the Pearson correlation coefficient (r). Except for one special mold, the relation between the two variables was good (r = -0.90). That pavement surface consisted of crushed sand in an epoxy overlay and was extremely smooth. The impression made of the surface contained air bubbles and produced a bad mold, which was eliminated from later studies. Since all of the surfaces seemed to fit the same general relation between gradient and mean texture rating, the molds were rated from all three surface types as a single group of 12 in the second study.

Study 2

In the second study the 12 molds were rated into five classes. Two of the original raters were unavailable for the second study, and the ratings were made by the remaining 10. The relation between gradient and mean texture rating in the second study is shown in Figure 5. Again, the relation is good (r = -0.92), and the coefficient of concordance (an index of how well the raters agreed on each mold) among raters was 0.90.

Study 3

In the third study, the individuals rated photographs of the pavement from which the molds had been made. The photographs were taken while the inventory van was stationary over the exact spot from which the molds had been made. The relation between gradient and mean texture rating for the still photographs is shown in Figure 6. The coefficient of concordance dropped to 0.75 for the still photographs.

Study 4

In the fourth study, the individuals rated the macrotexture photographs taken while the van was moving at 64 km/h (40 mph). The location of the pavement photographed was within 3 m (10 ft) of the spot of the impression in all cases. The relation between gradient and mean texture rating is shown in Figure 7. The coefficient of concordance increased to 0.92 for this group of photographs. At first, the result seems surprising. However, more reasonable results were attained when peaks per centimeter were counted on moving photographs because the streaking washed out the microtexture and made the macrotexture more visible. In study 4, however, the shadow bars in the photographs were more visible on the pavement because of the streaking, and judgment was easier by viewing the irregularities in the bars than by directly viewing the surface texture.

Study 5

An analysis was done to determine the rank-order agreement (Spearman correlation) for pavement texture ratings of molds and photographs taken while the van was stationary and moving. The results are as follows:

Combination	Correlation
Molds and still photographs	0.83
Molds and moving photographs	0.71
Still photographs and moving photographs	0.80

We concluded that raters could rate the photographs of macrotexture made while the van was moving into surface-texture classes with good interrater agreement. In addition, the mean ratings for the photographs formed a good relation with the known gradient.

However, two possibilities could have led to biased results. One possibility was that the raters used the photographs to remember the molds and did not actually rate texture based strictly on the information in the photographs. The other possibility was that the high interrater agreement on the moving photographs occurred because raters had become better through practice on the first three studies. Consequently, a fifth study was conducted.

Ten stenographers, none of whom had seen the pavement molds, were asked to rate the 12 still photographs and the 12 moving macrotexture photographs. Half of the individuals rated the still photographs first, and half rated the moving photographs first. The relation between mean rank and gradient is shown in Figure 8 for still photographs and in Figure 9 for moving photographs. By comparing the curve in Figure 6 with that in Figure 8 and the curve in Figure 8 with that in Figure 9, one can see that the agreement between the two groups was good. The Spearman rank-order correlation between the two groups for mean ranking of textures in moving photographs was 0.90. Consequently, previous knowledge of the molds did not seem to bias the ratings.

The coefficient of concordance was 0.48 for still photographs and 0.69 for moving photographs. Again, the concordance for moving photographs was higher than that for still photographs. Because the order effect was controlled in this study, the superiority of moving photographs was apparently real and not a result of learning. This conclusion was reinforced when a Bartlett's test was made on the variance data, and no significant difference was found between the variance for first and second readings.

However, the fact that the first group of raters (who had seen the molds) had a higher coefficient of concordance than the second group could indicate that the high concordance was due to experience with the molds. Another possibility is that a basic difference existed between the two groups of raters. Neither of these two possibilities could be ruled out.

Updated SN data were received from a skid test center at the completion of the five studies. The test center data used in the studies were preliminary results obtained shortly after the test surfaces had been laid, and the updated data were obtained after the surfaces stabilized. Two of the surfaces (molds 9 and 10) had a higher SN at 97 km/h (60 mph) than at 64 km/h (40 mph). Both had an epoxy overlay such that no aggregate directly contacted the tire. The surface in mold 9 had previously been eliminated because of a bad mold. The surface in mold 10 was then eliminated from further consideration. The updated gradients for the skid test center surfaces 3, 4, and 5 (molds 11, 12, and 13) are as follows (1 km/h = 0.62 mph):

Mold	Previous G (ΔSN/Δkm/h)	Updated G (ΔSN/Δkm/h)
11	0.18	0.16
12	0.15	0.10
13	0.09	0.03

Standards

After the known gradients were updated, we found that the correlation between mean texture rating and known gradient for the first group of raters (raters in studies 1 through 4) was better than the correlation for the second group. Consequently, the five standards were chosen in accordance with the ratings of the first group of raters. Figure 10 shows the relation between mean texture rating

and known gradient for the first group of raters using updated gradients. Figure 11 shows the relation after the three outlying points were eliminated. Based on the least squares curve fit of the reduced data set, five standards were chosen that best represented the relation between mean texture rating and known gradient. The pavements selected as standards are as follows (1 km/h = 0.62 mph):

Standard	Mold	Known G (ΔSN/Δkm/h)	Standard	Mold	Known G (ΔSN/Δkm/h)
1	4	0.31	4	8	0.12
2	2	0.24	5	13	0.04
3	7	0.21			

We now had five standards for estimating SN - G, but the photo-estimation technique had not been tested to determine its accuracy. Fortunately, gradient data were

Figure 4. Mean texture rating versus known gradient—sequential ratings.

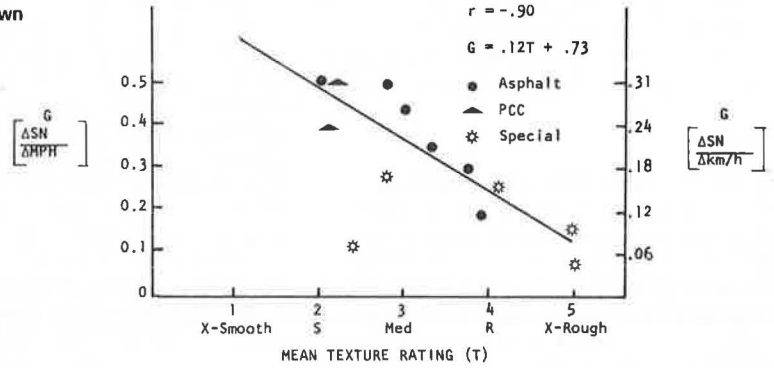

Figure 5. Mean texture rating versus known gradient—12 molds together.

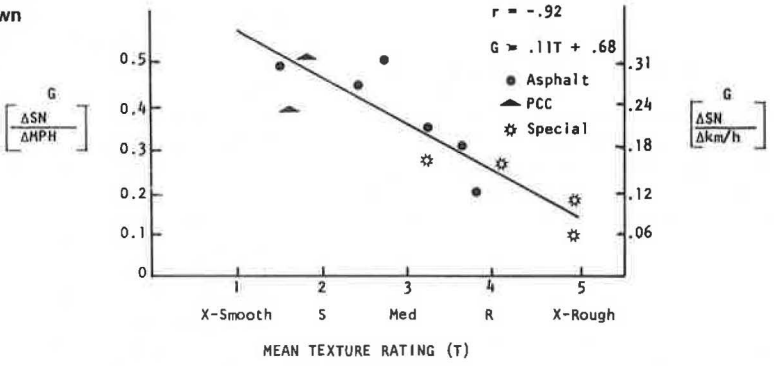

Figure 6. Mean texture rating versus known gradient—still photos, first group.

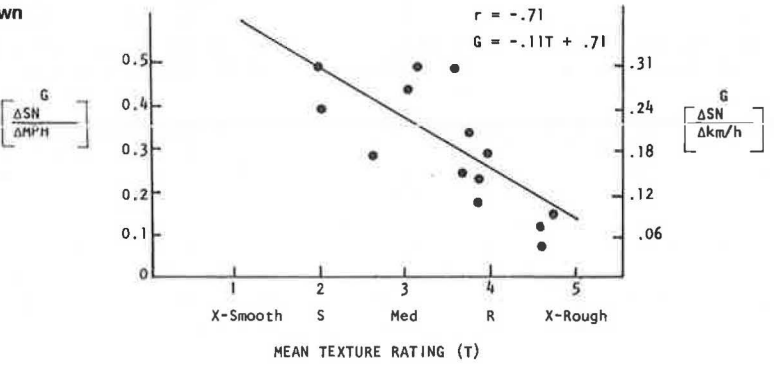

Figure 7. Mean texture rating versus known gradient—moving photos, first group.

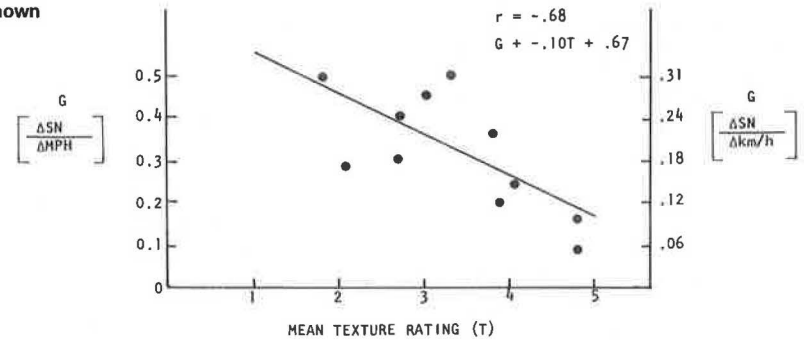

available on nine sections of pavement that had not been used in the earlier studies to develop the standards. A total of 208 photographs had been taken in the nine sections.

Negatives of the photographs of the five standards were cut into strips so that all five could be mounted on one 35-mm slide. This set of standards was projected onto half of a rear-projection screen. Then the 208 frames of negative film were each projected on the screen next to the standards. A photograph of the actual split projection is shown in Figure 12. The rater compared the pavement photograph with the five standards and then judged which standard the pavement photograph most resembled.

The ratings were converted into estimated gradient by the following procedure. The mean rating for each section of pavement was found. If the mean rating was an integer number, the known gradient of that standard was assigned to the pavement section as the estimated gradient. For example, if the mean rating was found to be

Figure 8. Mean texture rating versus known gradient—still photos, second group.

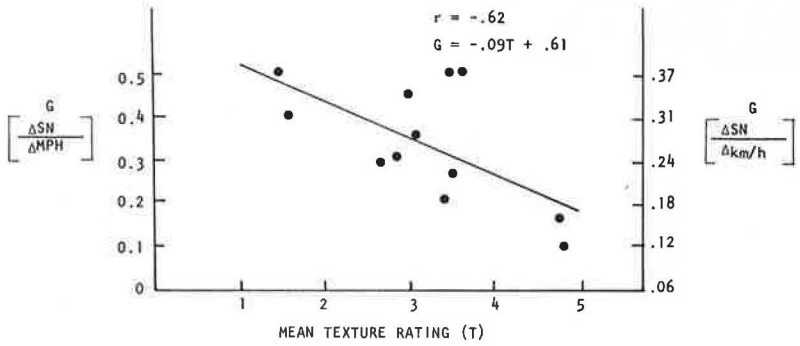

Figure 9. Mean texture rating versus known gradient—moving photos, second group.

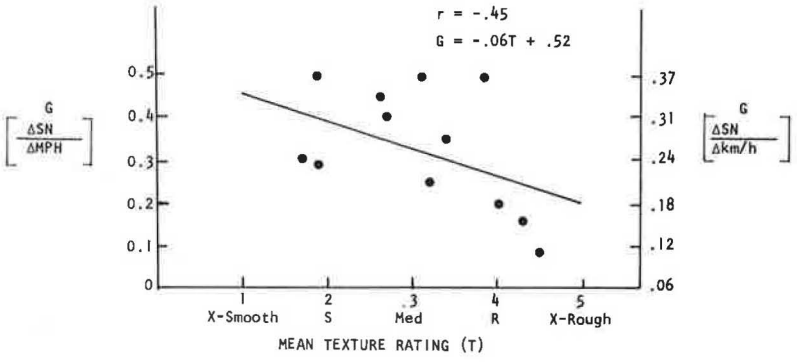

Figure 10. Mean texture rating versus known gradient—updated gradients.

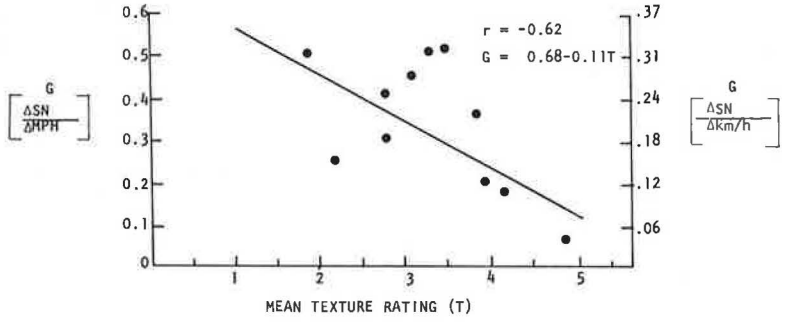

Figure 11. Mean texture rating versus known gradient—outlying points eliminated.

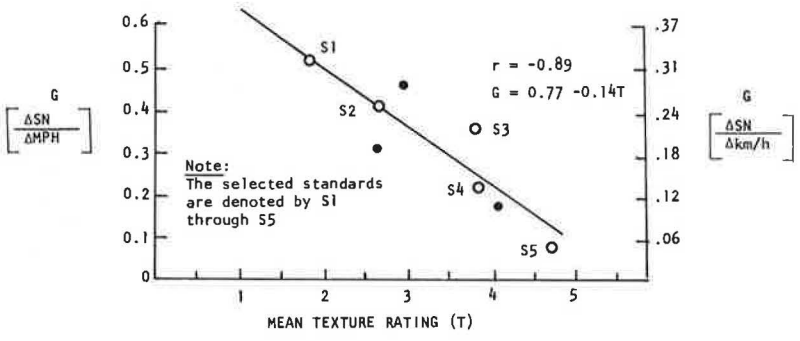

Figure 12. Negative photograph of pavement projected next to five standards.

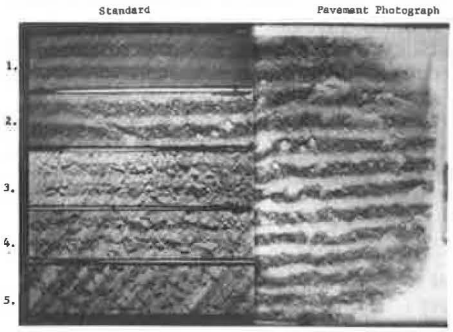

Figure 13. Relation between photo-estimated and known gradient.

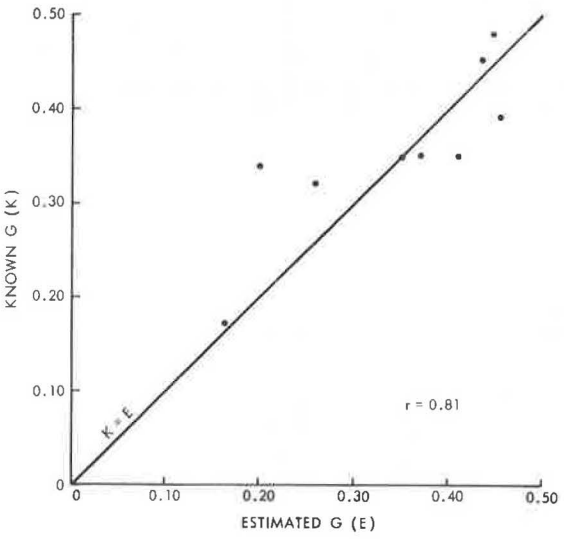

Figure 14. Relation between mean standard rating and known gradient.

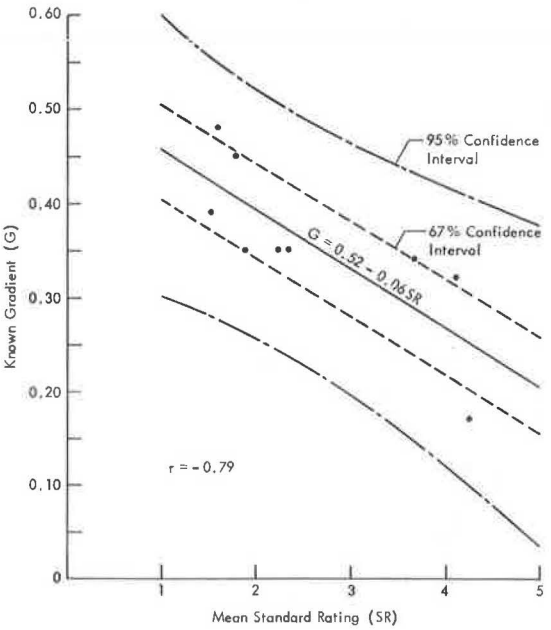

3.0, the known gradient (0.35) of standard 3 in the above table was assigned to the pavement section. If the mean rating was a fractional number, the estimated gradient was found by linearly interpolating between the two bordering known gradients. For example, if the mean rating was 1.5, the estimated gradient of 0.45 was assigned to the pavement section.

The relation between estimated and known gradients that was made by using the above procedure appears in Figure 13. The line represents where the points would fall if perfect correlation existed between estimated and known gradients. The points fall fairly close to the line, and the Pearson correlation coefficient between estimated and known gradient is 0.81.

Rating Conversion Equation

Once we observed that the technique was valid, we decided to improve the linear interpolation technique of converting standard ratings into estimated gradient. The relation between mean standard rating (SR) in the validation study and known gradient for each of the nine highway sections is shown in Figure 14. The best fit, least squares linear regression line for the points had the equation G = 0.52 - 0.06 SR. The correlation coefficient was -0.79, and the standard error of the estimate was 0.0578. The 95 and 67 percent confidence intervals are shown in dashed lines. The equation above then became the equation for converting mean SR to estimated SN - G.

Reliability

The technique described above was used to estimate SN - G on 580 sections of highway in 14 states. The standard ratings for each of 28 000 frames of film were placed on punched cards for later conversion to estimated gradient by the above equation.

The film-reading process took approximately 2 months of half-time work for two technician-level readers. At the end of the 2-month period the 208 photographs used in the validation study were reread. The mean standard rating for each of the nine sections of highway was found, and the Pearson correlation coefficient between first and second reading was +0.94, indicating high reliability of the technique.

As a further check, 168 frames of film for a section of highway (with unknown gradient) were reread. The standard ratings for each frame were compared to ratings given the frames when they were read along with the other 28 000 frames. The correlation between the first and second reading was +0.69, which is reliable. Mean rating was 1.82 on first reading and 2.37 on second reading. These ratings convert to estimated gradients of 0.38 and 0.41 respectively. An error of this magnitude is deemed acceptable when one considers the variance of the skid number data with which we were working.

ACKNOWLEDGMENT

This work was conducted as a part of a study performed for the Federal Highway Administration, U.S. Department of Transportation. The opinions and findings expressed or implied in this paper are ours and do not necessarily reflect those of the sponsor. We wish to express our appreciation to Andrew St. John for his valuable technical inputs to the project and to William Jellison and Melvin Lavik for their contributions to camera system developments. We wish to thank Patrick Heenan for his assistance in data analysis. Thanks are also due to Philip Brinkman, Office of Research, Federal Highway Administration.

REFERENCES

1. K. H. Schulze and L. Beckman. Friction Properties of Pavements at Different Speeds. ASTM, Special Technical Publ. 326, 1962, pp. 42-49.
2. K. H. Schulze. Einfluss der geometrischen Feingestalt der Strassenoberflache auf den Kraftschluss. Strasse und Autobahn, Vol. 10, No. 10, 1959, pp. 379-385.
3. T. D. Gillespie. Pavement Surface Characteristics and Their Correlation With Skid Resistance. Joint Road Friction Program, Pennsylvania State Univ., and Pennsylvania Department of Highways, Rept. 12, 1965.
4. H. A. Goodman. Pavement Texture Measurement From a Moving Vehicle. Joint Road Friction Program, Pennsylvania State Univ., and Pennsylvania Department of Highways, Rept. 19, 1970.
5. E. D. Howerter and T. J. Rudd. Automation of the Schonfeld Method for Highway Surface Texture Classification. TRB, Transportation Research Record 602, pp. 57-61, 1976.
6. H. W. Kummer and W. E. Meyer. Tentative Skid-Resistance Requirements for Main Rural Highways. NCHRP, Rept. 37, 1967.

Publication of this paper sponsored by Committee on Surface Properties-Vehicle Interaction.

**Mr. McDonald and Mr. Kobett were with the Midwest Research Institute when this research was performed.*

Relation of Accidents and Pavement Friction on Rural, Two-Lane Roads

Rolands L. Rizenbergs, James L. Burchett, and Larry A. Warren, Division of Research, Kentucky Department of Transportation

Friction measurements were made with a skid trailer at 50 km/h (40 mph) on 2350 km (1460 miles) of rural, two-lane roads (U.S. routes) in Kentucky. Maintenance sections or subsections were treated as test sections. Accident experience, friction measurements, traffic volumes, and other available data were obtained for each section. Various expressions of wet-pavement accidents and pavement friction were related and analyzed. Averaging methods were used in developing trends and minimizing scatter. A moving average for progressively ordered sets of 10 test sections and test sections grouped by skid numbers and peak slip numbers yielded more definite results. The expression of accident occurrence that correlated best with skid resistance and peak slip resistance was ratio of wet- to dry-pavement accidents. Wet- to dry-pavement accident ratios increased greatly as skid number decreased from approximately 40 and as peak slip number decreased from approximately 71.

To ensure safe highway travel in wet weather, pavements must have sufficient and enduring skid resistance to enable drivers to perform driving tasks without risk of skidding and loss of vehicle control. Investigations to establish minimum friction requirements in Kentucky have focused on analysis of accident experience as related to pavement friction (1). The primary objective of this study was to discern a relationship between accident experience and pavement friction for principal, two-lane roads (U.S. routes) in rural areas of Kentucky. Evaluation of such a relationship in conjunction with economical and technical considerations will guide the establishment of minimum friction requirements for pavements.

To define a relationship between accidents and pavement friction, we must know or hold constant the effect of all pertinent parameters to the extent possible. By limiting this study to the principal, two-lane roads in rural areas, we were able to assume that parameters such as highway geometrics, access, and traffic speed would remain within reasonable bounds. Traffic characteristics (volume and density) and pavement-surface condition (wet or dry and pavement friction when wet) are respectively the regenerative and causative factors.

Annual average daily traffic volumes were obtained for 1969 and 1971. Accident data were those reported during 1969, 1970, and 1971. Pavement friction measurements were made between June and December 1970 on 2350 km (1460 miles) of the principal, two-lane roads. Both locked-wheel and peak slip resistances were measured. The measurements that best correlate with wet-pavement accidents remain to be established.

DATA ACQUISITION AND COLLATION

Measurements of annual average daily traffic (AADT) are generally available biennially. AADT data for 1969 and 1971 were averaged and used in these analyses.

Friction measurements were obtained by using a surface dynamics pavement friction tester. The two-

Figure 1. Relationship between skid numbers measured at 63.4 and 96.6 km/h.

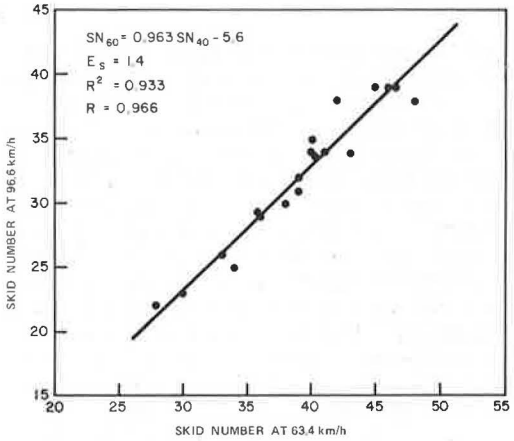

wheeled, skid-test trailer was acquired in 1969. This skid trailer complies with ASTM designation E 274 (2). The measurements represent friction developed between a standard test tire (ASTM designation E 249) and a wetted pavement. The locked-wheel measurement is expressed as a skid number (SN); incipient or peak friction is expressed as a peak slip number (PSN). Measurements were obtained during the summer and fall of 1970 on most of the roads having a posted speed limit of 96.6 km/h (60 mph). Tests were made in the left wheel path only and at 1.6-km (1-mile) intervals in each lane; no less than five tests per lane were made on each test section. The test speed was 63.4 km/h (40 mph). Additional tests were made on selected class 1 bituminous pavements at 96.6 km/h (60 mph). Comparison between the SNs obtained at the two speeds is presented in Figure 1.

Accident data were obtained from state police records, which are computerized and maintained by the Kentucky Department of Justice. All accidents reported during 1969, 1970, and 1971 were analyzed. Accidents for the 3-year period totaled 8481; of these, 1844 occurred during wet-pavement conditions. From these accident records, many expressions of accident occurrence may be calculated. However, based on the findings of an earlier study on the Interstate and parkway routes (1), rates of wet-pavement accidents and ratios of wet- to dry-pavement accidents were used primarily.

The ASTM definition of a test section was used: a section of pavement of uniform age and uniform composition which has been subjected to essentially uniform wear along its length. Almost all construction and resurfacing projects (maintenance sections) involved fit this definition. Because the direction of travel of vehicles involved in accidents was not given in the accident reports, test sections included both directions of travel. There were 230 test sections; 217 of these were bituminous pavements and the remaining 13 were portland cement concrete (PCC) pavements. The average length of the test section was 10.1 km (6.3 miles). Sections less than 3.2 km (2.0 miles) in length were not included.

The left wheel-path SNs and PSNs for both directions of travel were averaged to characterize the frictional properties of the test sections. Distribution of the SNs for the 230 test sections is shown in Figure 2. The relationship between SN and PSN is shown in Figure 3. Rates of wet-pavement accidents for 100 million vehicle·km (62 million vehicle-miles), the total distance traveled under all pavement conditions, and ratios of wet- to dry-pavement accidents were calculated for each test section. The rates were based on the lengths of sections and AADT (1969 and 1971). Both rates and ratios pertain to accidents for a 3-year period.

SKID NUMBERS AND ACCIDENTS

The ratio of wet- to dry-pavement accidents versus SN for the 230 test sections is shown in Figure 4. The data points are extremely scattered. The relationship between accident occurrence and skid resistance is obviously obscured by other causative factors. Multiple-regression analyses were performed with the ratio of wet- to dry-pavement accidents as the dependent variable and SN, AADT, pavement width, and access points per kilometer as the independent variables. The data were further stratified by AADT and SN. Similar analyses were performed with the wet-pavement accident rate as the dependent variable. The coefficients of correlation (R) indicated a substantially better correlation between SN and the ratio of wet- to dry-pavement accidents than with the wet-pavement accident rate. The correlation coefficients, however, were low (less than 0.430). For the ratio of wet- to dry-pavement accidents, some correlation with AADT was evident; but with pavement width or access points per kilometer, correlation was not evident in the range of SNs between 17 and 44. For the wet-pavement accident rate, there were stronger correlations with volume (above 2700 vehicles/d) and pavement width than with SN and to a lesser extent with access. These findings, however, must be viewed with caution because the data base was not sufficiently large to yield definitive results.

Two averaging methods were used to reduce variability and thus to more clearly discern general relationships in the data sets with and without volume stratification. In the first method of calculating averages, test sections were grouped by SN. The average ratio of wet- to dry-pavement accidents was calculated for each group of two SNs. These averages are plotted in Figures 5, 6, and 7. Lines were drawn to approximate trends. Reasonably distinct break points were evident. When all test sections were included (Figure 5), the trend line indicated the ratio of wet- to dry-pavement accidents decreased as SN increased to approximately 41; further increases in SN resulted in nominal reduction in the accident ratio. Stratification of data by AADT indicated that on the low-volume roads (650 to 2700 vehicles/d) the critical SN was about 43. On high-volume roads (above 2700 vehicles/d) the critical SN was about 38.

The second method involved calculation of an average ratio of wet- to dry-pavement accidents and average SN for progressively ordered sets of 10 test sections. The first average was of the 10 test sections with the lowest SNs. The test section with the lowest SN was then dropped, and a test section with the next highest SN was added. This procedure was repeated until all test sections had been averaged in a group of 10. In cases in which more than one test section had the next highest SN, one of these test sections was randomly added each time. Test sections were dropped in the same sequence as they were added. The resulting averages are plotted in Figures 8, 9, and 10. The trend lines were similar to those developed by the previous method. The break points in the trend lines, however, occurred at slightly different SNs. The following table gives the critical SN derived by using the two averaging methods.

AADT Stratification	Grouped by SN	Moving Average
650 to 8400	41	40
2700 or less	43	45
Above 2700	38	39

Plots of the 10-point moving average and test sections grouped by SN but involving wet-pavement accident rate were also prepared. The plots also indicated a relationship between accident occurrence and skid resistance, but the data points were more scattered; and, as stated above, other variables correlated with accident occurrence as well. The break points in the trend lines were at higher SNs than for the accident expression of ratio of wet- to dry-pavement accidents.

The above analysis showed that the critical SN was higher for the low-volume (650 to 2700 vehicles/d) roads than for the high-volume (2701 to 8400 vehicles/d) roads. Therefore, we had to ascertain whether traffic volume or other factors accounted for the differences in critical SNs. Information was available on pavement width, access, and pavement friction, but an inventory of highway geometrics was not available. Accident records did indicate whether the accidents occurred on grade or level and on curve or tangent sections. Various expressions of accident occurrence, such as ratio of wet-pavement accidents on curves to wet-pavement accidents on tangent sections and dry-pavement accidents on curves to dry-

pavement accidents on tangent sections, were calculated for test sections grouped by AADT. The results are given in Table 1 in addition to average SN and other data.

The high AADT roads exhibited slightly lower SNs and had wider pavements. There were no appreciable differences in access points per kilometer. The ratios of wet- to dry-pavement accidents, however, did not indicate trends consistent with the level of skid resistance. Obviously, other influences were present. The ratios of accidents grouped by other identifying conditions in dry weather and also in times of wetness showed marked differences between AADT groups—the ratios were substantially lower for test sections with high AADT. Also, the ratios within sorted wet-pavement accidents were much higher than the ratios of dry- to dry-pavement accidents within the same AADT group and, therefore, reflect increased hazards associated with wet-weather driving on curves and grades compared to driving on tangent sections. The ratios in the wet-pavement categories, of course, would also be affected by differences in skid resistance between level, tangent sections, and sections with other geometrical alignments.

The accident ratios given in Table 1 do suggest a difference between test sections with low and high AADT in regard to geometrics of the highway. The average adequacy rating (3) for each set of test sections was 60. However, when adjusted to the same traffic volume, the adequacy rating was substantially higher for the high

Figure 2. Distribution of SNs for 230 test sections.

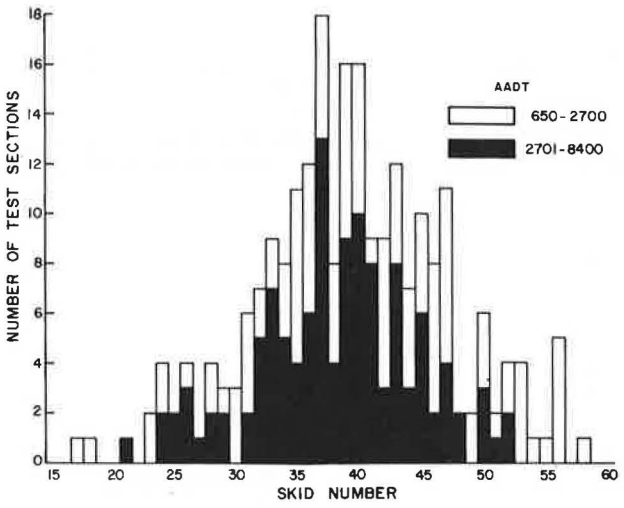

Figure 3. Relationship between SN and PSN at 63.4 km/h.

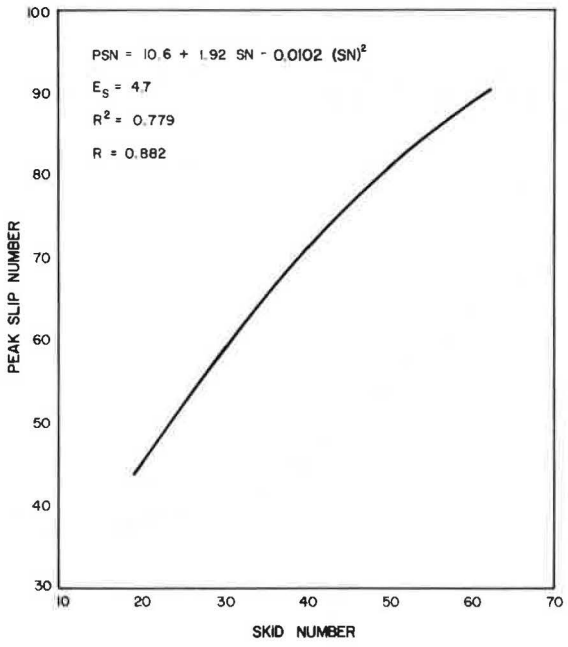

Figure 4. Ratio of wet- to dry-pavement accidents versus SNs for 230 test sections.

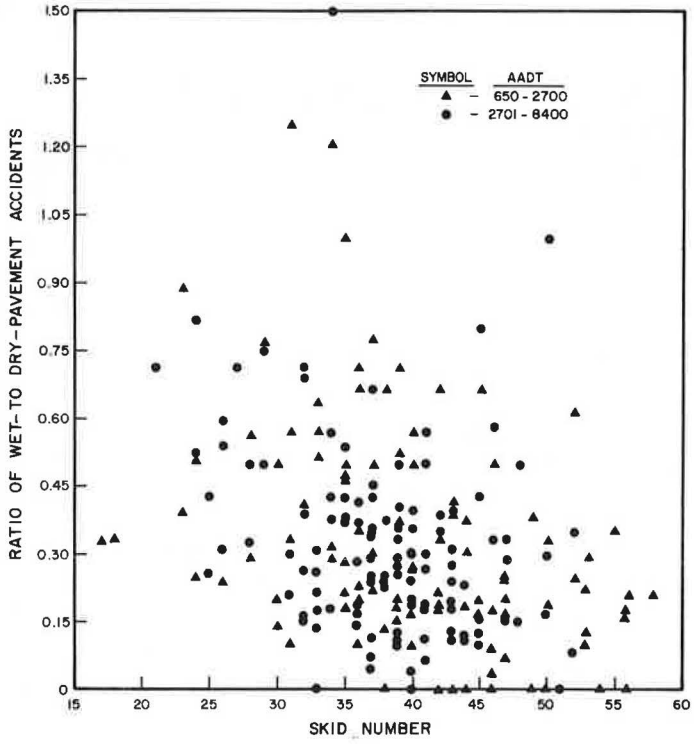

AADT roads than for the low AADT roads. This finding implied that the previous conclusion may be correct. The higher critical SNs derived from Figures 6 and 9, therefore, may be partially attributable to the poorer geometrics associated with the low AADT roads.

The accident data used in the analysis here pertained to the entire 3 years although skid resistance was measured in the summer and fall of 1970. Pavements, of course, exhibit lower friction during the summer and fall, but the measured values may not necessarily represent the lowest friction during the year for a particular test section nor for the road system as a whole. The rapid change in the slope of the curve in Figure 8, for example, may occur at some higher or lower SN depending on when the measurements were made. Measurements are normally conducted in the summer and fall,

Figure 5. Average ratio of wet- to dry-pavement accidents of 230 test sections (grouped by skid number) versus SN, without volume stratification.

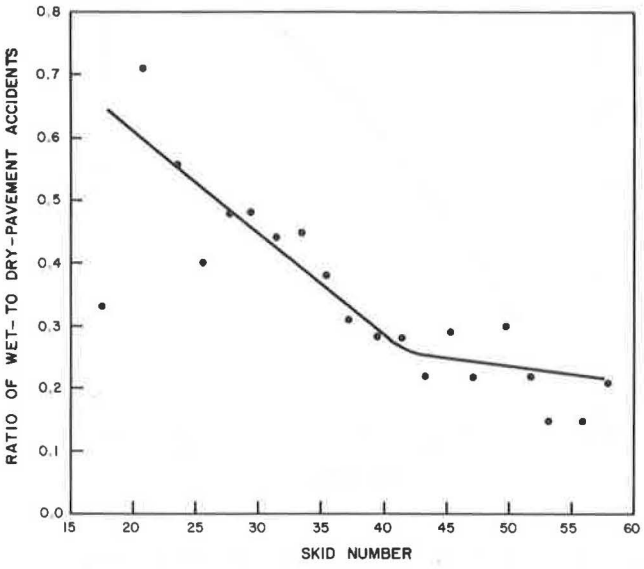

Figure 6. Average ratio of wet- to dry-pavement accidents of 230 test sections (grouped by skid number) versus SN, with volume stratification at AADT below 2701.

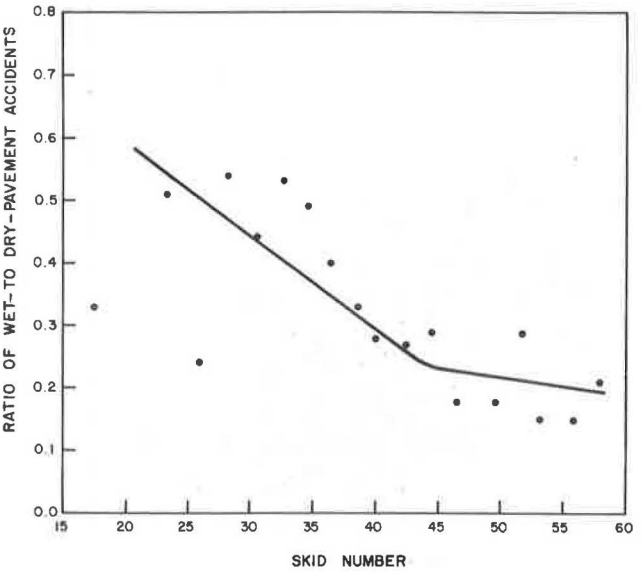

Figure 7. Average ratio of wet- to dry-pavement accidents of 120 test sections (grouped by skid number) versus SN, with volume stratification at AADT above 2700.

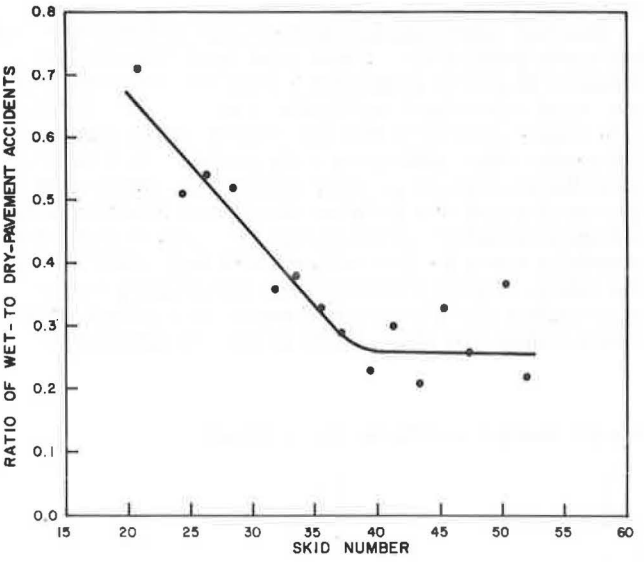

Figure 8. Ten-point moving averages: ratio of wet- to dry-pavement accidents for 230 test sections versus SN, without volume stratification.

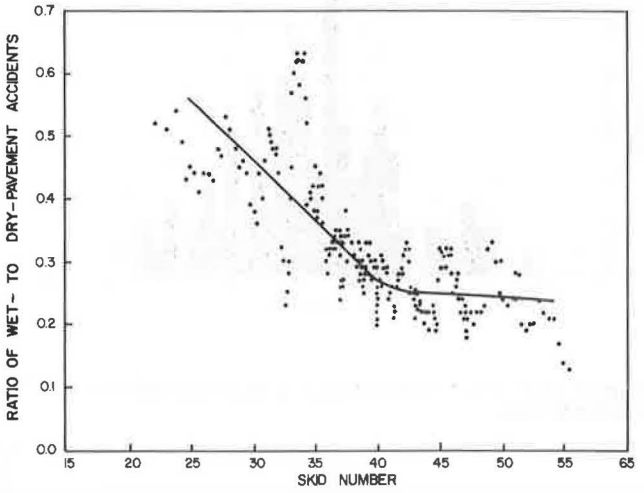

Figure 9. Ten-point moving averages: ratio of wet- to dry-pavement accidents for 110 test sections versus SN, with volume stratification at AADT below 2701.

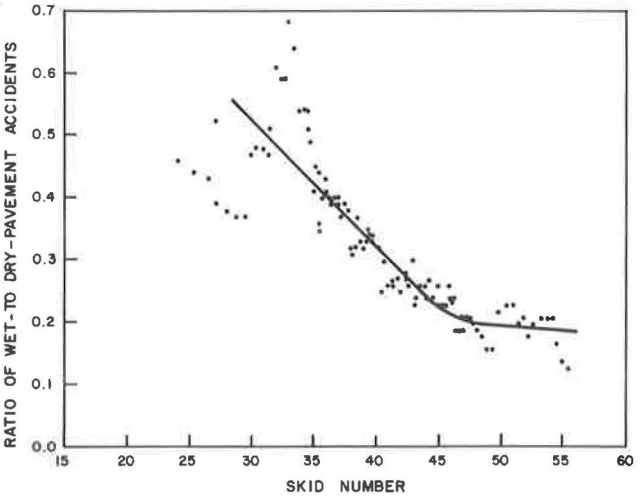

Figure 10. Ten-point moving averages: ratio of wet- to dry-pavement accidents for 120 test sections versus SN, with volume stratification at AADT above 2700.

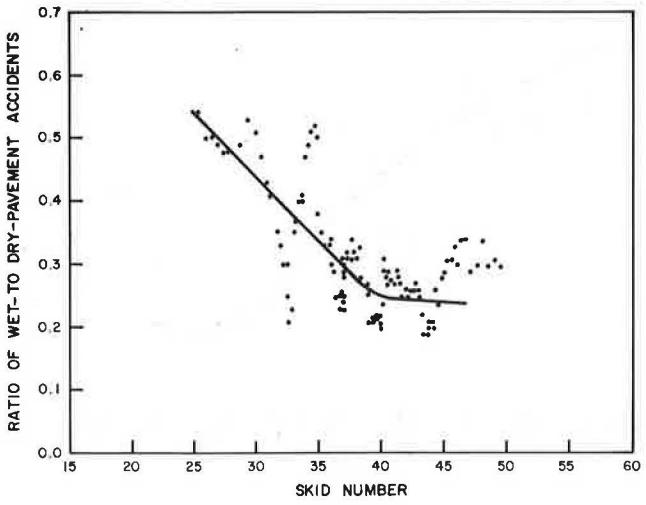

and the critical SN derived here will apply. If the measurements are conducted during other seasons of the year, the seasonal variation peculiar to a given pavement type must be taken into consideration.

Wet-pavement accident rates were calculated for 100 million vehicle·km (62 million vehicle-miles) for total travel under all pavement conditions rather than wet-pavement travel. The true accident rate for wet-pavement conditions would be nine times higher since pavements were wet only 11 percent of the time. Wet-weather accidents accounted for 22 percent of all accidents. Only 11 percent of all accidents, therefore, can be attributed to the time associated with wet-weather driving. This percentage, and the wet-pavement accident rate and the ratio of wet- to dry-pavement accidents vary from year to year according to the precipitation experience.

The influence of skid resistance on accidents for test sections with SNs above 41 was nominal. The ratio of wet- to dry-pavement accidents was approximately 0.23 (Figure 5). The lowest accident ratio would not be less than 0.13 since pavements were wet 11 percent of the time. Other factors related to wet-weather driving

Table 1. Data for test sections grouped by traffic volume.

Item	Annual Average Daily Traffic Volume							
	650 to 1700	1701 to 2700	2701 to 3700	3701 to 4700	4701 to 8400	650 to 2700	2701 to 8400	650 to 8400
Number of test sections	53	57	57	35	28	110	120	230
Skid number	42.8	38.2	39.2	37.0	37.6	40.4	38.2	39.3
Peak slip number	73.2	68.6	70.0	67.3	68.5	70.9	68.9	69.8
AADT	1263	2219	3159	4135	6036	1758	4115	2988
Access points per kilometer	5.2	5.3	5.2	6.1	5.5	5.2	5.5	5.3
Section length	6.9	7.2	6.2	5.6	4.8	7.0	5.7	6.3
Pavement width	19.7	20.4	20.4	21.7	22.0	20.1	21.2	20.6
Wet-pavement accident rate[a]	23.9	31.7	27.8	26.0	17.5	28.0	24.9	26.3
Ratio of wet- to dry-pavement accidents								
All sections	0.27	0.37	0.35	0.36	0.22	0.32	0.32	0.32
Tangent sections	0.25	0.28	0.27	0.32	0.20	0.26	0.27	0.27
Tangent sections on grade	0.28	0.40	0.33	0.37	0.35	0.34	0.35	0.34
All tangent sections	0.23	0.31	0.28	0.35	0.21	0.27	0.28	0.28
Level curved sections	0.30	0.52	0.39	0.49	0.24	0.41	0.38	0.40
Curved sections on grade	0.44	0.62	0.74	0.40	0.27	0.53	0.53	0.53
All curved sections	0.46	0.59	0.74	0.44	0.33	0.53	0.56	0.55
Ratio of dry- to dry-pavement accidents								
Level curved and level tangent sections	0.48	0.33	0.23	0.25	0.09	0.41	0.20	0.30
Curved and tangent sections on grade	0.99	1.58	0.77	0.58	0.25	1.30	0.59	0.93
All curved and all tangent sections	0.60	0.63	0.41	0.28	0.12	0.61	0.30	0.45
Ratio of wet- to wet-pavement accidents								
Level curved and level tangent sections	0.45	0.50	0.43	0.72	0.15	0.48	0.45	0.46
Curved and tangent sections on grade	0.72	1.24	1.45	0.62	0.21	0.99	0.92	0.95
All curved and all tangent sections	0.87	1.05	0.89	0.68	0.20	0.96	0.67	0.81

[a] Accidents/100 million vehicle·km.

Note: 1 km = 0.62 mile.

Figure 11. Average ratio of wet- to dry-pavement accidents of 230 test sections (grouped by peak slip numbers) versus PSN, without volume stratification.

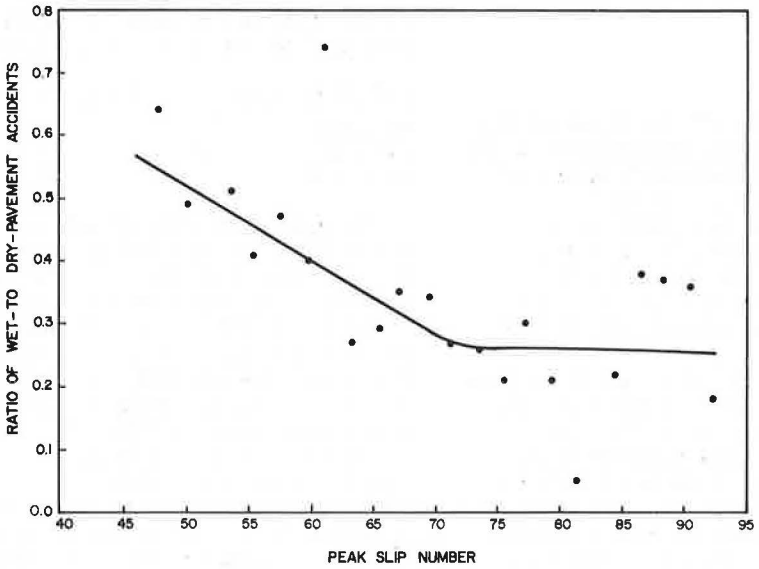

Figure 12. Average ratio of wet- to dry-pavement accidents of 110 test sections (grouped by peak slip numbers) versus PSN, with volume stratification at AADT below 2701.

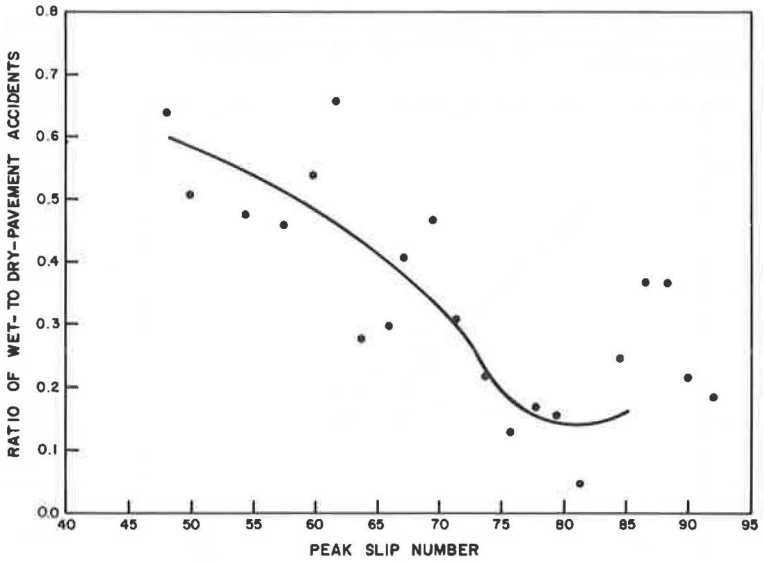

Figure 13. Average ratio of wet- to dry-pavement accidents of 120 test sections (grouped by peak slip numbers) versus PSN, with volume stratification at AADT above 2700.

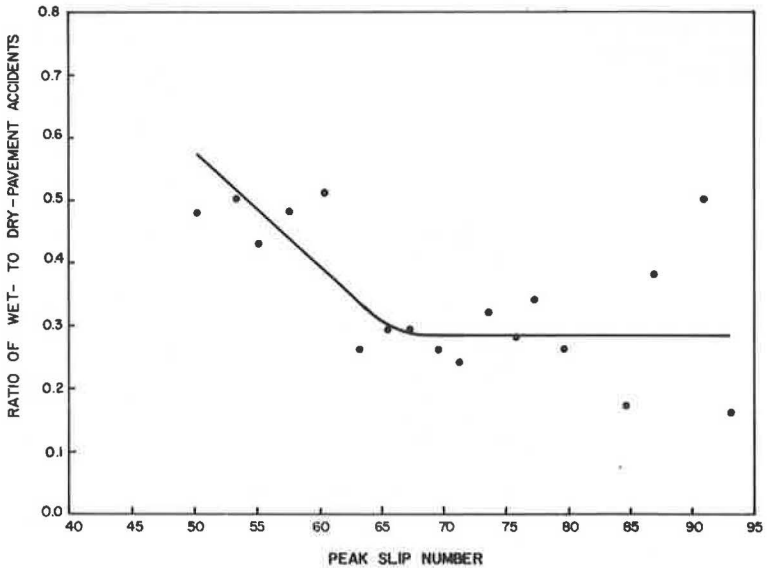

contributed to the elevated accident ratio.

PEAK SLIP NUMBERS AND ACCIDENTS

As stated above, the measurement that best correlates with accident experience remains to be established. The peak friction force was measured routinely during all tests; thus PSNs were available for analysis.

Multiple-regression analysis again indicated substantially better correlation between PSN and the ratio of wet- to dry-pavement accidents than with wet-pavement accident rate. The correlation coefficients were low (less than 0.350). Correlation with AADT was also evident.

Test sections were grouped by PSNs, and the average ratio of wet- to dry-pavement accidents was calculated for each group of two PSNs, as shown in Figures 11, 12, and 13. When all test sections were included (Figure 11), the greatest change in slope occurred at a PSN of 71. Stratification of data by AADTs indicated a change at a higher PSN for the low-volume roads and a lower PSN for the high-volume roads. Similar results were obtained by using the 10-point moving average; and the change in the slopes remained at the same PSNs. The critical PSNs are given in the following table.

AADT Stratification	Moving Average	Grouped by PSN
650 to 8400	71	71
2700 or less	74	74
Above 2700	65	65

The point of greatest change in slope of the curve in Figure 11 was at a PSN of 71 and in Figure 5 at SN of 41. According to Figure 3, a PSN of 71 is equivalent to SN of 40. The data were not so scattered in Figures 5, 6, and 7 as in Figures 11, 12, and 13; and, as cited above, there was a stronger correlation between accident occurrence and SNs than with PSNs. These findings, therefore, suggest that the SNs relate better to accident occurrence. This conclusion was not necessarily surprising because of the inherent measurement and chart analysis errors associated with peak slip resistance (PSN) determination. Peak slip resistance occurs for a very brief period of time during wheel lockup, and the measurement represents a much shorter length of pave-

ment than the locked-wheel test (SN). For that reason, the poor agreement between SN and PSN in Figure 3 was attributed largely to inaccuracies in PSN.

SUMMARY AND CONCLUSIONS

On rural, two-lane roads, ratio of wet- to dry-pavement accidents correlated best with pavement friction. Even using the best expression of accidents, we found that scatter and spurious variability in data seem inevitable. Averaging methods as a means of developing trends and minimizing scatter between variables were used in the study. Of the averaging methods investigated, the moving average and test sections grouped by SNs yielded more definite results. Definite trends were established in regard to the relationship between ratio of wet- to dry-pavement accidents and SN (Figures 5 and 10). When all test sections were included, the ratio of wet- to dry-pavement accidents decreased rapidly as SN increased to approximately 40; further increases in SN beyond this point resulted in only slight reduction in the ratio of wet- to dry-pavement accidents. Stratification of the data into two AADT groups showed that the critical SNs were higher for the low-volume roads than for the high-volume roads. Ratios of dry- to dry-pavement and wet- to wet-pavement accidents (Table 1) and sufficiency ratings suggested that the low-volume roads may have poorer geometric characteristics. The effect of traffic volume on the frictional demand of traffic, therefore, could not be separated from the other contributing influences.

Definite trends were also evident between ratio of wet- to dry-pavement accidents and PSN. The greatest change in slope of the trend line (Figure 11) occurred at a PSN of approximately 71. Scatter of data was somewhat worse than for SNs. This scatter was to be expected because of the inherent measurement and chart analysis inaccuracies associated with peak slip resistance determinations. A PSN of 71 is equivalent to an SN of approximately 40 (Figure 3); and, as shown in Figure 8, an SN of 40 also corresponds to the greatest change in slope of the trend line. Multiple-regression analysis, however, showed a stronger relationship between accident occurrence and SNs.

The curves shown in Figures 5 through 10 not only suggest critical SNs but may also be useful in ascertaining the level of accident experience peculiar to the roads involved in this study. No meaningful reduction in wet-pavement accidents may be realized by improving the skid resistance of those pavements that exhibit SNs above the critical value. Also, a low SN does not necessarily imply an accident problem. Some sections with low SNs obviously exhibited accident histories similar to sections with substantially higher SNs. Highway geometrics, pavement rutting and roughness, and so forth, of course, need to be considered in the selection of pavements for deslicking. However, the following general guide is suggested for assessing pavement skid resistance in Kentucky.

Skid Number	Skid-Resistance Assessment
Above 39	Skid resistant
33 to 39	Marginal
26 to 32	Slippery
Below 26	Very slippery

The ratio of wet- to dry-pavement accidents is particularly adaptable for screening sections because the ratio can be readily calculated. On the other hand, calculation of accident rates requires data on traffic volumes that are not always available or may be inaccurate. Also, a high wet-pavement accident rate may be misleading if the highway also has a high dry-pavement accident rate.

The findings cited in this study pertain to principal, two-lane rural roads (U.S. routes). These roads had posted speeds of 96.6 km/h (60 mph) for daytime and 80.5 km/h (50 mph) for nighttime. In response to the energy crisis, the posted speeds on these highways were changed on March 1, 1974, to 88.5 km/h (55 mph) for both daytime and nighttime. Fatalities, injuries, and accidents, as well as fatality rates, injury rates, and accident rates, have substantially decreased since the beginning of the energy crisis (4). Wet-weather accident experience has also been affected. The relationship between accident experience and pavement friction may have been altered as well.

ACKNOWLEDGMENTS

The work reported in this paper was done by the Bureau of Highways, Kentucky Department of Transportation, in cooperation with the Federal Highway Administration. Contents of the paper reflect our views and not necessarily the views or policies of the Kentucky Department of Transportation or the Federal Highway Administration.

REFERENCES

1. R. L. Rizenbergs, J. L. Burchett, J. A. Deacon, and C. T. Napier. Accidents on Rural Interstate and Parkway Roads and Their Relation to Pavement Friction. TRB, Transportation Research Record 584, 1976, pp. 22-36.
2. R. L. Rizenbergs, J. L. Burchett, and C. T. Napier. Skid Test Trailer: Description, Evaluation and Adaptation. Division of Research, Kentucky Department of Highways, Sept. 1972.
3. Field Procedure Manual for Sufficiency Ratings on All Systems. Kentucky Department of Highways, 1963.
4. K. R. Agent, D. R. Herd, and R. L. Rizenbergs. First-Year Effects of the Energy Crisis on Rural Highway Traffic in Kentucky. TRB, Transportation Research Record 567, 1976, pp. 70-81.

Publication of this paper sponsored by Committee on Surface Properties-Vehicle Interaction.

Critique of Tentative Skid-Resistance Guidelines

Stephen N. Runkle and David C. Mahone, Virginia Highway and Transportation Research Council, Charlottesville

The selection of appropriate minimum skid number (SN) values for wet pavements remains a major issue in skid-resistance research. The purpose of the research presented in this paper was to critique several reported accident and driver behavior studies related to skid resistance in an attempt to determine the most reasonable tentative guidelines for use in Virginia. The review confirmed our belief that required SN_{40} values vary with roadway and traffic conditions and that much work remains to be done regarding the determination of required SN_{40} values for specific roadway and traffic characteristics. For these reasons we concluded that accident data should continue to be the primary basis in Virginia for identifying wet-pavement sites that have high accident rates. However, general SN_{40} guidelines were selected for the purpose of determining potentially hazardous wet-pavement accident sites, that is, sites with SN_{40} values below the guideline values. Sites selected in this manner will be included in the normal site review process of the program to reduce wet-pavement accidents and may or may not be treated, depending on the results of the review process. The tentative SN_{40} guidelines selected and stated in terms of Virginia's survey of locked-wheel-trailer values are 30 for Interstate and other divided highways and 40 for two-lane highways.

The selection of appropriate minimum skid number (SN) values for wet pavements remains a major issue in skid-resistance research and a practical problem for organizations responsible for the construction and maintenance of highways. For the purpose of this discussion, SN refers to the locked-wheel skid number obtained with a skid trailer meeting the requirements for ASTM designation E 274-70.

Several studies have been undertaken to define the minimum desirable wet-pavement, skid-resistance level. As recognized by Kummer and Meyer, these studies can be divided into three groups (1):

1. Studies relating total accidents, wet-pavement accidents, or wet-pavement skidding accidents to some measure of skid resistance for the pavements on which the accidents occurred;
2. Driver behavior studies that usually involve measuring accelerations (usually negative) and relating these accelerations to SN values [the friction demand determined in this way is labeled FN, where FN = 100 (a/g), a is the measured acceleration in meters per square second, and g is the gravitational constant ($32.2/s^2$)]; and
3. Studies based on vehicle and pavement design (requisite FN levels based on vehicle design and highway geometric design are obviously limited only by the design criteria and not by driver behavior, and thus FN levels defined in this way may not agree with levels required for normal driving behavior).

The method used in the first of these study categories has the advantage of directly relating SN values as normally obtained in skid survey testing to accident experience. However, comparisons of various research results are difficult because of the variabilities involved in testing, even when the same test method is employed, and because of differences in traffic and highway characteristics.

The FN values developed in the second and third study categories must be converted to corresponding SN values. Assumptions regarding the relationship of FN to SN, including the question of whether FN represents the critical slip value obtained prior to skidding (and thus a higher value) or the locked-wheel skid value, vary among researchers. Furthermore, several researchers have indicated that modifications, in which such things as tire tread depth, pavement texture, and water depth are considered, should be made to SN values obtained from FN values so that they represent SN values available under normal driving conditions. Therefore, even if researchers determine a need for like FN values, they may specify different SN values because of varying philosophies regarding the relationship of FN to SN.

PURPOSE AND SCOPE

The purpose of this paper is to critique reported studies concerning minimum skid resistance (SN_{40}) guidelines. The critique resulted from a review of several studies to determine the most reasonable tentative guidelines for Virginia. The guidelines that have been established are tentative because they are based on the currently available research results we reviewed. These guidelines will be modified as necessary by future research results and used as secondary input to Virginia's program to reduce wet-pavement accidents. Wet-pavement accident statistics will be the prime indicator of pavements most in need of improved skid resistance.

Accident and driver behavior studies have been used to establish and modify these tentative guidelines. Studies concerning the required skid resistance as determined on the basis of vehicle or pavement design were not considered because these studies relate to theoretical limits that may or may not be exceeded in practice.

The guideline SN values presented in this paper are stated in terms of Virginia's current skid-trailer measurements. An evaluation of the skid trailer was conducted June 16 to 24, 1975, at the Field Test and Evaluation Center for Eastern States (EFTC) in East Liberty, Ohio. The conclusion was that the unit performed well; it obtained SN_{40} values approximately three units above those for the EFTC reference tester (2).

ACCIDENT STUDIES

Virginia Study

In a previous study we researched the relationship between skid resistance and percentage of wet-pavement accidents on 502.1 km (312 miles) of the Interstate highway system in Virginia. Based on our judgment, we separated the sites into the following four categories:

1. Open roadway—level and tangent noninterchange areas;
2. Nonopen roadway—vertical and horizontal curves at noninterchange areas;
3. Open interchange—level and tangent interchange areas; and
4. Nonopen interchange—vertical and horizontal curves at interchange areas.

Sight distance was considered highly important in the classification of sites; therefore, areas with gentle horizontal and vertical curves affording good sight dis-

tances were classified as open roadway. Estimated speeds for the sites studied were between 104.6 and 112.7 km/h (65 and 70 mph). Skid resistance was measured with the research council's locked-wheel trailer at 64.4 km/h (40 mph) but converted by correlation to predicted 64.4-km/h (40-mph) stopping distance skid numbers ($PSDN_{40}$) for comparison with the accident data.

We concluded that the percentage of wet-pavement accidents increased significantly below an SDN_{40} of 42; there was little difference among the categories. In terms of Virginia's current survey skid trailer, the SDN_{40} value of 42 would be equivalent to an SN_{40} of 29 based on the latest available correlation between the survey trailer and the stopping-distance method (4).

Texas Study

McCullough and Hankins studied the relationship of accidents per 161 million vehicles·km (100 million vehicle-miles) and skid resistance on 517 rural road sections that represented a random sample of Texas highways (5). Skid resistance was measured with a locked-wheel trailer at 32.2 and 80.5 km/h (20 and 50 mph), and the results of the study indicated that accidents increased at SN values below approximately 45 at 32.2 km/h (20 mph) and 35 and 80.5 km/h (50 mph). A straight-line extrapolation indicates an SN_{40} value of approximately 38.

A direct comparison of the results of the Virginia and Texas studies is difficult because we do not know how the sections studied in each case compared relative to roadway characteristics or mean traffic speeds, nor is there any way to relate the skid trailers involved. McCullough and Hankins recommend, based on the accident data and design practice, minimum SN values of 40 at 32.2 km/h (20 mph) and 30 at 80.5 km/h (50 mph) as a guide for surface improvements, which indicates a minimum desirable SN_{40} value of 33.

Tennessee Study

Moore and Humphreys studied 75 high accident sites in Tennessee to relate percentages of wet-pavement accidents to SN_{40} values obtained with a locked-wheel trailer (6). They concluded that the percentage of wet-pavement accidents increased significantly below an SN_{40} value of 40. The same difficulties discussed above are encountered in trying to relate those results directly to the Virginia results.

Kentucky Studies

Rizenbergs, Burchett, and Napier studied the relationship of pavement friction and wet-pavement accident experience on rural Interstate and parkway roads in Kentucky (7). Both SN and PSN were measured with a skid trailer at 112.7 km/h (70 mph). Several methods of relating wet-pavement accident data to SN_{40} and PSN_{70} were tried; the result was that wet-pavement accidents per 1.6 million vehicle·km (1 million vehicle-miles) correlated best. They concluded that the minimum desirable values were an SN_{70} of 27 and PSN_{70} of 57. Their reported correlations between SN_{70} and SN_{40} for bituminous and portland cement concrete pavements permit the determination of the minimum desirable SN_{40} value, which is approximately 40.

Because the data in the Kentucky and Virginia studies were for similar types of highways, the results would be expected to be fairly close, but, in fact, Kentucky results seem to indicate almost a 40 percent higher minimum desirable SN_{40} (40 versus 29). A comparison of the performance of the Kentucky and Virginia trailers at the Ohio test center indicated that the two units perform about the same.

In a second Kentucky study, Rizenbergs, Burchett, and Warren studied the relationship of wet-pavement accidents and skid resistance on rural, two-lane roads (8). In this study the test speed was 64.4 km/h (40 mph). For the roads studied, the ratio of wet- to dry-pavement accidents correlated best with pavement friction, and increases in SN_{40} above 40 resulted in only a slight reduction in the ratio. The authors also concluded that a low SN_{40} value does not necessarily imply an accident problem, and the general guidelines in the table below were suggested for assessing pavement skid resistance.

Skid Number	Skid-Resistance Assessment
>39	Skid resistant
33 to 39	Marginal
26 to 32	Slippery
<26	Very slippery

Arizona Study

Burns and Peters, as part of a general skid-resistance study of Arizona highways, determined a Mu-meter reading of 40 to be the desirable minimum value when one considers wet-pavement accident data (9). Based on a correlation contained in their paper, the Mu-meter value of 40 is equivalent to an SDN_{40} of 42 and thus an SN_{40} value of 29 for the Virginia survey trailer.

British Studies

Giles, Sabey, and Cardew correlated British portable tester (BPT) results with the risk of being in a skidding accident by measuring skid resistance at known high skidding-accident sites and several randomly selected sites. They developed the curve shown in Figure 1 (10) and, based on this curve, suggested minimum guidelines for the British portable tester as given in Table 1 (10). Similarly, minimum sideway friction coefficient (SFC) standards were suggested based on work by Giles (11). These suggested standards are given in the following table (1 km/h = 0.6 mph). Site categories are given in Table 1.

Site Category	Skidding Resistance: Test Speed (km/h)	Skidding Resistance: Sideway Force Coefficient
A	50	0.55
B	50	0.50
	80	0.45
	50	0.50
C	50	0.40

For the above standards to be meaningful to this study, the relationship of SFC_{30} values (as measured by the British portable tester) to locked-wheel skid trailer values (SN_{40}) must be known.

Giles developed the relationship shown in Figure 2 (10) between BPT values and locked-wheel retardation values at 48.3 km/h (30 mph) for a vehicle equipped with treaded tires. Dillard and Mahone reported on two studies relating the BPT and stopping distance skid values; the results are shown in Figure 3 (12). The 1960 and 1962 data shown in Figure 3 indicate quite different relationships between the two devices. There were several possible reasons for the differences as explained by Dillard and Mahone. One reason is that the 1960 data were collected on in-service road surfaces; the 1962 data, however, were obtained on specially prepared test surfaces.

In a discussion of the Dillard and Mahone paper,

Enrick offered several possible explanations for the different results; his evidence indicates that several of the 1962 test sites produced misleading results. Also, the 1960 data by Giles and a Purdue study cited by Enrick produced similar results though nearly 170 varied road surfaces in Great Britain and America were employed in the latter. Further, the use of the 1960 results as opposed to the 1962 results only serves to indicate a higher, and thus more conservative, SDN_{40} as the desirable minimum.

The following table gives SN_{40} values corresponding to the minimum BPT values given in Table 1. Set 1 values were determined by estimating required SDN_{40} values based on Figure 3 and converting them to SN_{40} values based on latest Virginia correlation results. Set 2 values are based on Figure 2 assuming retardation at 48.28 km/h (30 mph) is equal to SN_{30} and assuming a gradient of 0.5 SN. The two sets of SN_{40} values closely agree.

Category	BPT	Set 1	Set 2
A	65	51	51
B	55	39	39
C	45	26	28

Figure 1. Relative risk of a surface being a skidding-accident site for different values of skid resistance.

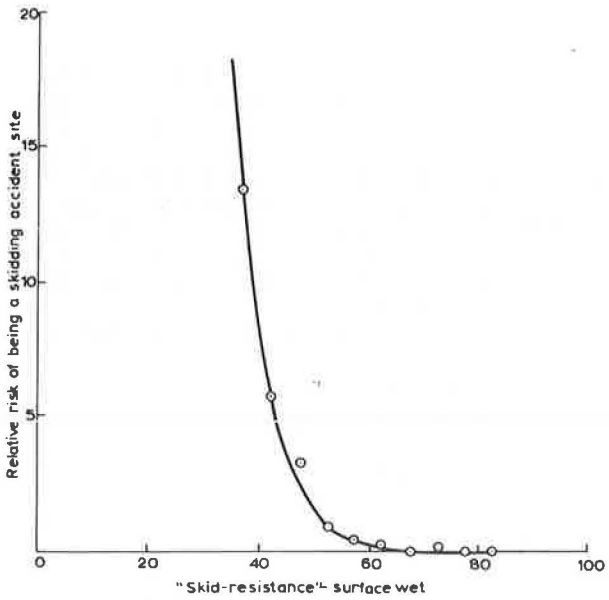

Desirable minimum SN_{40} values as derived from the various sources are summarized in the following table.

Source	Category A	Category B	Category C
Mahone and Runkle			29
McCullough and Hankins		38	
Moore and Humphreys		40	
Rizenbergs and others		40	40
Burns and Peters		29	
Giles, Sabey, and Cardew	51	39	27
Suggested composite	50	40	30

The values are grouped in accordance with those categories given in Table 1 although we felt that none of the accident studies would pertain in general terms to category A. Results of studies pertaining to roads like Interstate highways are given in category C; however, those pertaining to a cross section of rural highways are given in category B. The SN_{40} values equivalent to the BPT values for each category as determined by Giles are also given. Suggested composite SN_{40} values for all categories are indicated, based on the individual SN_{40} values given.

There is not total agreement on the SN_{40} values given, and no explanation can be offered as to why some of the differences exist. However, one could conclude that, in general, an SN_{40} value of 30 is the minimum desirable and probably is sufficient only on highways with good geometric conditions and moderate to low traffic congestion within normal traffic speeds. Higher SN_{40} values obviously are required in other cases, and in general terms an SN_{40} of 40 appears to be the desirable minimum for many two-lane rural highways. At severe curves, some interchange ramps, and some intersections, values as high as 50 may be required, as is suggested by the British guidelines.

DRIVER BEHAVIOR STUDIES

NCHRP Report 37

Probably the most referred to research in this country regarding minimum SN values is the report by Kummer and Meyer (1). Although results of some accident studies and vehicle and highway design criteria were evaluated by the study, the basis of the recommended minimum SN values was the maximum deceleration patterns of three drivers in local traffic and on long-distance trips. Data were obtained by a device mounted in the vehicle and with the knowledge of the driver. The minimum values recommended are intended to allow for normal driving maneuvers, including cornering and braking, by the majority of drivers under usual traffic conditions.

Table 1. Suggested values of skid resistance for use with portable tester.

Category	Type of Site	Skid Resistance on Wet Surface	Standard of Skidding Resistance Represented
A	Most difficult Roundabouts Bends with radius less than 150 m on derestricted roads Gradients, 1 in 20 or steeper, longer than 90 m Approach to traffic lights on derestricted roads	Above 65	Good (fulfilling the requirements even of fast traffic and making it unlikely that the road will be the scene of repeated skidding accidents)
B[a]	Roads and conditions not covered by categories A and C	Above 55	Generally satisfactory (meeting all but the most difficult conditions encountered on the roads)
C[a]	Easy Straight roads Easy gradients and curves No junctions Free from mixed traffic and emergency-creating conditions	Above 45	Satisfactory only in favorable circumstances
D	All sites	Below 45	Potentially slippery

Note: 1 m = 3.3 ft.

[a]On smooth-looking or fine-textured roads, in these categories, vehicles having smooth tires may not find the skid resistance adequate. For such roads, accident studies should also be made to ensure that there are no indications of difficulties due to skidding under wet conditions.

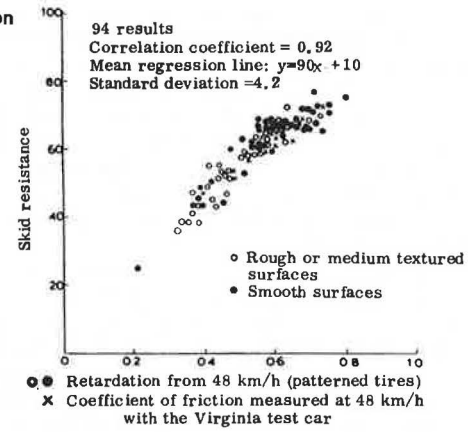

Figure 2. Comparison of measurements made with portable tester and locked-wheel braking method on all textures of road surface.

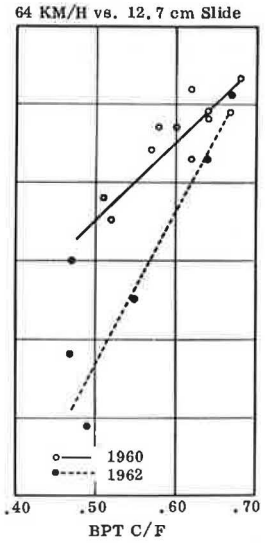

Figure 3. Relations between SDN_{40} and BPT.

Emergency maneuvers that might be the result of unforeseen traffic changes, driver misjudgment, or recklessness are not accounted for.

A summary of the deceleration data is given in Table 2 (1). In general, the higher decelerations occurred toward the end of a stop and thus were accompanied by low speeds. The six deceleration values above 40 on the 444.2-km (276-mile) trip all occurred at speeds below 32.2 km/h (20 mph). They concluded that FN values of 40 seemed to satisfy the normal needs of traffic, and higher values might be called for toward the end of a stop.

Table 3 (1) gives the selected FN values deemed desirable at different speeds based on the deceleration data (FN_0) and the conversion of these FN values to SN values. CSN indicates the additional FN value necessary to account for lateral decelerations during braking on a straight course as measured by Kummer and Meyer. $\Delta L/L$ represents the additional FN value necessary due to fluctuations in average wheel load. The values of $\overline{FN}$ and FN_d were computed as follows:

$$\overline{FN} = [(FN_0)^2 + (CSN)^2]^{1/2} \quad (1)$$

$$FN_d = [1/(1 \pm \Delta L/L)]\overline{FN} \quad (2)$$

In essence, then, the FN_d figures are the FN values recommended by Kummer and Meyer for the speeds shown.

The remaining conversions given in Table 3 are those required to change FN values to SN values. The K-factor is equivalent to FN/SN, assuming that FN represents critical braking and cornering slip numbers that occur prior to skidding and are normally larger than the locked-wheel SN values. SN_t and SN represent additions to the required SN necessary to compensate for fluctuations in measured SN values due to temperature changes and machine error. Table 3 thus gives the required SN values [SN(rounded)] at the speeds indicated, which account for each of the items as discussed above, and the recommended minimum SN_{40} values.

Table 2. Decelerations of three drivers in local traffic and on long-distance trips.

Deceleration FN		Combined Performance (Drivers A and B)				Combined Random and Square Courses				Driver C on 444.2-km Trip	
		Random Course		Square Course		Driver A		Driver B			
Range	Mean	No.	Percent	No.	Percent	No.	Percent	No.	Percent	No.	Percent
2.5 to 7.5	5	—	—	—	—	—	—	—	—	2	1.6
7.5 to 12.5	10	15	10.0	3	2.2	12	8.3	6	4.2	30	24.5
12.5 to 17.5	15	45	30.0	23	16.7	39	27.1	29	20.3	24	19.6
17.5 to 22.5	20	40	26.7	46	33.4	46	32.0	40	27.7	27	22.2
22.5 to 27.5	25	36	24.0	48	34.6	38	26.4	46	31.8	17	14.0
27.5 to 32.5	30	11	7.3	18	13.1	8	5.5	21	14.6	13	10.7
32.5 to 37.5	35	3	2.0	0	0	1	0.7	2	1.4	3	2.5
37.5 to 42.5	40	—	—	—	—	—	—	—	—	4	3.3
42.5 to 47.5	45	—	—	—	—	—	—	—	—	2	1.6
Total		150	100.0	138	100.0	144	100.0	144	100.0	122	100.0

Note: 1 km = 0.6 mile.

Table 3. Conversion of FN to corresponding SN.

Conversion Steps	SN for Mean Traffic Speed								
	0 km/h	16 km/h	32 km/h	48 km/h	64 km/h	81 km/h	97 km/h	113 km/h	129 km/h
FN_0	50	47.5	45	42.5	40	40	40	40	40
CSN	—	—	1.6	3.6	6.4	10.0	14.4	19.6	25.5
$\overline{FN}$	50	47.5	45	42.7	40.4	41.1	42.4	44.5	47.0
$\Delta L/L$(%)	—	—	2.5	5.0	7.5	10.0	12.5	15.0	18.5
FN_d	50	47.5	46.1	44.8	43.5	45.0	47.7	51.2	55.2
K-factor	1	1.3	1.6	1.8	2.0	2.2	2.4	2.6	2.8
SN_0	50	37.5	28.8	25	21.8	20.5	20	19.7	19.8
SN_t	56	43.5	34.8	31	27.8	26.5	26	25.7	25.8
SN	61	48.5	39.8	36	32.8	31.5	31	30.7	30.8
SN (rounded)	60	50	40	35	33	32	31	31	31
SN_{40}*	—	—	—	30	33	37	41	46	51

Note: 1 km/h = 0.6 mph.

*SN_{40} required based on SN (rounded) value (assuming a speed-SN gradient of 0.5).

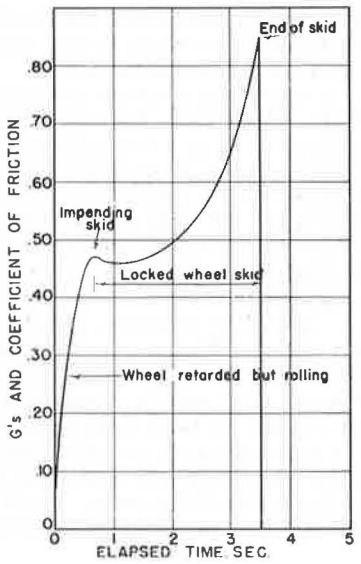

Figure 4. Typical change in coefficient of friction during skid.

Several observations are made regarding the conversion of FN to SN as given in Table 3. The equating of FN to critical brake or cornering slip resistance is not a procedure approved by all researchers; FN often is equated directly to SN (or locked-wheel deceleration). The critical slip values have often been shown to exceed the locked-wheel values, but the magnitude of the difference and the ability of an automobile braking on four wheels to achieve the difference in practice are somewhat uncertain.

Table 4 gives K-factors as determined from various sources. Those developed by Maycock were used by Kummer and Meyer in their conversion of FN values to SN values. Maycock's values were obtained by progressively braking the front wheels of an automobile to the locked condition and represent values obtained with treaded tires for water depths of 2.0 mm (0.8 in) or less [tests with bald tires were also run by Maycock (13), but the results were not used by Kummer and Meyer]. Dillard and Allen determined K-factors as part of a correlation study in Virginia during 1958 by comparing

Table 4. K-factors determined from various sources.

	16 km/h		32 km/h		64 km/h		80 km/h		88 km/h		97 km/h		113 km/h	
Sources	Avg	Range	Avg	Range	Avg	Range	Avg	Range	Avg	Range	Avg	Range	Avg	Range
Maycock			1.6	1.2 to 2.6	2.0	1.4 to 4.1					2.4	1.6 to 4.1		
Dillard	0.9	0.80 to 0.94			1.2	1.0 to 1.3			1.5	1.1 to 2.5				
Moyer			1.5	1.2 to 1.8	1.7	1.4 to 2.1					1.9	1.5 to 2.4		
Rizenbergs					1.8	1.5 to 2.2							2.0	1.4 to 2.6
Hartranft					1.8	1.5 to 3.8								
Lister			1.3	1.2 to 1.7										
Selected values	1.2		1.4		1.8		1.9				2.0		2.1	

Note: 1 km/h = 0.6 mph.

Table 5. Influence of K-factor on minimum SN_{40} values.

Speed (km/h)	FN_3[a]	Kummer and Meyer K[a]	Kummer and Meyer SN	Kummer and Meyer SN_{40}[b]	Selected Avg Values K[c]	Selected Avg Values SN	Selected Avg Values SN_{40}[b]	Selected Low Values K[d]	Selected Low Values SN	Selected Low Values SN_{40}[b]
32	46	1.6	29	19	1.4	33	23	0.9	51	41
48	45	1.8	25	20	1.6	28	23	1.0	45	40
64	44	2.0	22	22	1.8	24	24	1.1	40	40
80	45	2.2	21	26	1.9	24	29	1.3	35	40
97	48	2.4	20	30	2.0	24	34	1.5	32	42
113	51	2.6	20	35	2.1	24	39	1.7	30	45

Note: 1 km/h = 0.6 mph.

[a] From Table 3.
[b] Gradient assumed to be 0.5 SN.
[c] From Table 4.
[d] Estimate based on values in the tabulation at the bottom of next page and general change with speed as indicated in Table 4.

Table 6. 95th percentiles, 99th percentiles, and maximum required skid resistance and associated speeds, decelerations, and distances for 12 sites.

	Site Characteristics			95th Percentile				99th Percentile				Maximum			
Site Number	Highway Type	Mean Initial Speed (km/h)	Mean Hourly Traffic Count	Deceleration (g)	Speed (km/h)	Required SN_{40}	Distance From Stop Line[a] (m)	Deceleration (g)	Speed (km/h)	Required SN_{40}	Distance From Stop Line[a] (m)	Deceleration (g)	Speed (km/h)	Required SN_{40}	Distance From Stop Line[a] (m)
1	4	36	450	0.35	40	33	20	0.38	50	41	34	0.41	53	47	34
2	1	36	412	0.25	60	27	58	0.46	34	46	15	0.47	55	56	34
3	5	40	426	0.34	56	38	58	0.38	63	47	58	0.46	84	64	79
4	1	36	104	0.24	66	28	58	0.39	37	37	11	0.43	63	54	68
5	2	38	448	0.31	69	39	58	0.44	50	50	34	0.48	58	59	34
6	4	30	116	0.29	35	22	20	0.38	31	33	11	0.51	72	68	117
7	6	39	94	0.36	47	37	34	0.46	42	50	26	0.44	68	57	49
8	6	40	112	0.29	58	32	49	0.49	21	43	6	0.52	77	71	58
9	3	41	282	0.30	77	39	91	0.38	87	53	68	0.49	82	68	58
10	2	37	406	0.30	53	31	41	0.38	71	49	68	0.47	64	61	49
11	5	40	592	0.35	58	40	41	0.46	60	57	34	0.62	70	84	41
12	3	35	370	0.21	66	23	79	0.28	61	32	79	0.43	64	55	117

Note: 1 km/h = 0.6 mph; 1 m = 3.3 ft.
[a] Distance of first switch of deceleration interval relative to stop line.

Table 7. Required SN_{40} values at intersections under varying assumptions.

Maximum Deceleration From Table 6 (g)	Kummer and Meyer K-Value	Runkle and Mahone K-Value	Low K-Value	Table 6 SN_{40} Values
0.41	19	22	38	47
0.47	22	26	44	56
0.46	27	30	41	64
0.43	17	19	39	54
0.48	23	25	44	59
0.51	27	31	45	68
0.44	23	25	39	57
0.52	28	31	46	71
0.49	28	31	43	68
0.47	24	26	43	61
0.62	33	33	55	84
0.43	22	24	39	55
Average for all intersections	24	27	43	62

results obtained by a National Aeronautics and Space Administration trailer measuring incipient friction and a General Motors trailer measuring locked-wheel skid resistance (14). These values may be low relative to the others given because two test vehicles were used rather than one as in the other cases. Moyer developed the K-factors based on tests on various pavements in California (15, 16). Rizenbergs and others developed the K-factor at 112.7 km/h (70 mph) in the Kentucky accident studies previously cited (8, 9). Hartranft developed the K-factor at 64.4 km/h (40 mph) as part of a Pennsylvania State University correlation study of locked-wheel, peak slip, and peak side friction (17). Lister developed the K-factor by braking the front wheels of an automobile (18).

In each of the above situations the K-factors represent something other than an automobile braking all four wheels. When the automobile is braked, all four wheels do not reach the incipient friction stage simultaneously; therefore, the resulting averaged incipient friction and K-factors are somewhat lower than those thus far discussed. Dillard and Allen, in the 1958 Virginia research mentioned previously (14), also studied deceleration patterns throughout skids by an automobile in locked-wheel tests from a speed of 64.4 km/h (40 mph). Typically, the data indicated trends as shown in Figure 4; the incipient values were slightly higher than the initial locked-wheel values.

SN_{40} values were determined by two locked-wheel trailers at the same sites at which the peak decelerations were determined for the automobile. Thus, locked-wheel trailer skid values can be compared to peak skid values for the automobile as given in the table below. The speed is the speed at which peak deceleration occurred. SN_{40} was measured at 64 km/h (40 mph) corrected to speed shown, based on a gradient of 0.5 SN.

Site	Deceleration (g)	Speed (km/h)	Trailer A SN_{40}	Trailer A K-Factor	Trailer B SN_{40}	Trailer B K-Factor
1	27	61	27	1.00	24	1.12
2	38	56	40	0.95	34	1.12
3	52	56	53	0.98	–	–
4	72	53	71	1.01	67	1.07

The K-factors determined by this means are about equal to 1 for speeds between approximately 48.3 and 64.4 km/h (30 and 40 mph) and thus are lower than the values given in Table 4. Although these conclusions are based on an extremely limited amount of data, the K-factors used by Kummer and Meyer appear to be somewhat high. More research is desirable to determine what peak decelerations can be attained by an automobile and how they relate to locked-wheel decelerations and SN_{40}.

Table 5 indicates the effects of various assumptions regarding K-factors on desirable minimum SN_{40} values; allowances were not made for temperature corrections or machine error. The SN_{40} values are 2 to 4 units higher for selected average K-factors than for the K-factors used by Kummer and Meyer; when selected low K-factors are used, the SN_{40} values are much higher (10 to 22 units).

The comparison of the SN_{40} values in Table 5 with the composite minimum SN_{40} values given in the tabulation on page 3, column 2, is interesting. Since the values as determined by Kummer and Meyer apply to main rural highways (not Interstate), it seems reasonable to compare their results with category B in the above table of desirable SN_{40} values, for which a minimum SN_{40} value of 40 is indicated. Because these roads are likely to have traffic speeds between 80.5 and 96.6 km/h (50 and 60 mph), the selected low K-factors appear to yield the most reasonable SN_{40} values of 40 and 42.

NCHRP Report 154

A second major study dealing with the establishment of minimum SN_{40} values based on driver behavior is the one described in NCHRP Report 154 (19). The intent of the study was to determine that level of lateral or longitudinal acceleration that accommodated a reasonable maximum demand in cornering or braking and to relate this level to an SN_{40} value, thus determining an appropriate K-factor. Acceleration data were obtained on dry pavements by using tape switches to sample from the normal traffic flow without the drivers' knowledge. Data were obtained at 12 intersection sites and 10 curve sites.

Table 6 (19) contains the data obtained at the 12 intersection sites. The SN_{40} values given were determined empirically by relating locked-wheel deceleration values as obtained with a 1970 Plymouth Fury and a 1971 Ford Mustang to SN_{40} values obtained with the National Bureau of Standards skid trailer. Conventional bias ply, belted bias ply, and radial tires were used on the Plymouth and belted bias tires on the Ford. The tests were conducted at the Texas Transportation Institute skid pad facility. The relationships determined are considered by the authors of this report to be generally applicable to U.S. automobiles that have tires in good condition. The relationships developed are based on the maximum decelerations from among the four vehicle and tire combinations and are thus conservative.

As with the Kummer and Meyer study, the required SN_{40} values for the 12 intersections studied by the authors of NCHRP Report 154 vary widely, depending on the K-values selected for the conversion of FN to SN. Table 7 shows SN_{40} values determined by using three sets of K-values—the ones developed by Kummer and Meyer, the average of selected values by the present authors, and the low values previously mentioned—and by using the SN_{40} values required as determined by the authors of NCHRP Report 154.

Unfortunately skid tests were not performed at the 12 intersections with an ASTM 274 trailer. We feel that it is quite unlikely that the average SN_{40} value for all intersections would approach the average SN_{40} value of 62 as computed from the required SN_{40} values given in NCHRP Report 154. Therefore, we believe it is more reasonable to assume that rolling incipient friction should be considered, and a set of the K-values as given in Table 7 would provide a means of calculating the needed friction. Since the surfaces are located at intersections, we prefer the low K-values. In addition, intersections would intuitively seem to need SN_{40} values in the range of 38 to 55.

SELECTION OF TENTATIVE SN_{40} GUIDELINES

Different SN_{40} values are required for varying roadway and traffic conditions. Also, much work remains to be done regarding the determination of required SN_{40} values for specific roadway and traffic characteristics, including the determination of the proper relationship between FN and SN. For these two reasons, it appears that accident data will continue for some time to provide the primary basis for identifying high accident sites on wet pavement; survey skid data will be used once sites are selected.

Nevertheless, selecting minimum SN_{40} guidelines is desirable for the purpose of identifying potentially hazardous sites for inclusion in the routine site review process in Virginia's program to reduce wet-pavement accidents. For this purpose, an SN_{40} value of 30 is considered to be the minimum guideline value for Interstate and other divided highways in Virginia, and an SN_{40} value of 40 is considered to be the minimum guideline value for two-lane highways. Sites with values below these guideline values will not automatically be scheduled for treatment, but will be included for evaluation with sites selected by use of accident data. Site treatments should be allocated on a priority basis to achieve the maximum reduction of wet-pavement accidents.

REFERENCES

1. H. W. Kummer and W. E. Meyer. Tentative Skid-Resistance Requirements for Main Rural Highways. NCHRP Rept. 37, 1967.
2. E. A. Whitehurst. Field Test and Evaluation Center for Eastern States, East Liberty, Ohio. Skid Measurement System Evaluation, Ohio State Univ., Columbus, 1975.
3. D. C. Mahone and S. N. Runkle. Pavement Friction Needs. HRB, Highway Research Record 396, 1972, pp. 1-11.
4. S. N. Runkle. Methodology for Utilizing Survey Data. Virginia Highway and Transportation Research Council, Charlottesville, Oct. 1975.
5. B. F. McCullough and K. D. Hankins. Skid Resistance Guidelines for Surface Improvements on Texas Highways. Research Section, Texas Highway Department, Austin, May 1965.
6. A. B. Moore and J. B. Humphreys. High Speed Skid Resistance and the Effects of Surface Texture on the Accident Rate. Department of Civil Engineering, Univ. of Tennessee, May 1972.
7. R. L. Rizenbergs, J. L. Burchett, and C. T. Napier. Accidents on Rural Interstate and Parkway Roads and Their Relation to Pavement Friction. Division of Research, Kentucky Department of Transportation, Lexington, Oct. 1973.
8. R. L. Rizenbergs, J. L. Burchett, and L. A. Warren. Accidents on Rural, Two-Lane Roads and Their Relation to Pavement Friction. Division of Research, Kentucky Department of Transportation, Lexington, April 1976.
9. J. C. Burns and R. J. Peters. Surface Friction Study of Arizona Highways. HRB, Highway Research Record 471, 1973, pp. 1-12.
10. Symposium on Skid Resistance. ASTM, Philadelphia, Special Technical Publ. 326, Dec. 1962, pp. 50-74.
11. G. F. Salt and W. S. Szatkowski. A Guide to Levels of Skidding Resistance for Roads. U.K. Transport and Road Research Laboratory, Crowthorne, England, Rept. LR 510, 1973.
12. J. H. Dillard and D. C. Mahone. Measuring Road Surface Slipperiness. ASTM, Philadelphia, Special Technical Publ. 366, June 1963.
13. G. Maycock. Studies on the Skidding Resistance of Passenger-Car Tyres on Wet Surfaces. Proc., Institute of Mechnical Engineers, Automobile Division, Vol. 180, Pt. 2A, 1965 to 1966, pp. 122-141.
14. J. H. Dillard and T. M. Allen. Correlation Study: Comparison of Several Methods of Measuring Road Surface Friction. Proc., Pt. 2, International Skid Prevention Conference, Virginia Council of Highway Investigation and Research, Charlottesville, Aug. 1959, pp. 381-410.
15. R. Moyer. A Review of the Variables Affecting Pavement Slipperiness. Proc., Pt. 2, International Skid Prevention Conference, Virginia Council of Highway Investigation and Research, Charlottesville, Aug. 1959, pp. 411-433.
16. R. Moyer. Effect of Pavement Type and Composition on Slipperiness: California Experience. Proc., Pt. 2, International Skid Prevention Conference, Virginia Council of Highway Investigation and Research, Charlottesville, Aug. 1959, pp. 469-484.
17. T. J. Hartranft. The Relationship of Locked-Wheel Friction to That of Other Test Modes. Pennsylvania Transportation Institute, Feb. 1975.
18. R. D. Lister. Some Problems of Emergency Braking in Road Vehicles. Proc., Symposium on Control of Vehicles During Braking and Cornering, Institute of Mechanical Engineering, London, June 1963.
19. Determining Pavement Skid-Resistance Requirements at Intersections and Braking Sites. NCHRP Rept. 154, 1974.

Publication of this paper sponsored by Committee on Surface Properties-Vehicle Interaction.

Notice: The Transportation Research Board does not endorse products or manufacturers. Names of manufacturers appear in this report because they are considered essential to its object.

Rehabilitation Decision Model

Douglas I. Anderson, Dale E. Peterson, and L. Wayne Shepherd,
Utah Department of Transportation

A study was made of Utah's flexible pavement performance system to introduce new procedures and to alter existing procedures. The terminal serviceability concept was revised to consider functional class as well as average daily traffic. Highways with high average daily traffic were assigned a high terminal serviceability index to reduce user costs. A computerized pavement-rating system was developed to aid maintenance personnel in making the most appropriate pavement rehabilitation decision. The system can also be used by planning and programming personnel to

estimate future expenditures in each district. A computer program generates priority listings based on the failure modes of serviceability, distress, structural adequacy, and skid resistance. An overall listing is produced that considers failure modes with respect to average daily traffic, 80-kN (18-kip) loads, running speeds, and functional class.

Maintenance of bituminous-surfaced pavements requires periodic rehabilitation. The need for maintenance, the type needed, and the optimum time for rehabilitation are key elements. Systems designed to accomplish these tasks are needed also to establish administrative policies and to aid in the programming of appropriate amounts of construction and maintenance funds.

A model was developed to help planning and maintenance personnel plan rehabilitation strategies. The model deals only with a limited number of variables and does not consider all of the variables related to pavement aging, economic constraints, and political decisions.

Experience shows that a detailed printout of pavement condition is needed only for projects under consideration for major rehabilitation, i.e., reconstruction, overlay, recycling, and surface seals. The use of field data, such as pavement-distress values, deflection readings, and roughness, is necessary to establish priorities; however, these data supplied in their entirety are overwhelming to anyone attempting to compare pavement conditions of a large number of highway sections. Therefore, detailed analysis is reserved for pavements chosen for rehabilitation. An example of a detailed data sheet is presented in Figure 1. These data are used to review the range and magnitudes of deflection readings, to estimate surface and base structural conditions, and to predict the remaining life of a given pavement. Visual inspection data on the surface condition and objective data related to transverse, longitudinal, and load-cracking conditions are listed. The pavement roughness incorporated into the present serviceability index (PSI) and actual skid-meter data that measure the slipperiness of the surface are made available. These data and the route description, pavement dimensions, and traffic measurements can be used by the maintenance engineer to determine the specific type of rehabilitation needed.

The preliminary analysis is aimed at the selection of those highways that will be upgraded and is based on the output of the computer program that contains a set of condition and priority listings to be used by maintenance and planning personnel.

In the Utah system, ranking the pavements to receive maintenance and determining the most effective method for rehabilitation are based on present pavement condition and deterioration history, properties of the materials and mixes in place, traffic requirements, functional class, highway geometry, and environmental conditions. Information on each of these areas must be gathered to isolate modes of deterioration, extent of progress, and rate at which deterioration is occurring. Once this information has been gathered, a priority listing can be made based on functional class and traffic demands to minimize user costs and future maintenance costs due to pavement deterioration. The number of highways rehabilitated and the extent of rehabilitation are dependent on the funds available and the urgency of the problem (1).

The significance of each of the areas mentioned varies for each highway and failure mechanism in determining the extent of further testing or analysis. For example, deterioration apparently related to materials may lead to tests such as asphalt stiffness or density calculations. Pavements that fail because of increased traffic load should be subjected to increased testing with the dynaflect to check the structural adequacy of each kilometer of the section.

The following sections discuss the major factors related to pavement condition and their use in the preliminary analysis.

PRESENT SERVICEABILITY INDEX

Utah uses the present serviceability index as an indicator of the rideability of a pavement. Data gathered from the Mays road meter is the main determinant of PSI; the meter, mounted in an automobile, is positioned to measure the vertical movement of the rear axle. The PSI rating of pavement is given below.

PSI Rating	Pavement Condition	PSI Rating	Pavement Condition
4 to 5	Very good	2 to 3	Fair
3 to 4	Good	1 to 2	Poor

The following formula for PSI was developed at the AASHO Road Test (2), and customary units are therefore used.

$$PSI = 4.18 - 0.007\,(RC)^{0.658} - 0.0.\quad C + P - 1.34\,RD^2 \qquad (1)$$

where

RC = sum of roadmeter roughness counts per mile,
C = square feet of cracked area per 1000 ft^2 of flexible pavement surface,
P = square feet of patched area per 1000 ft^2 of pavement surface, and
RD = average rut depth measured at deepest part of rut.

As the PSI of a pavement decreases, the cost of vehicle operation increases. Figure 2 shows the relationship between operating costs, running speed, and PSI (3). Pavement roughness also has an effect on highway safety. Figure 3 shows the relationship between the probability of accident occurrence, running speed, and PSI. At any speed, accidents are more apt to occur on rough pavement surfaces.

For planning and maintenance purposes, one must not only know the magnitude of the PSI at any particular time but also the relative change in PSI with time. If rideability declines rapidly, the pavement will most likely reach the terminal serviceability index (TSI) sooner (Figure 4A). The TSI is the value of serviceability of the pavement in need of rehabilitation before it deteriorates beyond repair by normal maintenance (4).

High-volume highways, such as Interstate highways, are assigned a TSI value of 2.5, and most low-volume highways are assigned a value of 2.0. The values are based on user costs, which include fuel consumption. Reports show that fuel consumption at a speed of 80.5 km/h (50 mph) increases by 50 percent when the vehicle is driven on badly broken patched asphalt compared to when the automobile is driven on smooth pavement (1).

Figure 5 shows the relation of TSI to average daily traffic (ADT). Functional class remains a controlling factor at low and medium traffic levels; minimum values are specified at 2.5 and 2.0 as before. At high traffic volumes, TSI is increased to ensure a higher level of service.

The pavements in each maintenance district are listed in order from the roughest to the smoothest on the basis of average PSI of that highway section (Table 1). This

Figure 1. Detailed data sheet.

PAVEMENT EVALUATION FOR STATE ROUTE 016 SECTION 2 SUB SECTION 0 RICH COUNTY (17) DISTRICT 1 FAP-12
FROM WOODRUFF-NORTH-LIMITS MILEPOST 10.06 TO RANDOLPH-NORTH-LIMITS MILEPOST 21.00 LENGTH 10.94
MATERIAL BITUMINOUS SURFACE COARSE (BSC) MAINTENANCE SHED 137 I.D. NO. 445 WIDTH 12.
YEARLY INCREASE IN 18K LOADS 5.0 % PRESENT 18K LOADS 1.16850+04 T.S.I. 2.0

* * DYNAFLECT TEST DATA * *

NO. OF TESTS 11 DATE 9/11/75 HR 15 MIN 10
TEMPERATURES: AIR 67.00, SURFACE 69.00, PAVEMENT 70.00
WHL PATH OSWP LANE NBL LAST REVISION
F= 2.325

	DMD	SNSR 2	SNSR 3	SNSR 4	SNSR 5
OUTLYING VALUES	1.62	****	****	****	****
MEAN	1.21	.82	.52	.36	.25
STANDARD DEVIATION	.16	.12	.07	.07	.04
VARIANCE	.03	.01	.01	.00	.00
T(N)	2.58	2.22	1.66	1.87	1.40
ACTUAL READINGS	1.14	.72	.44	.29	.22
	.99	.68	.42	.29	.22
	1.14	.74	.46	.29	.20
	1.26	.90	.52	.30	.22
	1.32	.96	.64	.44	.30
	1.62	1.08	.62	.48	.30
	1.20	.80	.54	.38	.29
	1.14	.78	.46	.30	.23
	1.14	.82	.58	.40	.22
	1.14	.76	.48	.36	.25
	1.20	.80	.54	.38	.28

* * DYNAFLECT SUMMARY AND AVERAGE CONDITIONS * *

	DMD	SCI	BCI	18K LOADS TO FAIURE	YLTF
MIN	.99	.31	.07	1.2502+06	14
MAX	1.62	.54	.18	2.5856+05	10
AVE	1.21	.39	.11	6.6099+05	13

STRUCTURAL NO. REQUIRED FOR 10, YEARS ADDITIONAL LIFE IS .00
AVERAGE SCI & BCI INDICATE PAVEMENT AND SUBGRADE STRONG.
IF PRESENT TRENDS CONTINUE, THE STRUCTURAL NEEDS ARE
LOW AND THE ROAD WILL PROBABLY LAST OVER TEN YEARS.

SCIREQ= .59 BCIREQ= .14 DMDREQ= 1.74 IDSYRS= 13

* * SERVICEABILITY SUMMARY AND AVERAGE CONDITIONS * *

NO. TESTS 11 DATE 12/ 9/75 MPH 50. PSI: AVERAGE 3.1 MINIMUM 2.9 MAXIMUM 3.4

AVERAGE SURFACE WEAR 3.5 AVERAGE POPOUTS 3.
AVERAGE WEATHERING 3.5 AVERAGE UNIFORMITY 4.3
AVERAGE RUT DEPTH (IN) .18 YN 14 YX 24 YA 24

AVERAGE P.S.I. INDICATES THAT THE SERVICE NEEDS ARE LOW AND WILL PROBABLY FALL BELOW THE T.S.I. IN NOT LESS THAN TEN YRS

AVERAGE CRACKING PER 1000 SQ. FT. TRANSVERSE SEALED	TRANSVERSE NOT SEALED	LONGITUDINAL SEALED (FT)	LONGITUDINAL NOT SEALED	LOAD MAP TYPE SQ.FT.	LOAD ALLIG. TYPE SQ.FT.	AVERAGE PATCHING PER 1000 SQ. FT. SKIN SQ.FT.	PATCHING DEEP SQ.FT.	AVERAGE CONDITION OF TRANSVERSE AND LONGITUDINAL CRACKS OPEN.	AURAS.	MULT.
0.	0.	0.	0.	833.	0.	0.	0.	3.8	3.8	3.8

* * SKIDMETER TEST DATA * *

NO. TESTS 6 DATE 9/11/75 TEMPS: AIR 53.00 ASPHALT 55.0

TEST	01	02	03	04	05	06	07	08	09	10	11	12	13
SKD IND	50	50	62	69	66	64	**	**	**	**	**	**	**

* * SKIDMETER SUMMARY AND AVERAGE CONDITIONS * *

SKID INDEX: MINIMUM 50 MAXIMUM 69 AVERAGE 60

AVERAGE SKID INDEX INDICATES THAT THE ROAD IS MARGINAL, FURTHER MONITORING SUGGESTED.

Figure 2. Relationship between operating costs, running speed, and PSI.

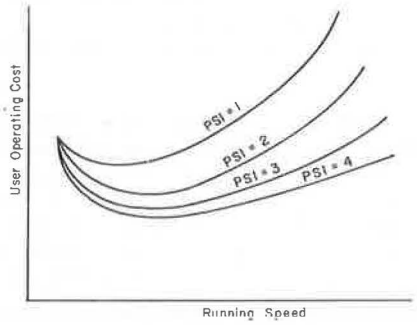

Figure 3. Relationship between accident occurrence, running speed, and PSI.

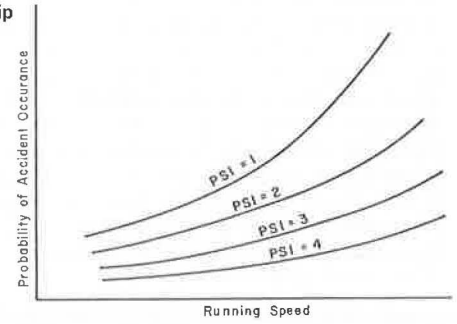

Figure 4. Pavement condition versus time.

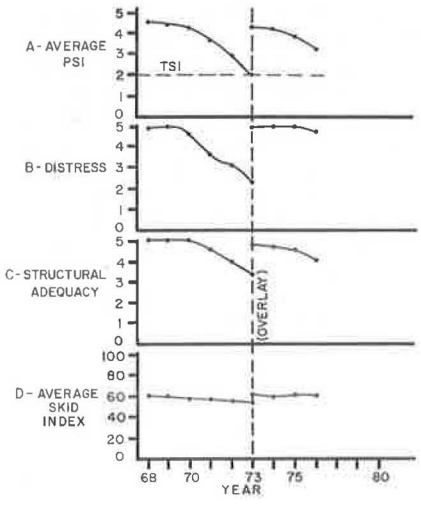

Figure 5. TSI versus ADT per lane.

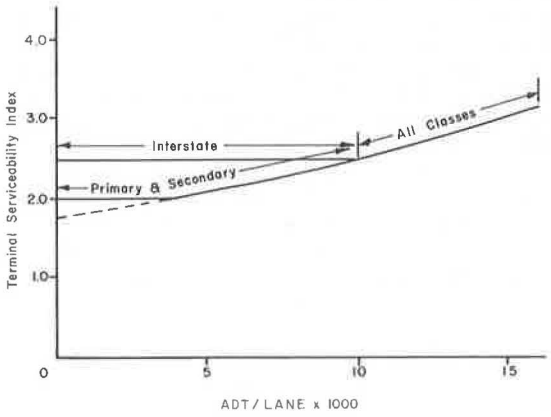

condition listing gives a preliminary indication of which pavements most need attention but not the best method for rehabilitation and can be used to establish the existing needs with respect to rideability for each district. The total lane kilometers of pavement below a specific level of service can be obtained and related to the cost needed to maintain or restore those areas by reference to the appropriate detailed data sheets. Also by comparing listings from previous years, one can predict failures and estimate future needs.

A similar listing based on the minimum PSI reading within each highway section is also provided in the program. This list reflects short rough areas requiring maintenance such as patches, bridge decks, and utility construction sites. This list is required because a short rough stretch could be left unidentified if the average PSI value on that pavement is adequate.

A third serviceability listing identifies sections that have reached the TSI specified for these sections. The sections that have dropped below TSI by the greatest amount appear first on the list. Before the pavement is programmed for rehabilitation however, consideration must be given to things such as costs due to maintenance delays, impacts on the present and future economics of the area, and changes in traffic configurations on adjoining facilities.

PAVEMENT DISTRESS RATING

In the routine evaluation of distress, 11 pavement parameters are reviewed; the 7 parameters that are given a rating on a scale from 0 to 5, where 5 is a condition showing no distress, are opening, abrasion, multiplicity of cracks, wear, weathering, popouts, and uniformity of surface. The other 4 parameters, given an approximate value per 1000 square units of pavement, are transverse cracking, longitudinal cracking, map cracking, and patching. Definitions of the conditions for each rating used in Utah are given in a previous report (4). This evaluation should be done only by trained personnel so that consistency throughout the state can be maintained. Each number on the rating scale should be well defined, and the evaluator should be familiar with each pavement condition.

Pavement distress does not necessarily indicate a rough condition that would be noticeable to materials. For example, a cracked pavement may provide a smooth ride for a period of time. However, a cracked surface allows moisture to reach the subgrade; a loss in matrix and erosion around the cracks may then occur and eventually lead to complete failure. Rutting can occur without creating a rough situation under certain driving conditions but can cause difficulty when drivers change lanes. Also, rutting can cause hydroplaning when pavement is wet and will eventually lead to strain cracking along the wheel path. The Maintenance Division must not only correct deteriorated pavements but also recognize which pavements most need attention to prevent extensive deterioration and greater costs.

STRUCTURAL ADEQUACY

The structure of a pavement being considered for rehabilitation must be analyzed for ability to support traffic loads. The Dynaflect is used to predict the remaining years to failure based on measured traffic loading on the highway and projected yearly increase. A listing is then made of the pavements in each district in the order in which they will probably fail structurally. Sections can be selected from this list for increases in structural adequacy. The maintenance engineer may request a secondary analysis, which also would incorporate use of the Dynaflect, to obtain a more extensive testing of weak areas. If an overlay is selected as the mode of upgrading the structure, the deflection data can be used to design the thickness of the overlay. A thicker overlay may be placed on the deteriorated areas, and some areas may even be left untouched rather than overlay the entire section with one thickness (5). Skipping nondeteriorated areas could greatly reduce the cost of a rehabilitation.

For comparison, the structural adequacy prediction was modified to a 0 to 5 rating similar to those used in the PSI and distress analyses. This system should be more compatible with the rest of the pavement rehabilitation model. In cases where a years-to-failure criterion is desired, the following can be used:

Structural Rating	Years to Failure	Structural Rating	Years to Failure
5.0	>10	2.5	3
4.5	8 to 10	2.0	2
4.0	6 to 7	1.5	1
3.5	5	1.0	0
3.0	4		

In the past, failure predictions based on structural adequacy have been misused; Dynaflect data cannot be used absolutely to predict the failure of a pavement. The analysis can only indicate structural failure based on the load-carrying capacity of the pavement structure. The modes of failure of a highway are interrelated. The presence of any one of the three basic failure modes (roughness, distress, or structural) usually precedes the appearance of the remaining two. Theoretically, years to failure based on a structural analysis should result in a decrease by 1 year each successive year; for example, at 10 years 1 year, at 9 years another year, and so forth, to 10 years and failure. In reality, however, we often observe predictions such as 10 years to failure the first year, 5 years the next year, and 2 years the next year. This apparent accelerated failure can be due to increased traffic loading, a rough condition, or distress weakening of the pavement structure. The observation of any single year's prediction can be misinterpreted, misused, and inevitably mistrusted. Therefore, adopting the 0 to 5 rating system of structural failure prediction rather than years to failure seems reasonable. The basic theory, however, remains sound. A reasonable indication can be obtained of how well the structure is supporting the present traffic loadings and how long the structure will perform adequately under projected traffic loadings if pavement distress or other factors do not accelerate failure.

SKID RESISTANCE

The Mu-meter is used to evaluate pavement surfaces for slipperiness. This device estimates surface skid resistance by pivoting the testing wheels to an angle with the line of movement at 64.4 km/h (40 mph) and measuring the resulting side force generated. The skid indexes range from 0 to 100; any surface that measures below 35 is considered to be in a hazardous condition. Lengths of 402 m (0.25 mile) are tested every 3.22 km (2 miles) within each section (plus any areas that appear to be slippery). Two listings of highway sections are needed to properly select highway sections for skid improvements. The average skid values of each section are listed in order from most slippery to least slippery to isolate sections that need surface rehabilitation. Minimum skid reading within each section is also listed to indicate smaller areas that need attention such as patches, nonuniform construction, or bleeding areas.

OVERALL PRIORITY RANKING

When reviewed individually, these lists can be helpful in establishing priorities as to which pavements are in need of maintenance, what type of failure is present, and to some extent how far the problem has progressed. However, to obtain an indication of the overall condition and to gain insight as to the most efficient form of rehabilitation to pursue, one must analyze the listings collectively as well as individually.

The interrelation between the general failure modes is important in determining the type and time of a rehabilitation effort because one form of deterioration leads to another. The degree to which deterioration progresses indicates when and how extensive the maintenance strategy must be to ensure proper service. Figure 6 is a diagram of the development of pavement failure. Because skid problems are surface problems and only slightly related to other modes of failure, they are not included in the flow chart. In new highway construction the intent is to obtain a pavement system that is structurally sound, has no initial pavement distress, and has a smooth riding surface. Pavement deterioration can occur if one of these requirements is not fully met in construction, if some unexpected problem occurs while the pavement is in service, or as the natural pavement aging processes take place. When

Table 1. Pavement sections ranked by average PSI.

Number	State Route	Length (km)	Beginning Terminus	Ending Terminus	Index
1	E02	13.52	Saltair	SLC Airport	1.9
2	106	0.56	Junction Utah-131	4th N. Bountiful	2.3
3	171	2.82	Redwood Road	Junction Utah-I15	2.7
4	201	1.27	Junction I-15	Junction Utah-271	2.7
5	186	1.61	East end US-40	2500 West	2.9
6	171	8.53	Junction Utah-111	4000 West	3.0
7	E02	5.79	Coalville	Echo Dam	3.0
8	270	1.21	East end I-15	1st W. Railroad	3.0
9	201	3.27	Redwood Road	Junction I-15	3.1
10	071	1.61	Draper West	11 400 South	3.1

Note: 1 km = 0.6 mile.

Figure 6. Development of pavement failure.

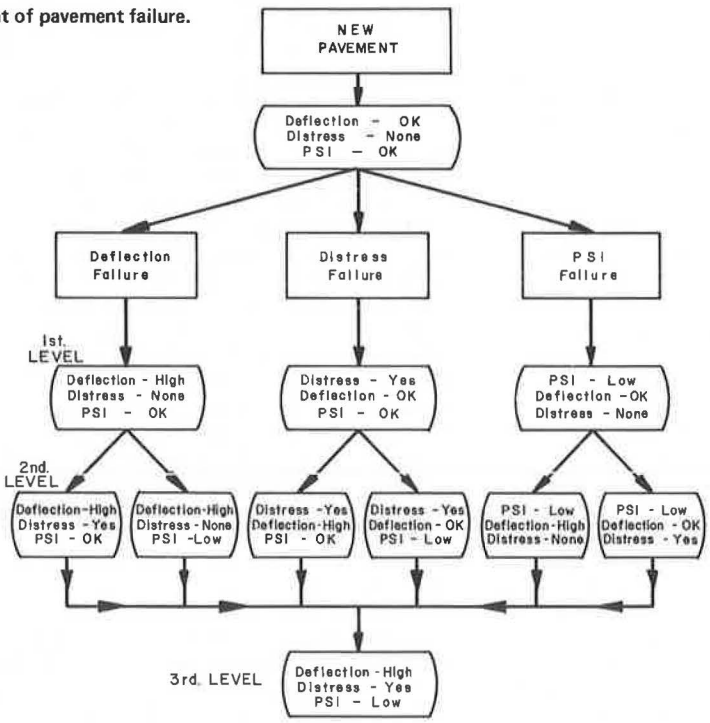

Table 2. Pavement sections ranked by final index number.

Number	State Route	Length (km)	Beginning Terminus	Ending Terminus	Final Index	Structure	Distress	PSI	Avg Skid
1	106	0.56	Junction Utah-131	4th N. Bountiful	2.4	4.0	1.0	2.3	70
2	E02	13.52	Saltair	SLC Airport	2.4	1.0	4.2	1.9	58
3	201	1.27	Junction I-15	Junction Utah-271	2.4	1.0	3.6	2.7	63
4	186	1.61	East end US-40	2500 West	2.5	4.0	1.0	2.9	35
5	201	3.27	Redwood Road	Junction I-15	2.6	1.0	3.8	3.1	51
6	071	1.61	Draper West	11 400 South	2.7	5.0	1.0	3.1	29
7	270	1.21	East end I-15	1st W. Railroad	2.8	1.0	5.0	3.0	33
8	171	2.82	Redwood Road	Junction Utah-I15	2.9	4.0	3.0	2.7	49
9	E02	5.79	Coalville	Echo Dam	3.0	3.0	3.7	3.0	43
10	171	8.53	Junction Utah-111	4000 West	3.2	5.0	3.3	3.0	56

Note: 1 km = 0.6 mile.

Figure 7. Pavement evaluation system.

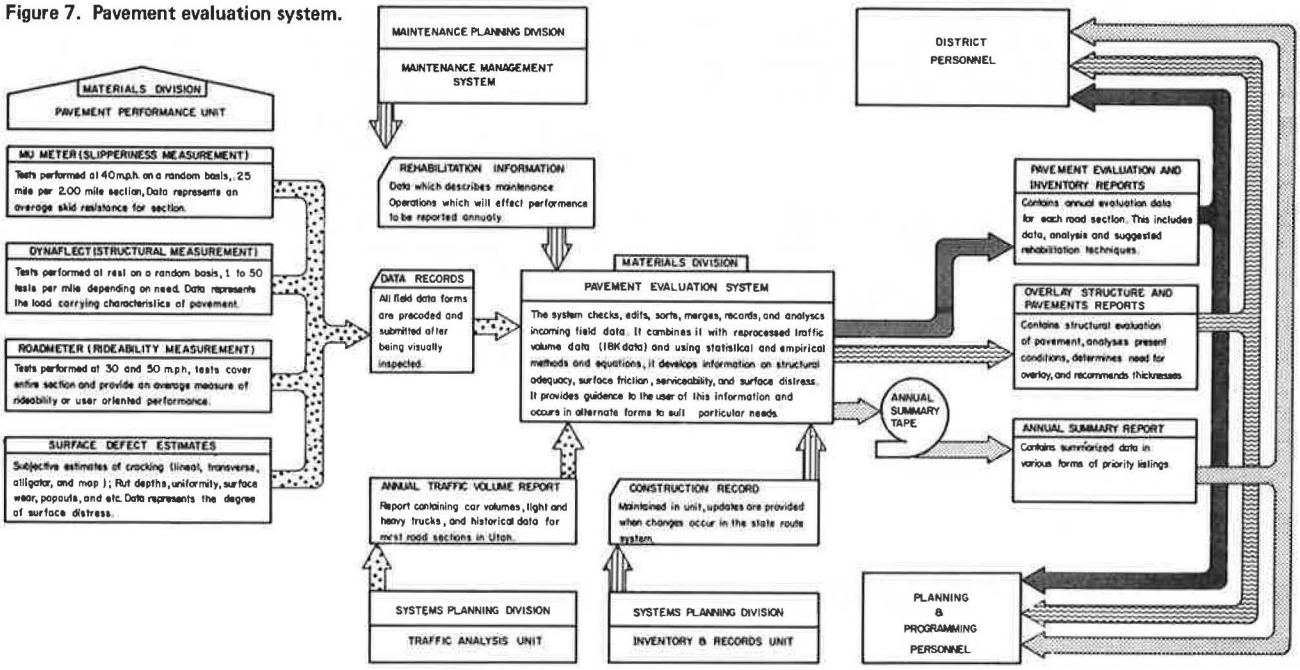

one of these modes of failure appears the pavement has reached first-level deterioration. If not corrected, the deficiency can lead directly to further problems, or the pavement could continue to age naturally, until the appearance of a second mode of failure. The pavement is then at the second level of deterioration. Inevitably the pavement system reaches the third level of deterioration if no rehabilitation effort is made at the appearance of any of the three modes of failure.

Each year data are added to a graph containing data from previous years. General trends are illustrated and made easily comparable for the four main failure modes (Figure 4).

The most efficient level for rehabilitation of a pavement depends on traffic demands placed on the system, which include ADT, 80-kN (18-kip) loads, functional class, and running speed. These parameters were used to list overall maintenance priorities. For highways with high ADT, the system weights the PSI proportionately to account for user costs. Structural adequacy of pavement is given extra attention where there is much truck traffic. An overall 0 to 5 rating that considers these variables is thus obtained for each pavement.

A final summary table (Table 2) gives the value of each of the four failure modes for each specific section of highway. This listing enables the reviewer to observe the section's relative condition and aids in choosing a rehabilitation strategy. For example, pavement 1 is structurally sound and has good skid resistance, but rates poorly in the distress and PSI columns. Although a more detailed analysis and field evaluations would be necessary before a final decision on rehabilitation could be made, some form of stress-relieving interlayer with overlay seems to be a consideration. This could minimize reflective cracking and create a smooth riding surface. Because the structure appears to be adequate, possibly enough material is in place. Therefore, recycling may be considered; however, bringing in the necessary machinery for such a short section may not be possible.

Pavement 2 is deficient in structural adequacy and PSI but has little distress and fair skid resistance. Further Dynaflect testing should be requested, and an overlay should be designed to support the traffic loading; thus, the PSI measurement of the section would be upgraded. Action should be taken before heavy distress occurs.

Reviewing the lists indicates direction for further analysis of various rehabilitation strategies. A flow chart of the entire evaluation system is presented in Figure 7 (6). The pavement condition evaluation conducted annually by the Materials and Research Section is limited to number of kilometers of highway that can be tested. To realize the greatest benefit from this program, we must make a careful selection of which pavements to test. The following are used as criteria for establishing testing priorities for any given year:

1. Control sections tested every year to ensure consistency in data,
2. Pavements with indexes below 3.0 on any failure mode listing for the previous year,
3. Sections requested for testing by district personnel, and
4. Pavements that have not been tested for 3 years.

CONCLUSIONS

The goal of pavement evaluation and rehabilitation is to minimize cost of constructing, maintaining, and operating on any given highway and still maintain level of safe service. To minimize user costs and prevent total loss of a pavement, a minimum value of the serviceability index should be specified where rehabilitation is indicated. This TSI, as defined in this report, is dependent on ADT as well as functional class.

The priority listings developed in this report give serviceability, distress, structural adequacy, and skid resistance of each pavement tested. These lists can be used in the development of highway rehabilitation strategies, programs for pavement testing schedules, and maintenance budgets to be submitted to legislative bodies.

ACKNOWLEDGMENT

This report was prepared in cooperation with the U.S. Department of Transportation. The contents reflect the views of the Utah Department of Transportation, which

is responsible for the facts and the accuracy of the data. The contents do not necessarily reflect the official views or policy of the U.S. Department of Transportation. The report does not constitute a standard, specification, or regulation.

REFERENCES

1. P. J. Claffey. Running Costs of Motor Vehicles as Affected by Road Design and Traffic. NCHRP Rept. 111, 1971.
2. The AASHO Road Test: Report 5—Pavement Research. HRB, Special Rept. 61E, 1962.
3. R. Kher, W. A. Phang, and R. C. G. Haas. Economic Analysis of Elements in Pavement Design. TRB, Transportation Research Record 572, 1976, pp. 1-14.
4. D. E. Peterson, W. R. Delis, D. Mangrum, and C. C. Sy. Utah's System Design for Roadway Improvement. Utah Department of Highways, 1972.
5. N. K. Vaswani. Method for Separately Evaluating Structural Performance of Subgrades and Overlying Flexible Pavements. HRB, Highway Research Record 362, 1971, pp. 48-62.
6. L. W. Shepherd. Utah's Transportation-Related Information Systems. Utah Department of Transportation, 1976.

Publication of this paper sponsored by Committee on Pavement Condition Evaluation.

Prediction of Rigid-Pavement Performance From Cumulative Deflection History

William H. Highter and Edward L. Moore, Clarkson College of Technology, Potsdam, New York

Data from the AASHO Road Test were used to investigate a functional relationship between the cumulative deflections sustained by a rigid pavement and a quantitative measure of the corresponding condition of the pavement. Cumulative deflections were estimated from periodic Benkelman beam deflections. Deflections had been measured at approximate 2-week intervals during the road test, and we assumed in the analysis that such deflections were representative of those that would have been measured had Benkelman beam deflections been measured continually. The present serviceability index (PSI) was used as a quantitative measure of pavement condition. Because of wide variation in response to loading of similarly constructed test sections and even between replicate test sections, no definitive relationship could be established that could predict PSI as a function of cumulative deflection. However, when data from test sections having the same slab thickness were averaged, a PSI-cumulative deflection relationship could be described by two straight lines intersecting at a threshold cumulative deflection. For cumulative deflections less than the threshold, an increase in cumulative deflection produced small changes in PSI; for cumulative deflection larger than the threshold, relatively small increases in cumulative deflection produced large changes in PSI. The level of the threshold cumulative deflection increased with increasing slab thickness.

Most methods of rigid pavement design for airfields and highways are based on considerations of load-induced stresses in elastic slabs. Repeated application of loads that induce stresses well below the modulus of rupture of a given material can cause the material to fail. This phenomenon, fatigue failure, is attributed to the fact that materials are not ideal homogeneous solids (1). Portland cement concrete (PCC) exhibits this behavior. Pavement distress due to fatigue may become more important in the future as aircraft and highway loads increase and exceed those contemplated by designers because the number of load repetitions that produce fatigue distress decreases as the load-induced stress increases.

Curves depicting the fatigue phenomenon usually have stress or strain on the ordinate versus cycles of load on a logarithmic abscissa. Such relationships are difficult for the pavement engineer to apply to in-service rigid pavements because measuring in situ stresses or strains is difficult and time consuming. Deflection measurements are made much more easily; the Air Force has a vehicle-mounted, optical-deflection measuring system under development that will be able to measure and compile deflections accurately with little or no interruption to traffic. Thus a correlation of deflections with a rigid-pavement performance index, which includes fatigue effects, would provide a valuable tool to the pavement engineer.

BACKGROUND INFORMATION

Fatigue of concrete has been investigated in terms of stress by several investigators (2, 3, 4). Nordby (4) reviewed research findings involving the fatigue of PCC and noted that most of the research performed on both plain concrete specimens and those with reinforcement similar to that of highway pavements was motivated by the fact that many failures of concrete pavements by cracking were due to repeated applications of stress. Fatigue research on plain concrete beams indicates (4) that plain concrete may not possess a fatigue limit within 10 million cycles of load, that inadequately aged and cured concrete is less resistant to fatigue than well-aged, well-cured concrete, and that as the induced stress is decreased the fatigue strength is increased substantially.

There is substantial agreement among fatigue investigators that, for reinforced concrete specimens (4), (a) most failures of reinforced beams were due to failure of the reinforcing steel that was accompanied by severe cracking in the concrete and stress concentrations associated with these cracks and (b) beams accumulated residual deflections over many cycles of load but recovered somewhat during rest periods, indicating, at

least for reinforced concrete beams, that the fatigue phenomenon is a function of the frequency of loading.

Lloyd, Lott, and Kesler (2) found that under repeated loading the strength of a specimen was reduced and the strength at failure was usually much less than the static flexural strength. PCC was found to behave similarly to other materials under cyclic loading in that the strength reduction was found to be proportional to the logarithm of the number of load cycles to failure. Because concrete does not have a fatigue limit (i.e., there is no stress level below which concrete can be stressed an indefinite number of times without fatigue failure), reference is frequently made to the fatigue strength of concrete. The fatigue strength is the strength expressed as a percentage of the static ultimate strength corresponding to a given number (frequently 10 million) of cycles of load (5).

Linger and Gillespie (6) reported a comprehensive evaluation of results of previous investigations of the fatigue characteristics of PCC and determined that the cumulated deformation was an indication of fatigue damage. Awad and Hilsdorf (7) found that damage to plain concrete caused by large repeated loads depends on the number of stress cycles and the total time the concrete has to sustain the stress. This finding seems to indicate that fatigue of a rigid pavement would depend on the speed of a vehicle and its wheelbase; both affect the frequency of loadings. Traffic spacing would also be a factor.

The experimental fatigue research on concrete beams reported in the literature was carried out on plain or reinforced specimens for which the support conditions remained constant throughout the test durations, which is in contrast to in-service conditions for rigid pavements. Special studies undertaken at the AASHO Road Test (8) revealed that, during periods of changing air temperatures, points on the surface of slabs were in continuous vertical motion, which would cause a continuous change in the geometry of slab support. At times, the slab would only be partially supported.

When Burmister (9) developed a theory of the structural behavior of rigid pavements, based on a layered solid elastic model, it was suggested that the design be based on a criterion of limited deformation under load. Although the tentative suggestion was that the maximum allowable deflection for a 203-mm (8-in) PCC slab be approximately 3.05 mm (0.012 in) to prevent fatigue failure (10), most design procedures used today are based on stress because a relationship between deflection and performance has not yet been developed for rigid pavements (11).

Ahlvin and others (12) recommended that consideration be given to the determination of maximum allowable deflections that can be tolerated in a rigid-pavement structure. They questioned whether designing for a given number of loadings by the largest load expected to use the pavement is realistic and suggested that "designs which incorporate strain and/or deflection histories should be investigated" to analyze random loading characteristics (mixed traffic with aperiodic loading frequency).

THEORY

Recently, a functional relationship has been shown to exist between the cumulative deflection that a flexible pavement experiences in its service life and the performance history of the pavement (13). The objective of this research effort was to determine if a similar relationship could be established for rigid pavements. Highter and Harr hypothesized that there is a functional relationship between the total energy imparted to a given rigid-pavement system as measured by cumulative deflections and the condition of that system.

Some methods of rigid-pavement design assume the existence of a reproducible stress-strain relationship. However, the field measurement of load-induced stress is very difficult and time consuming. The prediction of load-induced stresses is even more tenuous because the dynamic loads imposed on pavements by highway vehicles and especially aircraft are difficult to assess because they depend not only on characteristics of the vehicle but also on pavement roughness (14).

A need for an index that characterizes the dynamic response of a rigid pavement and can easily be measured becomes apparent. Cumulative deflections may provide such an index for flexible pavements (15). A theoretical basis for the supposition that cumulative deflections may also provide such an index for rigid pavements can be shown by the relationship between the load-induced deflection and strain energy of a plate (slab) supported on a Winkler foundation.

Rigid pavements are commonly modeled as plates supported by Winkler foundations. Timoshenko and Woinowsky-Krieger (16) analyzed a circular plate supported by a Winkler foundation. Assuming as an approximation that the deflections can be expressed as

$$w(r) = A + Br^2 \quad (1)$$

where A and B are constants, the total strain energy of the system for a load P applied at the center was found to be

$$U = 4B^2D\pi a^2 (1 + \nu) + 1/2 \int_0^{2\pi} \int_0^a k(r)[w(r)]^2 \, r dr d\theta \quad (2)$$

where

$D = Eh^3/[12 (1 - \nu^2)]$, flexural rigidity of the plate;
h = thickness of the plate;
a = radius of the plate;
ν = Poisson's ratio of the plate; and
k = modulus of subgrade reaction.

A and B are constants that are determined by imposing the condition that the total strain energy of the system is minimum when stable equilibrium is achieved. Since the maximum deflection occurs directly under the load ($r = 0$), Equation 1 indicates that A is the maximum deflection, w_{max}. Therefore, examination of Equation 2 indicates that the strain energy is a function of the plate and foundation parameters and the deflections. Equation 2 indicates that load-induced deflections are related to the strain energy of a deflected plate supported by a Winkler foundation. Within this context, the maximum deflected shape of a pavement provides a measure of the net energy introduced into a pavement by a load (vehicle or aircraft).

PROCEDURE AND ANALYSIS USED TO TEST WORKING HYPOTHESIS

To test the working hypothesis, rigid-pavement deflection measurements and corresponding assessments of the condition of the pavement over a sufficient period of time were required. The time interval over which these data were needed was such that the condition of the pavement changed markedly within the time interval. A sufficient time interval, then, depended on the design of the pavement, ambient conditions, and the nature and frequency of the traffic.

Data required to test the hypothesis were available in

Figure 1. Typical edge and corner deflection histories of AASHO Road Test section.

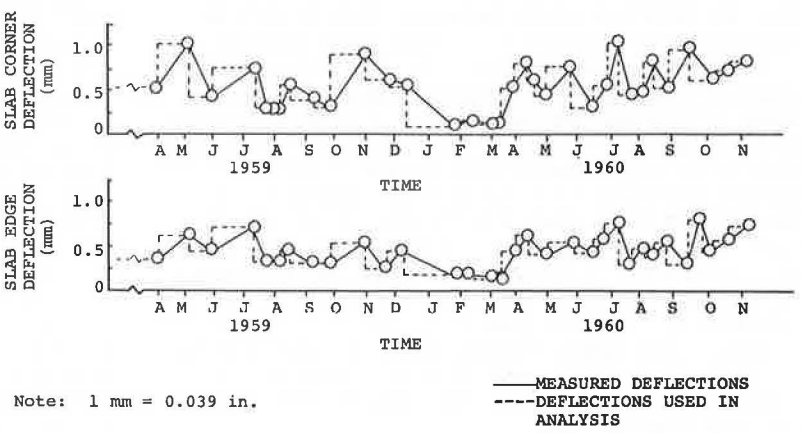

Figure 2. Serviceability versus cumulative corner deflection data for 203-mm slabs.

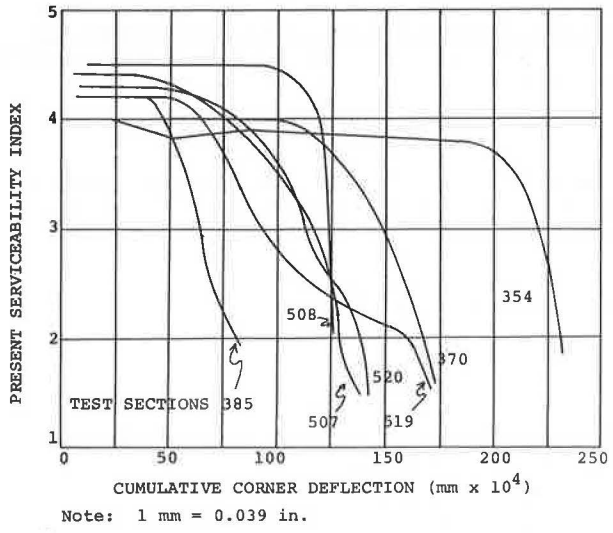

Figure 3. Curves of averaged data for three slab thicknesses.

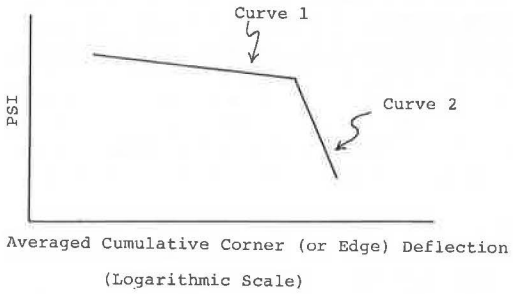

the histories of some of the test sections trafficked in the AASHO Road Test. The present serviceability index (PSI) (17) of some test sections did not change appreciably during the road test, and data from those test sections, which were considered to be overdesigned for the purpose of this study, were not used.

When assembling AASHO Road Test data, we selected five variables as likely to be related to the PSI: cumulative deflection, axle load, reinforcing, subbase thickness, and slab thickness. However, in performance analysis carried out on road test data by others (1), subbase thickness and reinforcing were not found to be statistically significant and these variables were not considered further.

A function was sought that would predict PSI as a function of cumulative deflection, load, and pavement slab thickness:

$$PSI = f_1 \text{ (cumulative deflection, load, slab thickness)} \quad (3)$$

If this function were known, predicting the serviceability level of a rigid pavement would be possible if deflection and traffic records were compiled.

A linear correlation analysis was carried out on the variables in Equation 3. The correlation matrix indicated a slight linear correlation between slab thickness and PSI and load and PSI. Further examination did not reveal a definite nonlinear relationship between slab thickness and PSI or load and PSI. Therefore, load and slab thickness were eliminated from Equation 3. Since both slab-corner deflections and slab-edge deflections were measured in the road test, regression analysis was performed on the following functions:

$$PSI = f_2 \text{ (cumulative edge deflection)} \quad (4)$$

$$PSI = f_3 \text{ (cumulative corner deflection)} \quad (5)$$

As expected, a strong linear correlation between edge and corner deflections was found to exist and Equations 4 and 5 were anticipated to have similar forms.

Throughout the duration of the AASHO Road Test, edge and corner Benkelman beam deflections were measured periodically. A typical deflection history for one test section is shown in Figure 1. Because deflection measurements were not taken continuously, estimating the deflections that occurred in the interval between contiguous deflection measurements was necessary. The deflection measurements (corner and edge) taken at the end of an interval were assumed to be representative of the deflections (corner and edge) throughout the interval. Deflections used in computing cumulative deflections are indicated by broken lines in Figure 1.

The wheel loads of the vehicles used in measuring Benkelman beam deflections were different from the wheel loads of the vehicles used for trafficking. To account for the change in load, we had to scale the Benkelman beam deflection data so that the deflections were representative of those caused by the vehicles used for trafficking. We assumed that the load-deflection relationship was linear. This assumption seems to be justified by previous findings (8, 18).

The traffic history of each test section was then applied to the scaled deflection measurements to obtain cumulative edge deflections and cumulative corner de-

Table 1. Results of linear regression analysis of averaged data for three slab thicknesses.

Slab Thickness (mm)	Cumulative Edge Deflection						Cumulative Corner Deflection					
	Curve 1			Curve 2			Curve 1			Curve 2		
	a_1	b_1	Range (mm)	a_1	b_1	Range (mm)	a_2	b_2	Range (mm)	a_2	b_2	Range (mm)
127	8.76	-0.85	<419 100	68.27	-11.44	>419 100	7.65	-0.63	<609 600	79.12	-13.04	>609 600
165	5.18	-0.14	<584 200	121.30	-20.27	>584 200	6.29	-0.35	<762 000	110.24	-18.05	>762 000
203	5.78	-0.30	<939 800	146.20	-23.81	>939 800	6.66	-0.45	<1 041 400	68.40	-10.74	>1 041 400

Notes: 1 mm = 0.039 in.
Curves are shown in Figure 3.

Figure 4. Serviceability versus averaged cumulative corner deflection for three slab thicknesses.

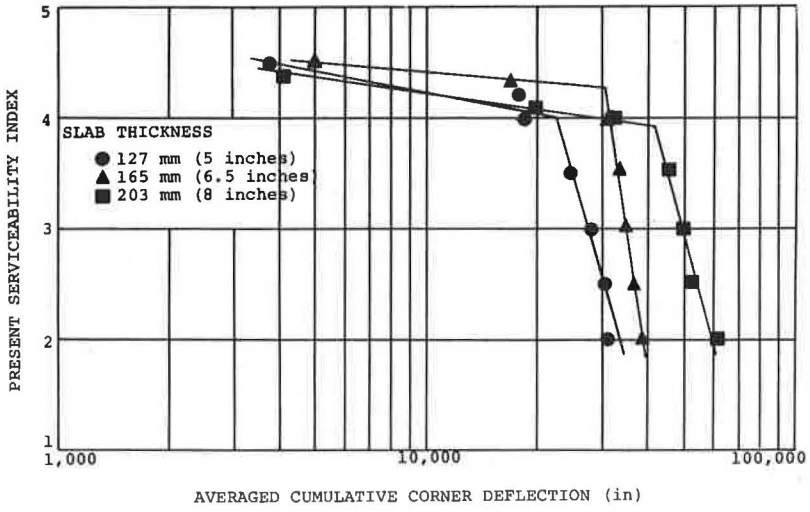

Figure 5. Serviceability versus averaged cumulative edge deflection for three slab thicknesses.

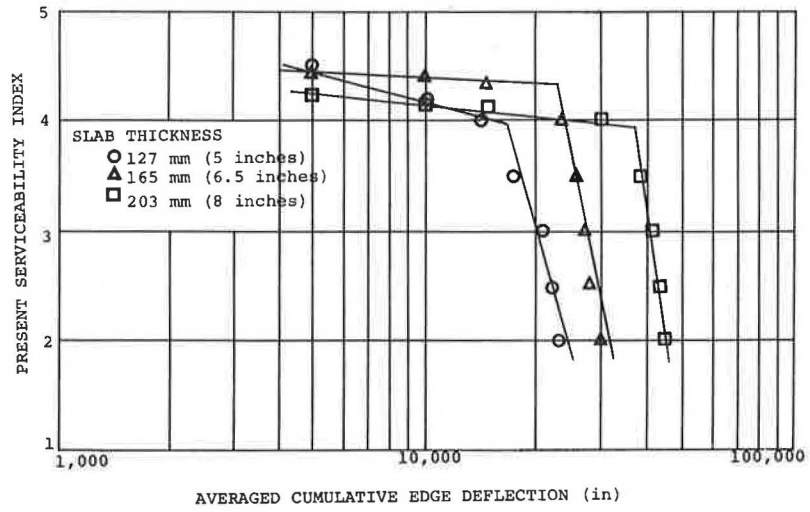

flections. The procedure whereby cumulative deflections were estimated for each test section can be expressed symbolically as

$$\text{Cumulative deflection} = \sum_{i=1}^{n} L/W_1 \, D_i \, N_i \qquad (6)$$

where

L = load of trafficking vehicles,
W_1 = wheel load of vehicle used in Benkelman beam deflection measurement,
D_i = ith Benkelman beam deflection, and
N_i = number of trafficking loads applied between ith and (i - 1) Benkelman beam deflection measurement.

To investigate the nature of the functions in Equations 4 and 5, we plotted PSI versus cumulative corner and cumulative edge deflection data. PSI versus cumulative corner deflection curves for seven test sections are shown in Figure 2. Two observations are suggested from examination of Figure 2: The data extend over a wide range, and most of the curves are nearly horizontal for PSI values greater than 4 and then a break occurs after which a

relatively small change in cumulative corner deflection produces relatively large changes in the level of serviceability.

Before regression analysis was performed, an attempt was made to linearize the PSI and cumulative deflection data. The shape of the curves in Figure 2 suggested that linearization might be achieved by transgenerating the data by taking the natural logarithm of both the PSI and cumulative deflection. Regression analysis on the transgenerated data gave a multiple correlation coefficient (R^2) of about 0.5 for both cumulative edge and cumulative corner deflections. Thus, only about half the variation in the PSI level is explained by cumulative edge and cumulative corner deflections, but there exists at least a general relationship between PSI and cumulative deflections.

The regression analysis did not differentiate between the various slab thicknesses because of the lack of linear correlation between cumulative edge deflection and slab thickness and between cumulative corner deflection and slab thickness discussed previously. However, slab thickness can be taken into account if the data from test sections having the same slab thickness are isolated and then analyzed. To establish a more definitive functional relationship between cumulative edge deflection, cumulative corner deflection, and PSI, we averaged the data for each slab thickness. When these curves representing the averaged data were plotted to a semilogarithmic scale, each curve could be represented by two straight lines (Figure 3). One line represented the PSI and cumulative relationship for the initial part of the curve when there were small changes in PSI, and the second line approximated the curve where small changes in cumulative deflection resulted in large changes in the level of PSI. Simple linear regression analysis was carried out on the averaged data to obtain the parameters of the following regression equations:

$$PSI = a_1 + b_1 \log_{10} (\text{cumulative edge deflection}) \quad (7)$$

and

$$PSI = a_2 + b_2 \log_{10} (\text{cumulative corner deflection}) \quad (8)$$

The results of the analysis are given in Table 1 and are plotted in Figures 4 and 5, which indicate the following:

1. The relationships between PSI and cumulative corner and edge deflections are well defined for the averaged data;
2. The cumulative deflection corresponding to the intersection of the two straight lines composing each curve, referred to as the threshold cumulative deflection, increases as the pavement slab thickness increases;
3. The position and slope of the initial part of each curve are nearly the same for each slab thickness, and one can reasonably assume that the positions of the curves are related to the as-built condition of the pavement rather than slab thickness; and
4. Although the slopes of the second part of each curve appear to be about the same when plotted to a logarithmic scale, the cumulative deflection associated with reducing the PSI of the 203-mm (8-in) thick slab from 3 to 2 is nearly three times as great as that corresponding to a similar change in PSI for the 127-mm (5-in) slab.

SUMMARY AND CONCLUSIONS

The objective of this research was to test the validity of the following hypothesis: There is a functional relationship between the total energy imparted to a given rigid-pavement system as measured by cumulative deflections and the condition of that system.

Analysis of AASHO Road Test data indicates the hypothesis is valid for rigid pavements if the behavior of an average pavement of given thickness is considered. In addition, the following conclusions and observations can be stated.

1. The PSI and cumulative deflection relationship determined from averaged road test data indicates that early in the service life of a pavement increases in cumulative deflection result in small changes in PSI until a threshold cumulative deflection is reached. For cumulative deflections greater than the threshold value, the pavement serviceability decreases more rapidly as the cumulative deflection increases. This phenomenon was noted for both slab-edge and slab-corner cumulative deflections.
2. The threshold cumulative deflection at which a sharp break occurs in the PSI and cumulative deflection curve increases as the slab thickness increases. All other factors being equal then, the effects of increasing slab thickness are twofold: The deflection caused by a given load decreases as slab thickness increases, and the cumulative deflection corresponding to a given level of pavement serviceability increases as the slab thickness increases.

ACKNOWLEDGMENTS

Support for this research was provided by the U.S. Department of the Air Force, Air Force Systems Command, Air Force Civil Engineering Center, Tyndall Air Force Base, Florida. We also wish to acknowledge the assistance of Feng-Bor Lin in the statistical analysis.

REFERENCES

1. L. H. Van Vlack. Elements of Materials Science and Engineering. Addison-Wesley Publishing Co., Reading, Mass., 3rd Ed., 1975.
2. J. P. Lloyd, J. L. Lott, and C. E. Kesler. Fatigue of Concrete. Engineering Experiment Station, Univ. of Illinois, Urbana, Bulletin 499, 1968.
3. J. T. McCall. Probability of Fatigue Failure of Plain Concrete. Journal of the American Concrete Institute, Vol. 30, No. 2, Aug. 1958, pp. 233-244.
4. G. M. Nordby. Fatigue of Concrete: A Review of Research. Journal of the American Concrete Institute, Vol. 30, No. 2, Aug. 1958, pp. 191-219.
5. C. E. Kesler. Fatigue and Fracture of Concrete. National Sand and Gravel Association and National Ready Mixed Concrete Association, 1970, 19 pp.
6. D. A. Linger and H. A. Gillespie. A Study of the Mechanics of Concrete Fatigue and Fracture. HRB, Highway Research News, No. 22, Feb. 1966, pp. 40-51.
7. M. E. Awad and H. K. Hilsdorf. Strength and Deformation Characteristics of Plain Concrete Subjected to High Repeated and Sustained Loads. American Concrete Institute, Publ. SP-41, 1974, pp. 1-13.
8. The AASHO Road Test: Report 5—Pavement Research. HRB, Special Rept. 61E, 1962, 352 pp.
9. D. M. Burmister. The Theory of Stresses and Displacements in Layered Systems and Applications to the Design of Airport Runways. Proc., HRB, Vol. 23, 1943, pp. 126-144.
10. F. N. Hveem. Pavement Deflections and Fatigue Failures. HRB, Bulletin 114, 1955, pp. 43-73.
11. J. W. Hall. Nondestructive Testing of Pavements: Final Test Results and Evaluation Procedure.

U.S. Air Force Weapons Laboratory, Kirtland Air Force Base, N.M., Technical Rept. AFWL-TR-72-151, June 1973, 82 pp.
12. R. G. Ahlvin and others. Multiple-Wheel Heavy Gear Load Pavement Tests. U.S. Air Force Weapons Laboratory, Kirtland Air Force Base, N.M., Technical Rept. AFWL-TR-70-113, Vol. 1, Nov. 1971, 212 pp.
13. W. H. Highter and M. E. Harr. Cumulative Deflections and Pavement Performance. Journal of Transportation Engineering, ASCE, Aug. 1975, pp. 537-551.
14. A. W. Hall and S. Kopelson. The Location and Simulated Repair of Rough Areas of a Given Runway by an Analytical Method. National Aeronautics and Space Administration, Technical Note D-1486, 1962, 36 pp.
15. W. H. Highter and M. E. Harr. Application of Energy Concepts to the Performance of Airfield Pavements. U.S. Air Force Weapons Laboratory, Kirtland Air Force Base, N.M., Technical Rept. AFWL-TR-72-225, June 1973, 172 pp.
16. S. Timoshenko and S. Woinowsky-Krieger. Theory of Plates and Shells. McGraw-Hill, New York, 1959, 580 pp.
17. W. N. Carey, Jr., and P. E. Irick. The Pavement-Serviceability Performance Concept. HRB, Bulletin 250, 1960, pp. 40-58.
18. R. E. Boyer and M. E. Harr. Predicting Pavement Performance Using Time-Dependent Transfer Functions. U.S. Air Force Weapons Laboratory, Kirtland Air Force Base, N.M., Technical Rept. AFWL-TR-72-204, July 1963.

Publication of this paper sponsored by Committee on Pavement Condition Evaluation.

Performance of the Mays Road Meter

Hugh J. Williamson, Yi Chin Hu, and B. Frank McCullough, Center for Highway Research, University of Texas at Austin

Serviceability index values obtained from the Mays meter and from the surface dynamics profilometer have been shown at times to differ by more than a point. A hypothesized explanation of these large discrepancies, based on the responses of the two machines to roughness with different ranges of wavelengths, is presented. Data from two sets of test sections are shown to be consistent with the hypotheses. The repeatability and day-to-day consistency of the Mays meter are also analyzed.

The Mays road meter (MRM) measures effect of the roughness of a road by summing the deflections of the rear axle of an automobile relative to the automobile body as the vehicle travels over the pavement. The mechanical details of the device, the measuring technique, and the calculation of a serviceability index (SI) from the MRM roughness measurement are discussed by Walker and Hudson (1).

The surface dynamics profilometer (SDP) is a more sophisticated device that can be used to obtain a measurement of road-surface elevation versus distance along the road in each wheel path. Obtaining an SI value for a road section as a function of the SDP measurements is also possible by using time-series analysis to compute characterizing measures of roughness and by using a regression model developed to relate roughness to serviceability.

Walker and Hudson discuss the calculation of SI values from measured profiles (2), and the measuring system is discussed by Walker, Roberts, and Hudson (3).

Periodically, an MRM must be recalibrated because of changes in the characteristics of the suspension system that affect the measurements (1). Significant changes in compression-rebound characteristics of shock absorbers or of stiffness of springs, for example, indicate the need for recalibration. The recalibration can be achieved by using SDP measurements because the performance of the SDP is very stable in time.

In addition to the shock absorber and spring characteristics, the following factors relating to the vehicle affect the MRM measurements: tire type and size, unsprung mass and sprung mass, including luggage and placement, mass of operating crew, and gasoline in tank. Sprung mass refers to the mass suspended by the springs. Because of hardware provisions within the SDP that are designed to remove the effects of the suspension system, the SDP measurements are affected drastically less by these factors than is the MRM (3).

An SDP measurement produces an approximate plot of the actual road profile (very long waves are removed by electronic filtering); however, the MRM produces only a single index that is believed to be related to the extent or severity of the roughness. Thus the two kinds of measurement are different in nature.

Because of the need for recalibration of MRMs and the much more detailed information provided by SDP measurements, the MRM will never completely replace the SDP and other similar systems. Because of its relatively low cost and simplicity of operation and maintenance, however, the MRM is more convenient for many purposes, particularly when only an overall indicator of roughness is needed and a large number of road sections are to be measured. Maintaining a fleet of MRMs to be used in different areas is feasible; however, owning a fleet of SDPs would involve a tremendous expense. Thus, there is considerable practical reason for interest in the adequacy of the MRM measurements.

Road meters similar to the Mays meter are used in many parts of the country. Although the results presented here apply only to the MRM, they are related in principle to the performance of other types of meters that are also based on the summation of rear-axle body deflections.

A set of roughness measurements were made on I-45 near Huntsville, Texas, to study the effects of swelling clay distress on the continuously reinforced concrete pavement (CRCP). Both the SDP and the MRM were operated on those sections, and large discrepancies between the SI values obtained from the two devices were observed.

DIFFERENCE BETWEEN SI VALUES FROM PROFILOMETER AND MAYS METER ON HUNTSVILLE SECTIONS

The CRCP test sections near Huntsville used in this study are sporadically affected by swelling clay and

intermediate-length roughness; also, wavelengths of 6.1 to 24.4 m (20 to 80 ft) appear sporadically. These long waves are caused in part by the swelling clay. Patching has been performed continually to repair structural failures in the pavement.

Serviceability indexes were obtained from both the MRM and the SDP on successive 347.5-m (1140-ft) sections along this project; for convenience, the SI values from the MRM and the SDP are denoted SI_m and SI_p, respectively. The SI_m values range from only 3.2 to 3.5; the SI_p values, however, vary from 2.5 to 5.0. Figure 1 shows a plot of $(SI_p - SI_m)$ versus SI_p. The linear nature of the plot is due to the small range of the SI_m values; $(SI_p - SI_m)$ is nearly the same as $(SI_p$ - a constant).

The differences between SI_m and SI_p cannot be explained in terms of random measurement errors alone. We hypothesized that the discrepancies could be explained in terms of the nature of the roughness measurements. The SDP is capable of measuring roughness with a wide range of wavelengths, and the SI model includes terms with wavelengths from approximately 2.6 to 26.2 m (8.6 to 86 ft) (2). The MRM, however, measures only that part of the roughness that causes the rear axle to deflect relative to the body of the automobile; although this is highly dependent on the suspension system of the particular automobile being used, one would suspect that the axle-body deflections would be more sensitive to short waves than to long waves.

Figure 2 shows conceptually the effects of different types of roughness on the SI_m and SI_p values. If, for example, the short waves are severe (have large amplitudes), the SI_m value will be low whether the long waves are severe (type d, Figure 2) or not (type b). The SI_p value, sensitive to both short and long waves, however, is much lower in type d than in type b. Thus, any time the long and short waves are greatly different in severity, the SI_m and SI_p values are likely not to agree. Comparing the severity of roughness with different wavelengths is a significant problem. Although a real road profile cannot easily be classified as one of these four hypothetical cases, they serve to illustrate the principle.

The mathematical methods most commonly used for analyzing highway roughness on the basis of wavelength are digital filtering (4, 5, 7) and power spectral analysis (2). These methods have been discussed in the literature and will not be treated in detail here. Because the computational speed of power spectral analysis is faster than that of digital filtering and because previous work (5) relating digital filtering output to serviceability was in a developmental stage when the Huntsville study began, power spectral analysis was employed.

Power spectral analysis is a method that can be used to compute amplitudes of surface undulations with different wavelengths. Figure 3 shows the amplitudes as a function of frequency (the reciprocal of wavelength) for two Huntsville sections for which SI_p = 5.0 and 2.5. The amplitudes are greater for the section with the lower SI_p value; however, this plot alone is not proof of the relative severity of the short as opposed to the long waves. There is clearly a need to convert the long waves, which have much larger amplitudes in general, and the short waves to a common scale to allow their comparison.

COMPARISON OF SEVERITY OF LONG AND SHORT ROUGHNESS WAVES

A scheme was devised to transform roughness amplitudes so that, for each of the wavelengths studied, derived roughness values fall within a range from 0 to 5, just as the SI values do. This approach involves the use of the power spectral values, which are directly related to the roughness amplitudes; the power spectral density corresponding to a given wavelength is the square of the roughness amplitude divided by a constant [the frequency bandwidth, 0.0381 cycle/m (0.0116 cycle/ft), in this case].

Walker and Hudson (2) averaged the power spectral values of 19 sections with present serviceability rating (PSR) values from 4.0 to 4.5 and of 10 sections with PSR values from 2.0 to 2.5 for a set of frequency bands. Thus, we have an estimate of an average power spectrum for a road with a PSR of 2.25 and for a road with a PSR of 4.25.

The results are given in Table 1 [in which a correction of a clerical error in Walker and Hudson's work (2) has been made in the power for a frequency of 0.0381 cycle/m (0.012 cycle/ft) for the low PSR values]. This table can be used to assess the severity of the roughness in different ranges of wavelengths. For example, if a road has a power of 0.0055 cm^2/cycle/m (0.0028 in^2/cycle/ft) at wavelengths 4.39 m (14.4 ft), this road can be said to be comparable to a road with a PSR of 4.25 with respect to the severity of the 4.39-m (14.4-ft) waves. Similarly, if the power is 0.0342 cm^2/cycle/m (0.0174 in^2/cycle/ft), then the road is comparable to a typical road with a 2.25 PSR with respect to 4.39-m (14.4-ft) waves.

Analysis of shorter wavelengths would be beneficial; because of high-frequency noise produced by the tape recorder originally used on the SDP, however, very short waves are not discussed by Shaw (2). The noise problem has subsequently been solved by installing a newer tape recorder. The transformation of a power value to a more easily interpreted quantity is achieved by the method described below.

Consider a wavelength of 4.39 m (14.4 ft). As indicated above, Table 1 gives two points on the SI versus power curve for this wavelength: SI ≈ 2.25 when the power is 0.0342/cm^2/cycle/m (0.0174 in^2/cycle/ft) and SI ≈ 4.25 when the power is 0.0056 cm^2/cycle/m (0.0028 in^2/cycle/ft). In addition, we assumed that SI = 5.0 if the power is 0 because 0 power is associated with a roughness amplitude of 0 at the wavelength in question. These three points on the SI versus power curve are joined by straight lines, as shown in Figure 4, to approximately the true function. Although this approach is somewhat crude because of the small number of points available on the power versus frequency curves, the interpolated SI values are much more easily interpreted than the power or amplitude values. Thus, the linear interpolation is adequate for the specific comparisons we wish to make.

Another condition that was imposed is that an additional point is added if negative interpolated SI values would otherwise have been obtained. Under this condition SI = 0 for the largest power observed in the sample of pavement sections used in the study. Figure 4 shows the piecewise linear function for a wavelength of 4.39 m (14.4 ft).

EXPLANATION OF MRM AND SDP DISCREPANCIES

Table 2 gives the interpolated SI values for each frequency for the sections shown as extreme points in Figure 1. The average interpolated SI, SI_m, and SI_p values are given below:

Wavelength (m)	Frequency (cycles/m)	Avg SI_p = 3.0 Avg SI_m = 3.4	Avg SI_p = 4.7 Avg SI_m = 3.2
8.8 to 26.4	0.039 to 0.115	2.3	4.1
2.6 to 3.3	0.302 to 0.381	3.6	4.2

For the two sets of sections, the SI_m averages differ by only 0.2 (3.4 versus 3.2), and the SI_p differs by 1.7 (3.0 versus 4.7). The interpolated SI means for short

wavelengths differ by a relatively small amount, 0.6. A statistical test revealed that this difference is not statistically significant at the 0.05 level. (A t-test for samples from populations with unequal variances was performed by using as data the individual section means over the three wavelengths (6, pp. 114-116).

A 1.8 difference, however, appears in the interpolated SI means for the long wavelengths. This difference is clearly statistically significant at the 0.05 level. The large variation in severity of long-wavelength roughness apparently affects the SI_p values but not the SI_m values.

Thus, the large difference in variation of SI_p values as opposed to SI_m values is explainable in terms of the responses of the different machines to roughness with different ranges of wavelengths. This explanation is in accordance with the conceptual hypotheses presented earlier about the reasons for differences between SI_m and SI_p values.

That there is not a perfect correlation between the SI_m values and the interpolated SI values for short wavelengths is probably due in part to the influence of shorter waves that were not analyzed because of the high-frequency, tape-recorder noise discussed above. The important point is that the interpolated SI means have sufficient physical meaning to shed light on the SI_m versus SI_p discrepancies.

Figure 1. (SI_p-SI_m) versus SI_p for Huntsville sections.

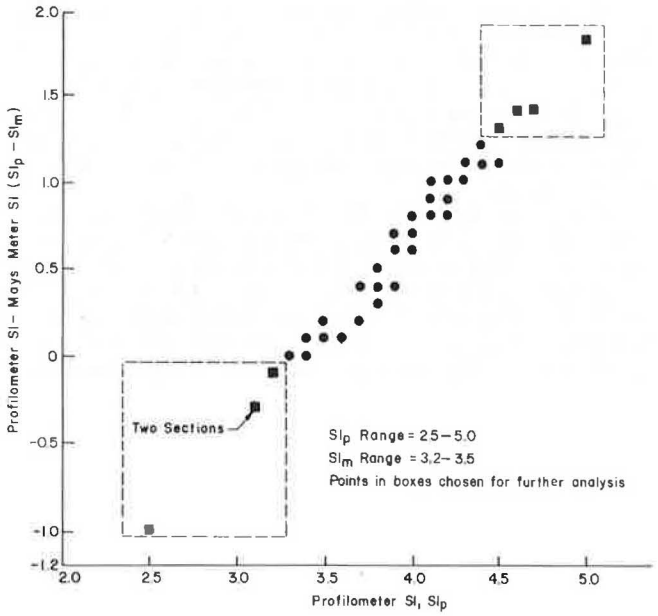

ROUGHNESS MEASUREMENTS ON A DIVERSE SET OF PAVEMENTS

Because of their special characteristics, the CRCP road sections discussed above are useful for illustrating certain differences between the SDP and the MRM. We felt,

Figure 2. Hypothetical road profiles and corresponding SIs.

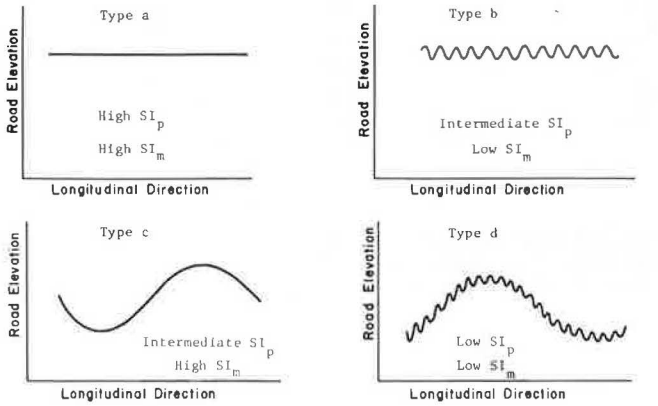

Figure 3. Amplitudes of roughness waves versus frequency.

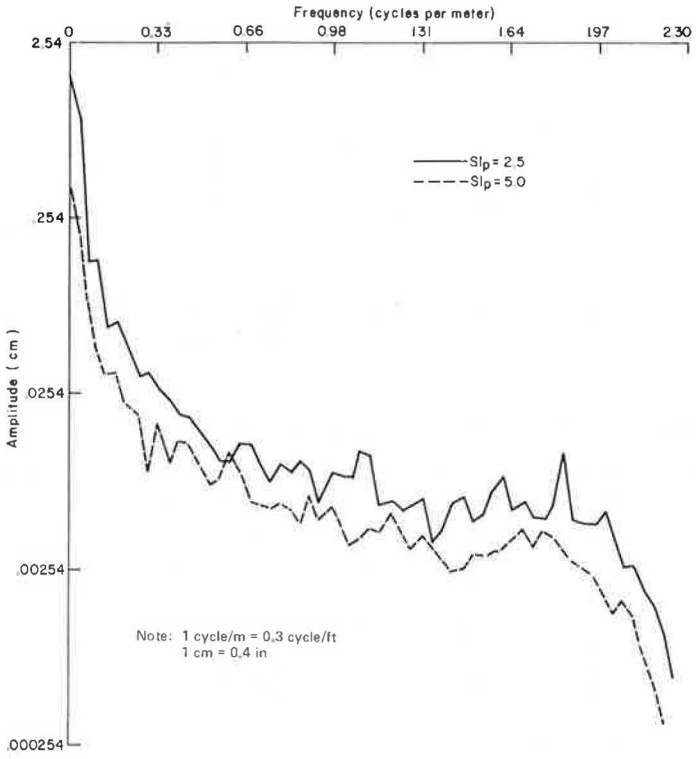

however, that the results should be supplemented with a study of a more typical set of pavements with a wider range of SI_m values. The Austin test sections, which are used to calibrate the Mays meters used in Texas, were selected because they are a diverse set of pavements and because MRM and profilometer data are readily available for those sections.

Figure 5 shows a plot of (SI_p - SI_m) versus SI_p for the Austin test sections. For this set of test sections, the SI_m and SI_p do not have a consistent discrepancy, as they did for the Huntsville sections; when SI_p is low, for example, the difference (SI_p - SI_m) is neither consistently low nor consistently high. The inconsistency is at least partly due to the fact that the conversion for the MRM roughness measurement to SI is based on the SI_p values for those sections; in spite of that conversion, a consistent discrepancy would still be possible if the SI_p values reflected information that simply was not present in the MRM roughness measurements.

The sections with moderate SI_p values, shown in the boxes in Figure 5, were selected for further analysis to explain differences in SI_m when SI_p varies within a very narrow range. The interpolated SI values are given in Table 3. Average values are given below (1 cycle/m = 0.3 cycle/ft, 1 m = 0.3 ft).

Wavelength (m)	Frequency (cycles/m)	Avg SI_p = 3.3 Avg SI_m = 2.6	Avg SI_p = 3.3 Avg SI_m = 3.7
8.8 to 26.4	0.039 to 0.115	3.5	3.6
2.6 to 3.3	0.302 to 0.381	3.8	4.4

The interpolated SI means for long wavelengths differ by only 0.1, which is practically and statistically insignificant. The interpolated SI values for short wavelengths differ by 0.6, however, and this difference is clearly statistically significant at the 0.05 level. (The section-to-section variation is smaller here than in the case in which a 0.6 difference was statistically insignificant for the Huntsville data.)

Thus, the larger variation in short-wavelength roughness has a stronger effect on the SI_m values than on the SI_p values. The wavelength analysis, then, is again consistent with the conceptual hypotheses stated earlier about SI_m and SI_p differences. The wavelength studies support, but do not constitute an absolute proof of, the hypothesis that SI_m and SI_p differences can be explained

Table 1. Power spectrum statistics.

Frequency (cycles/m)	Wavelength (m/cycle)	Power Mean (cm^2/cycle/m)	
		2.0 ≤ PSR ≤ 2.5	4.0 ≤ PSR ≤ 4.5
0.039	26.4	9.4390	2.5456
0.076	13.2	0.4991	0.1023
0.115	8.8	0.1493	0.0313
0.151	6.6	0.0604	0.0149
0.190	5.3	0.0490	0.0087
0.226	4.4	0.0342	0.0056
0.266	3.8	0.0212	0.0049
0.302	3.3	0.0171	0.0043
0.341	2.9	0.0161	0.0035
0.381	2.6	0.0165	0.0033

Note: 1 cycle/m = 0.3 cycle/ft; 1 m = 3.3 ft; 1 cm^2 = 0.16 in^2.

Figure 4. Piecewise linear model for 4.39-m wavelength and 0.23-cycle/m frequency.

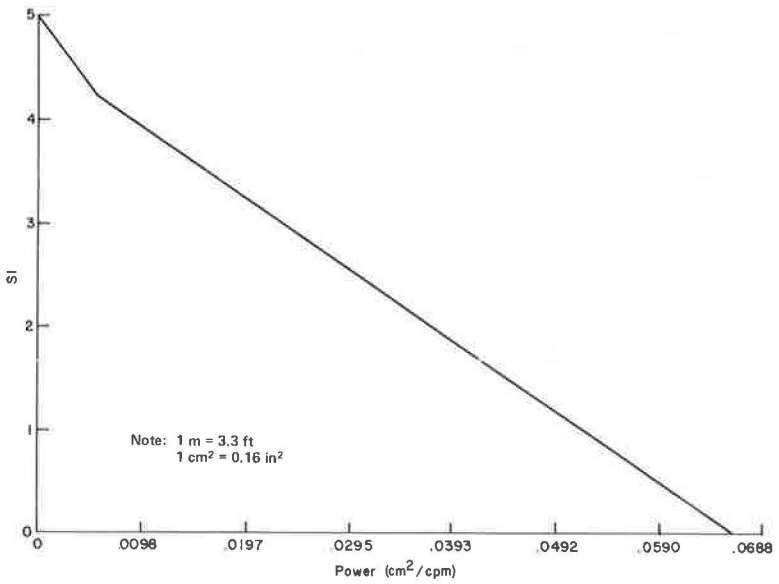

Table 2. Interpolated SI for each frequency band for Huntsville CRCP sections.

Wavelength (m)	Frequency (cycles/m)	Sections for Which SI_p < SI_m				Sections for Which SI_p > SI_m			
		SI_p = 2.5 SI_m = 3.5	SI_p = 3.1 SI_m = 3.4	SI_p = 3.1 SI_m = 3.4	SI_p = 3.2 SI_m = 3.3	SI_p = 4.5 SI_m = 3.2	SI_p = 4.6 SI_m = 3.2	SI_p = 4.7 SI_m = 3.3	SI_p = 5.0 SI_m = 3.2
26.4	0.039	1.5	3.1	4.4	1.8	4.1	4.8	4.8	4.8
13.2	0.076	3.3	0.0	3.2	2.3	3.5	4.2	4.0	4.1
8.8	0.115	1.6	1.6	2.6	1.9	3.4	3.6	3.7	4.3
6.6	0.151	2.7	2.0	1.8	2.1	4.4	4.0	3.8	4.2
5.3	0.190	2.0	0.0	3.0	3.0	4.3	4.1	3.6	3.9
4.4	0.226	2.6	1.3	3.8	3.2	4.4	4.1	3.6	4.1
3.8	0.266	3.1	2.0	4.0	3.4	4.4	3.9	3.0	4.2
3.3	0.302	2.2	4.2	3.8	3.5	3.9	4.1	3.8	4.6
2.9	0.341	3.3	3.7	4.1	3.9	4.2	4.2	3.8	4.1
2.6	0.381	3.7	2.9	4.1	4.2	4.1	4.3	4.1	4.7

Note: 1 cycle/m = 0.3 cycle/ft; 1 m = 3.3 ft.

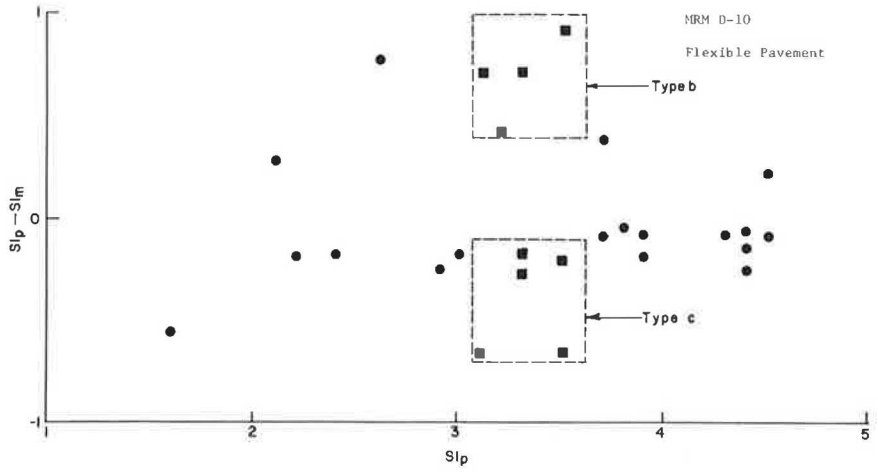

Figure 5. (SI_p - SI_m) versus SI_p for Austin sections.

Table 3. Interpolated SI for each frequency band for Austin flexible test sections.

Wavelength (m)	Frequency (cycles/m)	Sections for Which $SI_p > SI_m$				Sections for Which $SI_p < SI_m$				
		SI_p = 3.50 SI_m = 2.59	SI_p = 3.30 SI_m = 2.60	SI_p = 3.10 SI_m = 2.40	SI_p = 3.20 SI_m = 2.78	SI_p = 3.30 SI_m = 3.48	SI_p = 3.50 SI_m = 3.71	SI_p = 3.30 SI_m = 3.57	SI_p = 3.50 SI_m = 4.15	SI_p = 3.10 SI_m = 3.75
26.4	0.039	3.8	2.5	3.8	2.0	2.0	4.0	1.9	3.7	4.5
13.2	0.076	4.2	3.1	3.7	3.9	3.7	4.2	3.4	4.2	3.7
8.8	0.115	3.7	3.5	3.4	4.1	4.2	4.2	3.0	4.1	2.7
6.6	0.151	3.0	3.8	3.2	4.3	4.2	4.5	3.4	4.3	2.8
5.3	0.190	4.1	4.2	4.1	4.2	4.4	4.3	4.4	4.6	4.4
4.4	0.226	4.0	4.0	3.6	4.1	4.2	4.2	4.2	4.2	4.5
3.8	0.266	4.1	4.1	3.5	3.8	4.2	4.3	4.2	4.6	4.4
3.3	0.302	3.6	4.1	3.6	3.3	4.4	4.3	4.2	4.2	4.5
2.9	0.341	3.9	4.1	3.6	3.7	4.4	4.3	4.2	4.3	4.5
2.6	0.381	3.9	4.1	4.0	3.6	4.7	4.6	4.4	4.8	4.6

Note: 1 cycle/m = 0.3 cycle/ft; 1 m = 3.3 ft.

in terms of different responses of the two machines to long and short roughness waves.

REPEATABILITY OF THE MAYS METER

The Austin test sections were also used to test the repeatability of the Mays meter. The repeatability of an instrument refers to the degree to which the repeated measurements made with the instrument agree with one another. The sources of run-to-run measurement differences include variations in tire pressure and the inevitable small differences in the wheel paths traversed in successive runs. If sufficient distances are driven, the change in the weight of the gasoline in the tank can also have a significant effect. Gradual effects, such as changes in the shock absorbers and springs, would not be expected to cause run-to-run differences, although these gradual effects do cause long-term variations and necessitate recalibrations of the MRMs.

There were four repeated runs available for each section for each of two Mays meters. Under standard calibrating procedures, the MRMs are operated five times on each section, and the most deviate measurement is discarded. Thus, since the most extreme measurement for each section was not available, the variance estimates computed here are slightly low.

The conversion of each individual measurement to an SI value is possible. Standard statistical methods, then, can be used to compute the variance of the replication error. If SI_{ij}, j = 1, 2, 3, 4, are the SI values of the MRM corresponding to the ith section, and if $\overline{SI}_i$. is the mean of these four values, then

$$s^2 = \left[\sum_{i=1}^{n}\sum_{j=1}^{4}(SI_{ij} - \overline{SI}_{i.})^2\right] \Big/ 3n \qquad (1)$$

is an estimate of the error variance, where n is the number of sections used. Equation 1 is a standard one-way analysis of variance approach (6, 8).

The error variance for two MRMs used by the Texas State Department of Highways and Public Transportation is given below.

Mays Meter	Pooled Variance	d.f.	F
D-21	0.011 388	78	1.138
D-10	0.010 011	72	

An F-test reveals that, at the 5 percent level of confidence, one cannot conclude that either of the MRMs produces larger errors than the other. Since the error variances are both about 0.01, the standard deviation of the errors for both machines is about 0.1, which is only 2 percent of the scale, 0 to 5, for the SI values; thus, both machines are highly repeatable.

We suspected, because of their greater transverse surface irregularities, that roads with low SI values would induce greater measurement errors than would smoother roads. If this observation were true, more replicate measurements would be required on rough than on smooth roads to obtain average measurements with the same accuracy. The effect, however, was not observed in the Austin test-section data, but further study of this point would be beneficial.

CONSISTENCY OF THE TWO MAYS METERS USED

There has been much speculation about the consistency of the MRM measurements because these measurements are affected by some factors that are difficult to control [such as weight in the automobile (e.g., of the gasoline) and the tire pressure]. Because two MRMs were used in this study, comparison of their SI values is possible.

The runs with the two MRM machines were made a month apart, and a newer set of SI_p values was used to calibrate the second MRM. The SI_m values and the SI_p values for the sections whose SI_p values changed by 0.1 or less during the time interval involved are shown below.

Section Number	SI_p	SI_m (D-21)	SI_m (D-10)
41	2.45	2.44	2.57
34	2.90	3.15	3.14
33	2.95	3.24	3.17
13	3.10	2.14	2.40
8	3.15	3.54	3.75
6	3.30	2.73	2.60
21	3.50	3.75	3.71
15	3.65	3.08	3.31
28	3.85	3.98	4.10
7	4.45	4.61	4.59

Three points are important.

1. The SI_m values are in good agreement with the SI_p values. This agreement was expected because the SI_m values are computed by using calibrations developed from these SI_p values.
2. In 9 of 10 cases, the SI_m values are either both higher or both lower than the corresponding SI_p values, which indicates that the two MRMs are more consistent with each other than with the SDP. Thus, the systematic differences between the MRM and the SDP discussed above are consistent from Mays meter to Mays meter.
3. The fact that the pair of SI_m values for any of the 10 sections differs by no more than 0.26 indicates the excellent agreement between SI_m values obtained by operating different machines on different dates.

SUMMARY AND CONCLUSIONS

Devices such as the Mays meter will never replace more sophisticated instruments such as the SDP. The Mays meter is not stable in time and, hence, must be recalibrated periodically by using a time-stable device such as the SDP. In addition, the SDP provides much more detailed information about the roughness of a road and is therefore required for some applications. Such applications are discussed in other reports (2, 4, 5, 7). The less expensive Mays meters, however, provide adequate information in many cases if only a single overall measure of riding quality is needed and if the calibration is current.

The SI values for the same road section computed from SDP and from (calibrated) MRM roughness measurements sometimes desagree by over a point. The empirical evidence presented in this study indicates, however, that the differences are explainable by the fact that the Mays meter is sensitive primarily to short waves; however, the profilometer SI is based on roughness with a much wider range of wavelengths. In view of the observations made in the paragraphs below and the fact that the differences can be explained, this point does not indicate that measurements made with the Mays meter are invalid. The SI_m is best interpreted as a summarizing measure of short-wavelength roughness only. This type of measure is important because research results have indicated that ratings of riding qualtiy by human panels are highly correlated with short waves (5).

As a by-product of this study, the repeatability of the two Mays meters used and their day-to-day consistency were examined. The standard deviation of the measurement errors in replicate SI_m values for each of the two machines is about 0.1, which is only 2 percent of the range of the scale, 0 to 5, for SI. Thus, the repeatability is good for both machines.

Analysis of a small set of 10 sections measured on different dates with the two MRMs indicated high consistency between the two machines; the maximum SI_m difference for any section is 0.26. The tentative conclusion is that comparisons among SI measurements made under normal conditions with different MRMs can validly be made. This conclusion is consistent with the study of sources of MRM variations presented in (9).

ACKNOWLEDGMENTS

This study was carried out at the Center for Highway Research at the University of Texas at Austin. We wish to thank the sponsors, the Texas State Department of Highways and Public Transportation and the Federal Highway Administration.

REFERENCES

1. R. S. Walker and W. R. Hudson. A Correlation Study of the Mays Road Meter With the Surface Dynamics Profilometer. Center for Highway Research, Univ. of Texas at Austin, Research Rept. 156-1, Feb. 1973.
2. R. S. Walker and W. R. Hudson. The Use of Spectral Estimates for Pavement Characterization. Center for Highway Research, Univ. of Texas at Austin, Research Rept. 156-2, Aug. 1973.
3. R. S. Walker, F. L. Roberts, and W. R. Hudson. A Profile Measuring, Recording, and Processing System. Center for Highway Research, Univ. of Texas at Austin, Research Rept. 73-2, April 1970.
4. A. D. Brickman, J. C. Wombold, and J. R. Zimmerman. An Amplitude-Frequency Description of Road Roughness. HRB, Special Rept. 116, 1971, pp. 53-67.
5. H. J. Williamson, W. R. Hudson, and C. D. Zinn. A Study of the Relationships Between Road-Surface Roughness and Human Ratings of Riding Quality. Center for Highway Research, Univ. of Texas at Austin, Research Rept. 156-5F, Aug. 1975.
6. G. W. Snedecor and W. G. Cochran. Statistical Methods. Iowa State Univ. Press, Ames, 1967.
7. H. J. Williamson. Analysis of Road Profiles by Use of Digital Filtering. TRB, Transportation Research Record 584, 1976, pp. 37-54.
8. R. L. Wine. Statistics for Scientists and Engineers. Prentice-Hall, Englewood Cliffs, N.J., 1964.
9. C. W. Shaw. Influence of Testing Variables of the Mays Ride Meter. Texas A&M Univ., MS thesis, Dec. 1972.

Publication of this paper sponsored by Committee on Pavement Condition Evaluation.